NOAA Technical Memorandum NWS SR-117

1986 NWS SOUTHERN REGION QPF WORKSHOP

Houston, Texas
February 3-5, 1986

Scientific Services Division
Southern Region
Fort Worth, Texas
April 1986

UNITED STATES DEPARTMENT OF COMMERCE
Malcolm Baldrige, Secretary

National Oceanic and Atmospheric Administration
John V. Byrne, Administrator

National Weather Service
Richard E. Hallgren, Director

TABLE OF CONTENTS

PREFACE

This is the second in a series of Technical Memoranda which consolidates reports on work in the area of quantitative precipitation forecasting by field forecasters, meteorologists from National Centers, and researchers. The Tech Memo comprises papers which were planned for presentation at the Fifth NWS Southern Region QPF Workshop, scheduled for Houston in February, 1986. Although circumstances prevented the workshop from being held, it is hoped this compendium will provide a useful alternative. It also serves as an update on field projects and related studies which were reported upon at the Fourth QPF Conference (NOAA Technical Memorandum NWS SR-112).

ABSTRACTS

SYNOPTIC CLIMATOLOGY FOR HEAVY SNOWFALL ACROSS LOUISIANA

G. Alan Johnson and Edward Mortimer
WSFO New Orleans Area, LA

A climatological study of 22 heavy snowfall events in Louisiana during the period of November 1948 through March 1985 is presented. Seasonal variations indicate a strong preference for mid-winter with the greatest frequencies in January and the first half of February.

Geographic variations are strongly governed by the position of the polar jet as well as the strength and intensity of the surface polar high pressure system. Nearly 80 percent of the heavy snowfall events occurred when a wave or low pressure system developed in the Gulf. The majority of the events occurred in the northern half of the state.

Synoptic flow patterns were identified for all the events. These events were classified into two main pattern types based on the prevailing 500 mb long-wave flow. One of the patterns was subdivided to account for the split-flow with or without a closed low moving toward the state. These patterns closely followed the pattern types associated with heavy rain and flash flood events developed for Louisiana by Belville (1982). Characteristics of the surface and 500 mb patterns associated with each type are presented and discussed.

The forecasters' ability to detect and forecast an impending heavy snow event should improve when the results are used with numerical output in conjunction with a locally developed "decision tree" by G. A. Johnson (1982) for forecasting SNOW/HEAVY SNOW for Louisiana.

THE PRACTICAL REALITIES OF QPF

Charles A. Doswell III and Robert A. Maddox

presented by Charlie Chappell
Environmental Research Laboratories, Boulder, CO

The problem of quantitative precipitation forecasting (QPF) is discussed in terms of what is currently possible and what is likely to be possible in the near future. Discussion centers around the meteorological problem and the tools required in order to address it. It is pointed out that if one takes QPF to mean specific predictions of isohyets which represent what one would actually measure with a dense network of raingauges, we are unlikely to attain this goal in the foreseeable future. What seems more attainable is a sharpening of our ability to define areas of enhanced (or diminished) precipitation probability. Further, it is likely that we can improve our capacity to anticipate significant thresholds of precipitation amount within the areas of forecast precipitation.

Technology and its impact on QPF is discussed at some length, with the conclusion being drawn that purely technological proposals are not the best means of improving our service to QPF users. The QPF issue cannot be discussed as an independent problem -- it is linked to the whole range of meteorological forecast services, about which active debate is ongoing.

AN AUTOMATED QPF VERIFICATION PROGRAM WHICH PROVIDES BOTH REAL-TIME AND LONG-TERM STATISTICAL SCORES IN A USER-FRIENDLY ENVIRONMENT

Christopher D. Hill
WSFO Boise, ID

National Weather Service Forecast Offices (WSFOs) in Montana, Idaho, Washington and Oregon provide daily Quantitative Precipitation Forecasts (QPF's) to the Northwest River Center (NWRFC). The area covered is the Continental Divide westward to the Pacific Coast. Since this region is mountainous and characterized by considerable elevation differences, basin run-off is complicated by snowpack storage and also snowmelt. As a result, the QPF's prepared by the WSFOs consist of more than just forecasts of precipitation amounts. Forecasts of freezing levels and daily maximum temperatures are also required by the hydrologic model.

To assist NWRFC in fully utilizing these daily QPF packages and also to assist WSFOs in improving them, an automated verification system has been developed. The program runs on the NWS Western Region applications computer at WSFO Boise, Idaho. Forecasts and observational data are passed from the NWS AFOS network to the applications computer automatically. The data is not only stored, but it is also checked for internal consistency. If discrepancies are found, an error message is generated and routed via AFOS to the appropriate WSFO.

The forecast region is by any definition "data sparse." To overcome the lack of observational information, the program utilizes numerous statistical scores. These scores are used to produce profiles of forecaster or forecast technique skills in

1. Detecting precipitation events
2. Timing peak rainfall periods
3. Forecasting precipitation amounts
4. Detecting major temperature changes

Verification data is available in real-time and also stored for long-term statistical studies. The system is designed to be very user-friendly. Numerous menus are available which provide the user with great flexibility in output. The system can be accessed from any of the four WSFOs via a personal computer and modem.

Preliminary results from this program yield some interesting results. Based on a single year's data, it was found, for example, that the forecast

staff at a WSFO was reluctant to forecast a "peak" in the rainfall curve. When a peak was forecast, however, the forecaster chose the correct 6-hour period over 50 percent of the time. The correct 12-hour period was forecast 80 percent of the time. The staff also had a strong tendency to overforecast amounts when rainfall totaled less than one-tenth inch, and underforecast amounts when more than one-tenth inch was received.

A CLOSER LOOK AT THE NGM QPF

Frank Brody
National Meteorological Center
Forecast Branch/Heavy Precipitation Unit

The National Weather Service is currently implementing the Nested Grid Model (NGM) as part of the new Regional Analysis and Forecast System. Objective and subjective verification of the NGM Quantitative Precipitation Forecasts (QPF) has shown it is generally superior to the LFM QPF. The NGM QPF occasionally displays a remarkable consistency from one model run to the next on the placement, shape, and maximum amount of precipitation forecast during a particular 12-hour period. It has been observed that when this type of consistency occurs, the NGM is usually far superior to the LFM QPF. Examples of this NGM characteristic are shown, and implications for forecasting are discussed.

VERIFICATION RESULTS FOR NMC 24 HOUR QPFs

Robert E. Bell
National Meteorological Center
Forecast Branch/Heavy Precipitation Unit

Comparison of manual and model threat scores for 1985 are shown.

OPERATIONAL SATELLITE DERIVED RAINFALL ESTIMATES WITH HURRICANES BOB, DANNY AND ELENA

Dane Clark
NESDIS, Washington, D.C.

During the summer of 1985, three hurricanes made landfall along the coastline of the United States. Satellite Meteorologists, in the synoptic analysis branch of NESDIS, calculated rainfall potentials and real-time estimates of rainfall associated with each of the hurricanes. These potentials and estimates were disseminated operationally to NWS Forecast Offices, the National Hurricane Center, and NMC's Heavy Precipitation Unit. Preliminary results show good agreement between estimates and available observations.

TECHNIQUES AT THE NATIONAL HURRICANE CENTER FOR ESTIMATING MAXIMUM RAINFALL FROM TROPICAL DISTURBANCES

Jim Lynch and James B. Lushine
National Hurricane Center, NESS Unit

At the National Hurricane Center (NHC), forecasting the heavy rainfall associated with landfalling tropical disturbances and tropical cyclones has been an imprecise task. Two methods are used to estimate the rainfall potential for these tropical systems: a local rule-of-thumb developed by Kraft in the 1960's, and the Woodley-Griffith technique.

The rule-of-thumb was originally intended to forecast the maximum rainfall for hurricanes affecting the U.S. coast along the Gulf of Mexico. The rule provides rainfall in inches by dividing the system's speed of translation (in knots) into 100.

The Woodley-Griffith technique uses infrared satellite data to estimate area rainfall, averaged over the tropical disturbance cloud canopy. A modification to the original technique provides "core" rainfall, designed to estimate the maximum rainfall normally located near the core of tropical cyclones.

Selected cases of tropical rainfall are presented. Results and verification from the Woodley-Griffith technique are compared to rainfall estimates from the rule-of-thumb. A close examination of the rule-of-thumb indicates that different formulae should be used for different disturbance intensities. Both techniques are extremely susceptible to forecast error of the speed of translation during landfall.

SYNOPTIC CLIMATOLOGY OF HEAVY RAINFALL OVER SOUTH FLORIDA, NOVEMBER - APRIL

Frank J. Revitte
National Weather Service Forecast Office
Coral Gables, Florida

The annual rainfall across south Florida (south of 27N) is quite heavy, averaging between 55 to 60 inches. However, only 20 to 25 percent of the total occurs during the period November through April. Occasionally, daily rainfall during this "dry season" can be quite heavy as mid-latitude synoptic systems penetrate into south Florida.

Data from 25 rainfall reporting sites over south Florida were examined for the period 1948 through 1984 to determine the dates heavy rainfall (3 inches) occurred during the November - April period. A synoptic climatology of heavy rainfall events was then determined by classifying the 500 mb and surface pattern existing just prior to the occurrence of heavy rainfall. Three synoptic patterns accounted for 90 percent of the heavy rainfall events over south Florida during the period of study.

Once heavy rain synoptic patterns are recognized, forecasters can then concentrate on sub-synoptic scale features to decide if and where heavy rainfall is a threat.

A CASE STUDY OF THE AUGUST 1, 1985, FLOOD AT CHEYENNE, WYOMING

Robert T. Glancy
WSFO Cheyenne, Wyoming

Cheyenne, Wyoming, experienced the most devastating flood in its history on the evening of August 1, 1985. In less than four hours a severe thunderstorm dropped two to eight inches of rain on the city. The 6.06 inches of rain recorded at the forecast office was almost half of the average annual precipitation. Twelve people were drowned, and over 70 were injured.

In addition to flooding, the thunderstorm produced two short-lived tornadoes and hail up to two inches in diameter. Damages from the hail and flooding were estimated at over 65 million dollars.

Was this an abnormal storm? Large rainfall amounts are reported from high plains thunderstorms every summer, but rarely in populated areas. However, on August 1, one stationary severe thunderstorm produced torrential rains in Cheyenne.

Synoptic and mesoscale analyses were conducted for the afternoon and evening of August 1. The synoptic weather pattern showed a stationary low level boundary, deep low level moisture, strong instabilities, and approaching shortwave trough. This was not an unusual pattern for mid-summer in the high plains, and both severe weather and flooding were indicated.

Evening satellite pictures showed several areas of significant convection from the Texas Panhandle to eastern Montana, but the Cheyenne thunderstorm produced the most disastrous results. It is shown that the significant difference in the Cheyenne storm was mesoscale forcing which focused the convection over Cheyenne. Outflow boundaries from earlier convection and strong gradient wind flow produced an effective convergence area on which the Cheyenne thunderstorm developed and flourished.

If these situations are as common as suggested, National Weather Service forecasters should be aware of this type of synoptic pattern. But it is only through a dedicated surveillance of changing conditions that these developing mesoscale patterns can be discerned.

NORTH TEXAS HEAVY RAINS ASSOCIATED WITH 500 MB CLOSED LOWS

Ernest L. McIntyre
WSFO Fort Worth, TX

During the period 1974-1985 twelve North Texas heavy rain events (> = 5 inches in a 24 hour period) occurred which were associated with 500 mb closed lows in the southern branch of the westerlies. Data sets were assembled for each of the events in an attempt to identify common features.

In five of the twelve events, the heavy rain fell along north-northeast to south-southwest oriented stationary fronts. Thunderstorm outflow boundaries were present in an additional three events. One event occurred along a slow-moving north-northeast to south-southwest oriented cold front.

The remaining three events were associated with east to west oriented frontal boundaries. One of these events occurred just north of a slow-moving warm front while the other two events occurred well behind slow-moving cold fronts.

PUERTO RICO'S SEVERE RAINFALL EVENT MAY 15-19, 1985: AN INCIDENT OF HEAVY RAINFALL PRODUCTION IN THE CARIBBEAN INFLUENCED BY NON-TROPICAL CIRCULATION PATTERNS

Jere R. Gallup
WSFO San Juan, Puerto Rico

(No abstract)

THE RELATIONSHIP OF QPF TO THE MANAGEMENT OF HYDROELECTRIC POWER ON THE SANTEE RIVER BASIN IN NORTH AND SOUTH CAROLINA

Sam Baker
WSFO Columbia, SC

Hydroelectric power is well developed in the Santee Basin of North and South Carolina. Many of the reservoirs have little or no capacity to store excess water. As a result, water must be used as it comes down the river or be wasted over the spillway. In fact, some power companies in this basin show kilowatt hours wasted as well as flow in cubic feet per second in their spillway rating tables.

The QPF is a valuable tool for water managers in the Santee Basin. Using the QPF, the amount of additional water that will be available can be estimated. Power companies can then increase hydropower use on the assumption that the reservoirs will be replenished. This has the effect of utilizing the additional water for hydroelectric generation rather than wasting it over the spillway or through the floodgates.

This paper describes hydroelectric development in the Santee Basin and attempts to establish an economic relationship between an accurate QPF and hydropower generation.

THE EFFECTS OF URBANIZATION ON THE MINGO CREEK WATERSHED

Tim Marshall
Haag Engineering Company, Carrollton, TX

Mingo Creek is located just east of Tulsa, Oklahoma. The creek flows northward from rolling hills to a broad, shallow sloping floodplain. Over the last three decades, the floodplain has undergone intensive urbanization. Residential areas abut the creek channel. Bermed highways bisect the floodplain.

Mingo Creek has had a long history of flash flooding. The most recent flash flood occurred on May 27, 1984. Eight to fifteen inches of rain fell over the watershed in a four hour period, resulting in a flash flood that killed fourteen people and caused more than fifty million dollars in damage.

This paper will summarize the types of flood flow restrictions observed. Backwater resulted in areas where there were channel constrictions, elevated highway berms, dense channel vegetation, and underdesigned culverts. Of these, backwater from elevated highway berms was the worst. Berms essentially dammed water outside the flood channel elevating flood levels several feet. Steps to reduce the backwater problem are presented.

WATER VAPOR IMAGERY AND EXTRATROPICAL CYCLONES

Roderick A. Scofield
NESDIS, Washington, D.C.

This talk presents the use of water vapor imagery (6.7 um) for analyzing features associated with extratropical cyclones; the use of this type of imagery for analyzing convective systems is also briefly mentioned. Water vapor imagery can be used for the following:

Detect cutoff lows
Detect deformation zones
Detect building ridges
Track mid-upper level circulation systems
Track jet streams
Detect moist/dry zones
Track jet streaks (maxima)
Detect moist/dry couplets
Detect dry slots or surges
Detect areas of rapid drying (often near convective systems)

In addition, extratropical cyclone cloud categories have been developed for heavy precipitation systems. These categories are based on satellite (visible and infrared), radar, rainfall characteristics and surface and upper air data. Each category has distinctly different cloud patterns and/or cloud top temperature characteristics, life cycles, precipitation characteristics, and mechanisms which initiate, focus and maintain the heavy precipitation system.

SYNOPTIC CLIMATOLOGY FOR HEAVY SNOWFALL ACROSS LOUISIANA

G. Alan Johnson and Edward Mortimer

WSFO New Orleans
Slidell, Louisiana

1. INTRODUCTION

Twenty-two (22) heavy snow events were identified statewide from November 1948 through March 1985. These events were further subdivided into two geographical sections. The northern section was considered to be that portion of north and central Louisiana north of 31 degree N or generally along and north of Leesville-Old River Lock line. The southern sections consisted of parishes south of this line to the coast. See Figure 1 for a map of the geographical considerations for Louisiana. Seven of the cases affected portions of both the northern and southern sections. Twelve cases were confined to the northern section while only three cases were confined to the southern section.

The period of climatological data was November 1948 to March 1985. The daily series of synoptic weather charts (NOAA, 1968) for the period of November 1948 to April 14, 1968, and the daily weather maps (NOAA, 1983) for the period April 15, 1968, through March 1985, which include both 500 mb and surface analyses were used to examine the patterns that produced the heavy snow. These charts were for 1200Z data only. The pattern selected was based on the 12Z time and data closest to the beginning of the event.

Light snowfall has been reported in some portions of Louisiana nearly every winter season, but heavy snowfall is rare. An event was defined as a 24-hour snowfall of 3 inches or greater in the north and between 1 and 3 inches in the south (at two or more reporting stations). Since heavy snowfall is quite rare in the bayou state, amounts less than 4 inches statewide are economically significant. Most cities are not mechanically equipped for snow removal.

2. SEASONAL AND GEOGRAPHIC DISTRIBUTIONS

2.1 General Snowfall Climatology

Using climatological data for the 37 winter seasons of 1948-1949 through 1984-1985, it was noted that at least a trace of snow was reported in all but the 1951-1952 season. Measurable snowfall, considered to be 0.5 inch or more at two or more reporting stations, was observed in just over two-thirds of the seasons (25 of 37). This compared favorably with Ethridge (1978), who showed measurable snowfall occurred in northern Louisiana in about 75 percent of the winter seasons since 1893. For geographical comparison, the state was divided into northern (consisting of north and central parishes) sections and southern sections. This was done along 31 degrees north as described above. As would be expected, the majority of the snowfall cases (75%) were confined to the northern section, with only 3 events confined entirely to the south, see Table 1. However, as a note of interest, the greatest monthly snowfall total for the state occurred in southwestern Louisiana in 1895, see Table 2. During the 37 seasons of record, the snowfall amounts ranged from a trace to 14.0 inches. Table 3 shows a distribution of snowfall amounts over the state. Snowfall events in Table 3 were considered separate if they occurred in both the northern and southern sections. There were twelve such events, thus accounting for the difference in total events between Tables 1 and 3.

2.2 Heavy Snowfall Climatology

The monthly distribution of heavy snowfall events in Louisiana, November 1948-March 1985, is shown in Figure 2. Heavy snow has fallen in Louisiana as early as December 16 (which occurred in 1983) and as late as March 22nd (which occurred in 1968). Heavy snowfall was most frequent in January and early February (77 percent of the cases). The frequency increased rapidly in late December and diminished rapidly in late February. The greatest frequency of heavy snows in January and early February correlates quite well with the southward displacement of the polar jet. Also, heavy snows were generally triggered by mid and high level (above 8000 feet) tropical moisture of Pacific origin overrunning the polar airmass with a wave or low in the northern Gulf of Mexico.

With southern displacement of the polar jet in January and early February, surface cyclogenesis occurred in the northern Gulf about 80 percent of the time. This southerly displacement was the mechanism which forced the polar airmass southward over Louisiana and created the environment necessary for heavy snows. See Table 4 for the five heaviest snowstorms in Louisiana since 1948.

During the 37 winter seasons, 22 heavy snow events met the criteria. The average number of parishes affected by heavy snow per event was 21. The average width of the band of the heaviest snow within the general area of heavy snow was 40 to 50 miles. The band of the heaviest snow generally occurred about 240 nautical miles (276 statute miles) to the north or northwest of the track of the surface low. This is similar to the finding of Harms (1973).

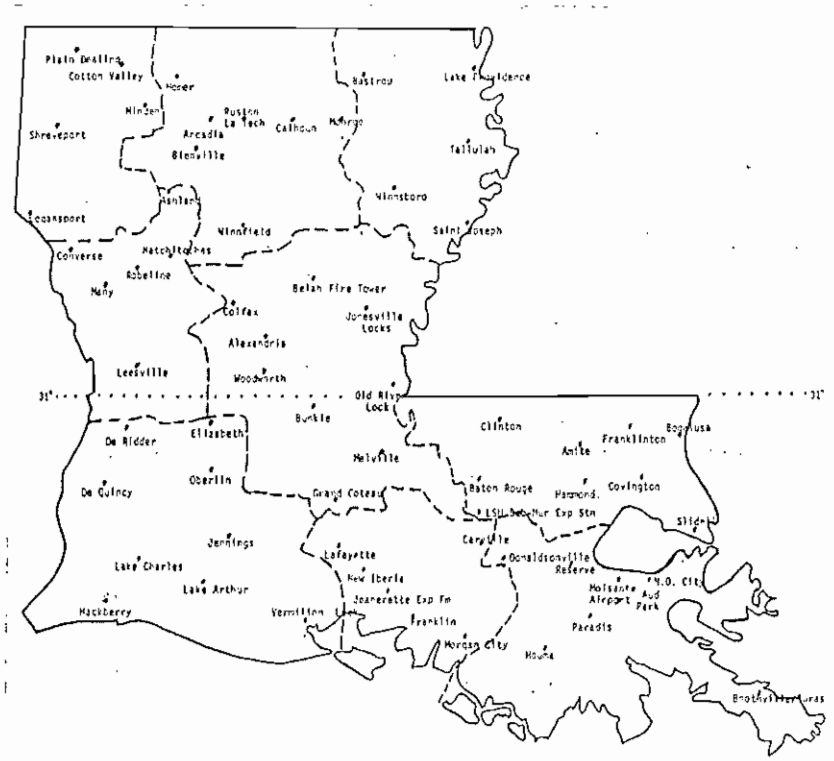

Figure 1. Map of geographical considerations for Louisiana.

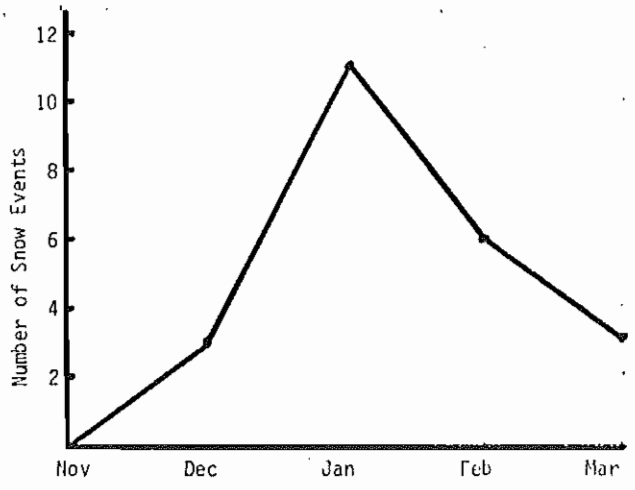

Figure 2. Monthly distribution of heavy snowfall events in Louisiana.

Several other characteristics were noted during these events. Most snow events occurred with surface temperatures in the upper 20s to lower 30s. Five of the 22 events preceeded a major arctic outbreak (Mortimer and Johnson, 1986). Several of the heavy snow events followed significant ice storms (accumulations of .75 inch or more) across northern Louisiana. In 1948 and 1978, the heavy snowfall in northern Louisiana consisted of two significant events within a 48-72 hour period (these were considered as separate in this study since they were separated by 24 hours or more between snows). In 20 percent of the events, Ethridge (1985) indicated that the heavy snowfall was associated with thunderstorms.

3. SYNOPTIC PATTERN TYPES

3.1 Upper Air

Only a few synoptic patterns caused heavy snow in Louisiana. Upper air patterns were identified for all of the events although several events fell into the "hybrid" type that exhibit qualities of two pattern types. These events were classified into two main pattern types based on the prevailing 500 mb long-wave pattern. One of the patterns was divided into two sub-parts to account for the split-flow with or without a closed low which was moving towards the state. Composite figures were developed for each pattern, see Figures 3 through 7. These patterns closely followed the pattern types associated with locally heavy rains and flash flood events which were developed by Belville (1982) for use by WSFO New Orleans. Belville described 6 upper air patterns related to heavy rains in Louisiana.

The pattern types were based on the following long-wave patterns:

3 - Migratory full-latitude trough over central North America

4 - Migratory short/wave (s/w) troughs in a split-flow pattern over the United States

4a - Migratory east or northeast moving short-wave (open trough) in a split flow

4b - Migratory eastward moving closed low towards the state in a split flow pattern (generally passes just north of the state).

Region	Month Nov.	Dec.	Jan.	Feb.	Mar.	Total
N	1	5	30	12	5	53
S	0	1	0	2	0	3
Both	0	0	7	3	1	11
Total	1	6	37	17	6	67

Table 1. Number of measurable snowfall events for winter seasons 1948-1949 through 1984-1985.

Climatological Region	Amount (inches)	Station	Mo/Year
Northwest	14.0	Sarepta	01/1948
North central	16.4	Arcadia	01/1948
Northeast	15.2	Bastrop	01/1948
West central	14.0	Robeline	01/1949
Central	15.0	Grand Coteau	02/1895
East central	12.5	Amite/Baton Rouge	02/1895
Southwest	24.0	Rayne	02/1895
South central	14.0	Lafayette	02/1895
Southeast	16.0	Houma	02/1895

Table 2. Greatest monthly snowfall (1893-1985). Unofficial reports showed 22.5 inches at Plain Dealing in NW Louisiana in 12/1876 (Ethridge, 1978).

Region	> 9.99	6.00-9.99	4.00-5.99	2.00-3.99	1.99-0.50	Total
N	2	7	10	17	29	65
S	0	1	5	3	5	14
Total	2	8	15	20	34	79

Table 3. Measurable snowfall by amounts and regions. Twelve cases occurred in both the north and south and are included separately for each region.

Date	Max Storm Total (Inches)	Pattern Sfc/500 mb
Jan. 30-31, 1949	14.0 at Robeline	A /4A to 4B
Feb. 12-14, 1960	13.0 at Colfax	C /4A to 4B
Jan. 31-Feb. 1, 1951	8.0 at Lake Providence	B /4A
Mar. 22, 1968	8.0 at Arcadia	A /4A to 3
Jan. 31, 1982	8.0 at Ashland	A /4A to 4B

Table 4. Five heaviest snowfall events in Louisiana, 1949-1985. Station locations are shown in Figure 1. Pattern type are discussed in Section 3. Note: The pattern types above are hybrid in nature. Prior to and during the event, the pattern translates into another pattern.

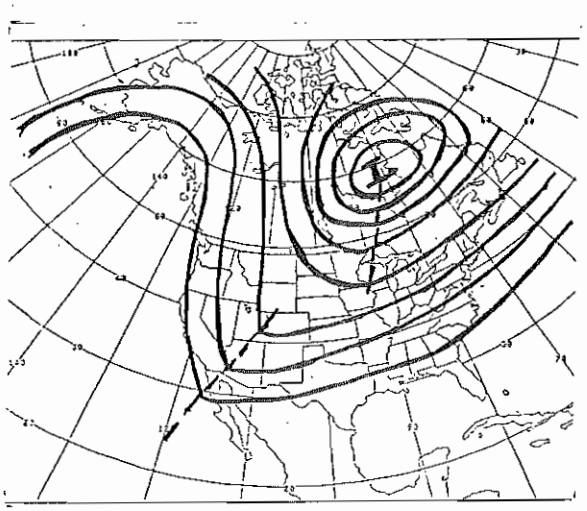

Figure 3. Pattern 4a, beginning of event. Migratory east or northeast moving s/w trough in a split flow.

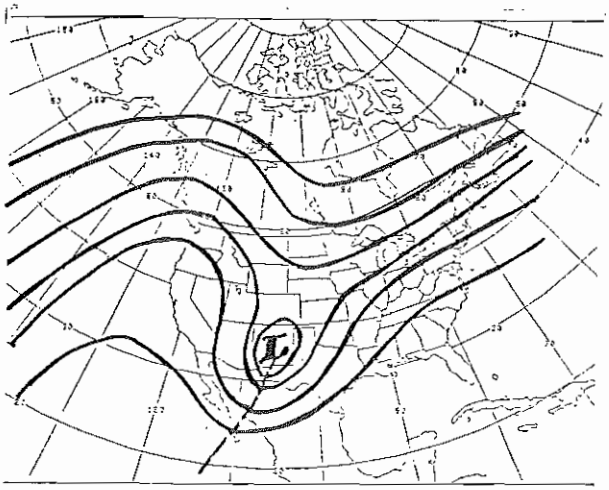

Figure 4. Pattern 4b, beginning of event. Migratory closed low in the southern branch of split flow moving eastward toward the state.

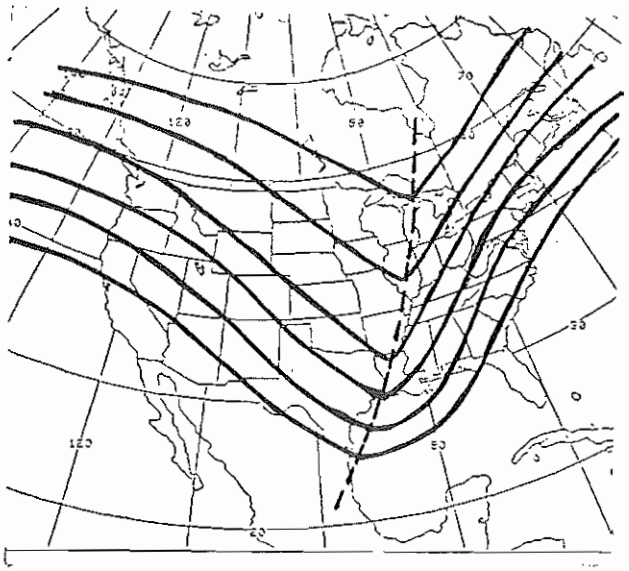

Figure 5. Pattern 3, end of event. Migratory full-latitude trough over central North America.

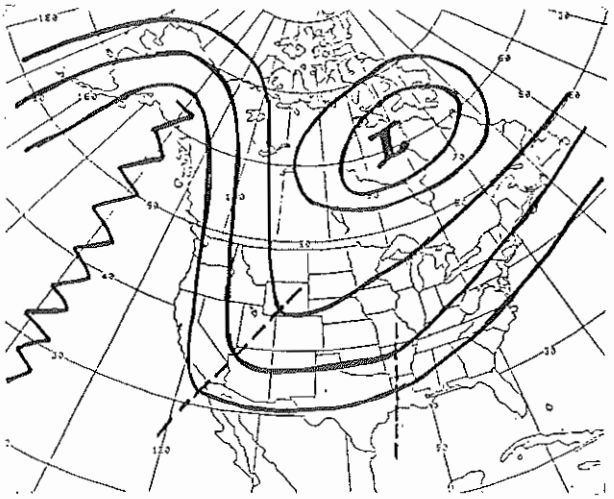

Figure 6. Pattern 4a end of event. Migratory east or northeast moving s/w trough in a split flow.

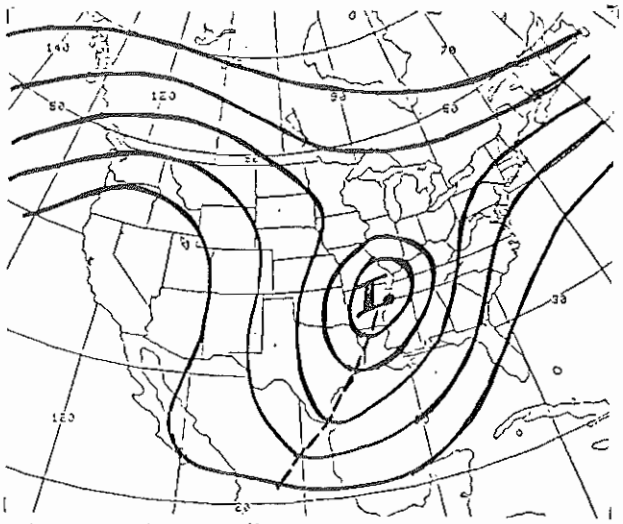

Figure 7. Pattern 4b, end of event. Migratory closed low in the southern branch of split flow moving eastward.

A split-flow pattern was evident at the beginning of all heavy snow events. The predominate pattern was 4a (16 of 22 cases) with a s/w trough in the southern branch generally located over the southwestern U. S. (Figure 3). An exception was the Dec. 31, 1963 - Jan. 1, 1964, event in southeastern Louisiana when the s/w trough was located over eastern Texas and extended southward into the western Gulf of Mexico. The 4b pattern was evident in the other 6 cases (Figure 4). In 4 events, a closed low in the southern branch was located over the southwestern states (New Mexico and Colorado), while in 2 cases the closed low was centered over the eastern Pacific. Branick (1985) found that over 50 percent of the heavy snow cases in Oklahoma were associated with upper level closed lows, while in Louisiana only 27 percent of the cases had a closed low.

The upper air patterns were also studied to correlate with the ending of the snow event. As would be expected, the snow ended as the s/w trough in the southern branch or major trough moved into Louisiana.

In one-half of the events, the upper air pattern changed from its original pattern (see Table 5). In 8 cases, the 4a or 4b pattern moved eastward and became orientated with the long-wave trough, pattern 3. The trough was along a western Great Lakes to southeast Texas/southwest Louisiana line in 6 out of 8 cases, see Figure 5. In the other two cases, the trough axis was: along a Lake Winnepeg, Canada to southern New Mexico line and along an eastern Great Lakes to southwest Texas line.

	Ending Pattern			
Beginning Pattern	3	4A	4B	Total
3	0	0	0	0
4A	4	9	3	16
4B	3	1	2	6
Total	7	10	5	22

Table 5. Change in the upper pattern through cycle of heavy snowfall events.

The ending of the snow event characterized by a 4A pattern showed the main trough continuing in the southwestern states while a s/w trough moved into Louisiana in 8 of 10 cases, see Figure 6.

The mean position of the closed low in the 4b ending pattern was over Arkansas with the trough extending southwestward to near Brownsville in 4 of the 5 cases, see Figure 7. In one case (1977), the closed low moved from off the southern California coast to the Gulf of California.

3.2 Surface

Characteristics of the surface patterns associated with the 500 mb pattern were also identified for each type. The four main surface patterns associated with the 500 mb long-wave pattern were as follows:

A - Surface front in or near southeast Louisiana
B - Surface wave or low in the northwest Gulf of Mexico
C - Surface wave or low in the middle Gulf of Mexico
D - Surface wave or low in the eastern Gulf of Mexico

See Figures 8-10 for composite examples of some of these patterns which were dominate during heavy snow events.

At the surface, a strong polar high pressure system builds southward from the northern Plains through the Lower Mississippi River Valley to the Gulf coast. In fact, frigid temperatures usually engulfed the entire region with a strong cold front located in or near southeast Louisiana. Winds were generally east to northeast when the snow began with speeds of generally 15 mph or less. However, by the time it ended, the wind had backed to a northerly component. Occasionally, this was due to the passage of an inverted trough or a surface low passing south or southwest of the snow area. The majority of the events occurred across a portion of the state when a wave or low developed in the northwest or

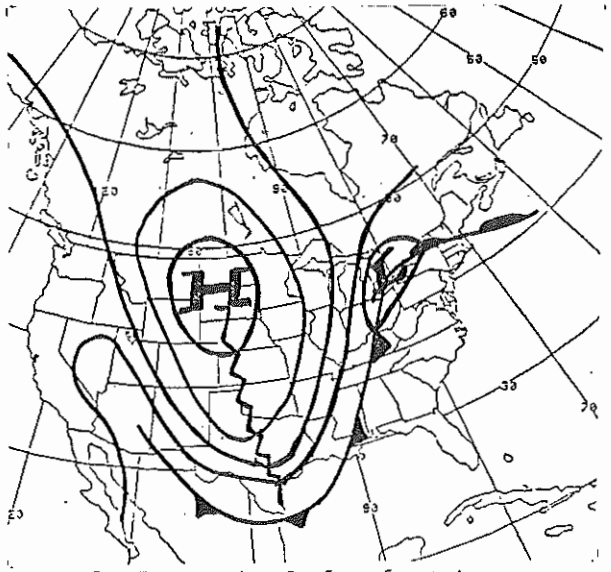

Figure 8. Pattern A. Surface front in or near southeast Louisiana.

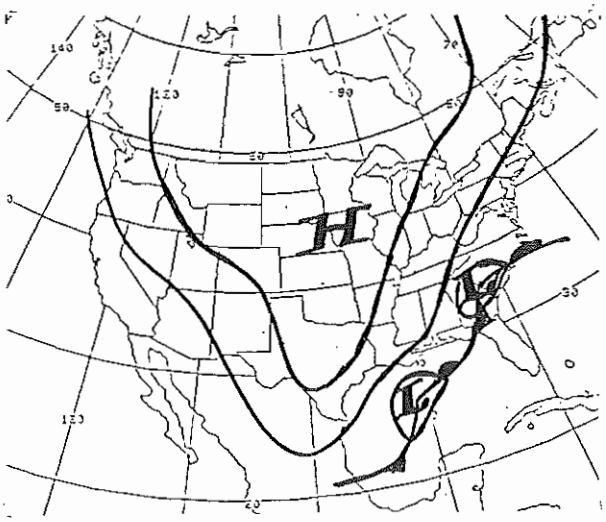

Figure 9. Pattern B. Surface wave or low in the northwest Gulf of Mexico.

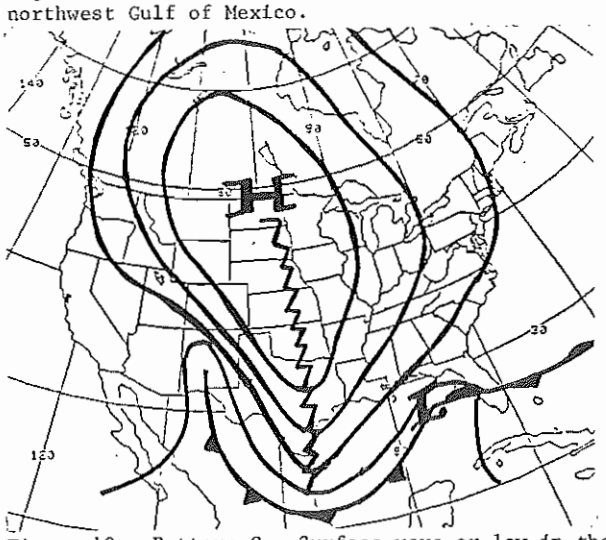

Figure 10. Pattern C. Surface wave or low in the middle Gulf of Mexico.

middle Gulf of Mexico. The value of the highest pressure in the center of the high averaged 1038mb.

In 4 of the cases, the snowfall developed shortly following the passage of a strong cold front through the state (pattern A, see Figure 8). The remaining 18 cases were associated with either a wave or a low in the Gulf of Mexico. Eleven of these low pressure systems developed in the northwest Gulf of Mexico and moved northeastward into portions of Florida, pattern B, see Figure 9. Six lows developed in the middle Gulf between 85W and 90W, pattern C, see Figure 10. The Dec. 31, 1963-Jan. 1, 1964, event produced the only low to develop in the eastern Gulf of Mexico. Table 6 shows the relationship between surface and upper air patterns for 12Z closest to the beginning of the snow event.

	Surface Patterns				
Upper Air Patterns	A	B	C	D	Total
3	0	0	0	0	0
4A	3	7	5	1	16
4B	1	4	1	0	6
Total	4	11	6	1	22

Table 6. Relationship between surface and upper air patterns at 12Z closest to the beginning time of heavy snow.

Many of these events are actually mesoscale not synoptic scale phenomena. Thus, with this in mind, the classification of synoptic pattern types will not likely provide sufficient information on the precise timing and location of the heaviest snow. Consequently, analyses are needed to ascertain the focusing mechanism and therefore "zero in" on the main threat area. This technique is similar to that developed by Belville (1982) and Belville et al (1978) in the analysis of heavy rainfall patterns in Louisiana and west Texas.

Of course, in addition to recognizing the proper pattern which might be conducive to the development of heavy snow, the forecaster must carefully evaluate the MOS guidance for sufficient moisture and the critical temperatures needed for the development of snow versus rain. A locally prepared "decision tree" can be utilized to aid this process (Belville et al, 1982). A modified snow/heavy snow "decision tree" developed for use in Louisiana by the WSFO New Orleans forecasters focuses on the major parameters and their critical values necessary for snow/heavy snow development. This "decision tree" was based on the one developed at WSFO Lubbock in the mid 1970's (Johnson, et al).

4. CONCLUSIONS

Light snowfall occurs across portions of Louisiana nearly every winter season, November through March. However, heavy snowfall is somewhat rare with only 22 events identified statewide from Nov. 1948 through Mar. 1985. It was found that the heavy snow events peak in January and early February and were not confined to only the northern section of the state. Seven cases affected the entire state while 12 cases were confined to the north and three cases to the south.

Two main pattern types were identified based on the prevailing 500 MB long-wave pattern. These were a long wave trough pattern and a split flow pattern, which was subdivided to indicate cases with or without a closed low. A split-flow pattern was evident at the beginning of all heavy snow events. In one-half of the events the upper air pattern changed from its original pattern to one of the other patterns. Synoptic surface patterns associated with the 500 MB pattern were also identified for each event. Eighty percent of the heavy snow cases were associated with a wave or low developing in the northern Gulf of Mexico.

Pattern recognition can play a very important role in the medium-range forecasting (one to two days in advance) of heavy snowfall. Numerical guidance may show a developing flow pattern that resembles one (or more) of the heavy snow patterns, thus alerting the forecaster that a heavy snow event may be developing. The most likely time and location of heavy snowfall across the state may be narrowed down as later data becomes available.

However, pattern recognition will only help alert the forecaster to the potential for heavy snowfall. Additional studies of subsynoptic and mesoscale flow patterns are needed to help with the assessment of heavy snow potential on a smaller time scale and areal delineation. With a series of synoptic flow patterns associated with heavy snow events and a "decision tree" for forecasting snow/heavy snow using mean threshold values of various parameters, a more complete climatology is now available to the meteorologist for forecasting a "heavy snow" event in Louisiana.

5. ACKNOWLEDGEMENTS

The authors would like to thank Dr. Robert A. Muller, State Climatologist, and his staff at LSU for their help in obtaining some of the climatological data used in this study, as well as reviewing this manuscript. Likewise, thanks are due to Ernie Ethridge, OIC, WSO, Shreveport, La., for providing some of the climatic data as well as reviewing the paper. Additionally, we would like to thank Gary Grice, WSFO, San Antonio, Tx., for his review of the manuscript, and for Gail Stein, Secretary, WSFO, New Orleans, who typed the manuscript.

6. REFERENCES

Belville, James., G. A. Johnson and J. D. Ward (1978): A Flash Flood Aid - The Limited Area Quantitative Precipitation Forecast. NOAA Tech. Memo. NWS-SR-97, 12pp.

Belville, James and G. A. Johnson (1982): The Role of Decision Trees in Weather Forecasting, Preprint 9th Conference of Weather Forecasting and Analysis (Seattle) June 28-July 1, 1982, AMS, Boston, pages 7-11.

Belville, James (1982): 500 MB Flow Patterns and Related Surface Features Associated with Heavy Rainfall Events in Louisiana. WSFO New Orleans Area Technical Note 12.

Branick, Michael L. (1985): Synoptic Pattern Type Associated with Heavy Snowfall Events in Oklahoma, 1985 NWS Southern Region QPF Workshop (San Antonio), NOAA Technical Memo NWS SR-112, pages 38-46.

Ethridge, Ernest S. (1978): North Louisiana Snow. Unpublished report for February 1978 WSFO/WSO Conference at New Orleans, La.

Ethridge, Ernest S. (1985): Personal correspondence.

Harms, Rheinhart W. (1973): Midwestern Snowstorm Models and the February 1973 Storm Over Georgia. NOAA Tech Memo NWS SR-74, 13 pp.

Johnson, G. A. and A. Castaneda (1975): Checklist for Forecasting Snow/Heavy Snow in West Texas. (Unpublished)

Johnson, G. A. (1982): Checklist for Forecasting Snow/Heavy Snow in Louisiana (Unpublished)

Mortimer, Edward and G. A. Johnson (1982) Study of Arctic Outbreaks in Louisiana (Unpublished)

NOAA, 1948-1985: Climatological Data for Louisiana. NOAA, EDIS, FEderal Bldg., Asheville, NC.

---, 1948-1968: Daily Series, Synoptic Weather Maps, Part I, Northern Hemispheric Sea Level and 500 mb Charts, Jan. 1948 to Apr. 14, 1968, NCDC, Asheville, NC.

---, 1968-1985: Daily Weather Maps--Weekly Series, Apr. 15, 1968 to March 31, 1985, U. S. Government Printing Office, Washington, DC.

The Practical Realities of QPF

Charles A. Doswell III and Robert A. Maddox*
NOAA/Environmental Research Laboratories
Weather Research Program
Boulder, CO 80303

I. Introduction

Quantitative precipitation forecast (QPF) products come in a variety of forms: predicted precipitation isohyets, a probability distribution with respect to expected amounts, a flash flood watch, agricultural forecasts, etc. In principle, all can be derived from a set of predicted isohyets, provided those isohyets represent what would be observed in a gage measurement. This is not a trivial point, because not all predicted isohyets are intended to fulfill this requirement. Another seemingly minor point is that true QPF products must be issued before the precipitation is to fall. How long before? For this discussion, the lead time must exceed the characteristic period of natural variability associated with the process producing the precipitation. For convective processes, this might be a few hours; for synoptic-scale events, it might be as long as a day or two. Finally, we wish to distinguish between forecasts made before precipitation events have begun from those issued after precipitation has commenced, since distinctly different forecasting methodologies are involved.

Some forecasts require one to combine hydrology with meteorology -- flash flood forecasts are the most obvious example. Nowhere is QPF more essential to the process than in issuing a flash flood watch (the warning is more of a "nowcast", although this should not be construed to mean it is easy). Flash flooding and heavy precipitation are not synonymous, since hydrology plays such an important role. If the hydrologist has predicted isohyets available, this makes the job of predicted stream flows and, hence, flash floods more or less straightforward. Unfortunately, those isohyets must be correct in a very detailed sense for this hydrological forecast to be correct. In order to be worthy of the adjective "quantitative" the predicted isohyets must give an accurate prediction of the total precipitation distribution, at least down to the scale of drainage basins. The basins of interest in flash flood prediction are those of the tributaries rather than the main channels, so the scale down to which we require accurate precipitation forecasts is quite small. This also implies small time scales -- an entire event can begin, mature, and decay within three hours (e.g., the recent Cheyenne, WY flash flood).

*Present Affiliation: National Severe Storms Laboratory, Norman, OK 73019

II. Scale interaction and QPF

Weather events are the result of meteorological processes. To be more precise, they arise through the interaction of a number of processes. For example, thunderstorms develop when the large-scale environment has evolved to bring together moisture, instability, and small-scale lifting mechanisms (fronts, drylines, upslope flow, etc.). The presence of thunderstorms can, in turn, modify that large-scale environment to make other processes (e.g., extratropical cyclogenesis) more (or less) likely. The formation of precipitation within clouds depends on other processes on scales above and below that of the precipitation formation region. Therefore, as a matter of principle, it is not hard to see that QPF requires one to know a great deal about a rather intimidatingly large number of processes.

The science of meteorology is best equipped to give insights to large-scale weather systems of middle latitudes (i.e., extratropical cyclones). There is a fair amount of knowledge about convective processes, although this is based on research data sets not generally available. There is relatively little known about mesoscale processes -- operating in, say, the size range between 1000 km and 10 km. Thus, the circumstances by which the potential for precipitation (created by synoptic-scale systems) comes to fruition in convective precipitation may be rather elusive and hard to anticipate. By implication, large-scale QPF is relatively easy, but the large-scale isohyets which one produces do not represent what one would measure with a gage. Instead, such large-scale QPF shows *an average* precipitation over a large-scale domain (say a large fraction of the area of a midwestern state). While such a product can be reasonably accurate in this limited interpretation of accuracy, it does not necessarily meet the needs of a forecaster concerned with flash floods.

In the discussion of QPF, we should distinguish between forecasting and nowcasting (a distinction to which we have already alluded). For a statement about the weather to qualify as a true forecast, some lead time is required, as mentioned above. By lead time we mean the difference between the statement's issue time and the time the event begins. When precipitation is already underway, one has to predict whether or not the event will *continue*. For precipitation events not in progress at forecast issue time, one must

predict whether or not precipitation will *develop*.

In the latter case, this cannot be done directly by linear extrapolation, since one does not use linear extrapolation for events which are not yet occurring. Of course, one may be able to employ linear extrapolation successfully for prediction of the large-scale features which make precipitation *possible*. Non-convective precipitation forecasting usually depends on large-scale processes, so large-scale methods (objective and subjective) can be used to *formulate* a prediction of non-convective precipitation. The most difficult QPF problem is *convective* QPF, because there is so little quantitative knowlege about the relationship between the synoptic weather systems and convection. This paper focuses on convective QPF for two reasons. First, intense precipitation events are almost invariably convective in nature. Second, we wish to consider the effect of the ignorance of mesoscale processes which dominates meteorology.

III. Convective precipitation events

At this stage in the science of meteorology, it is just marginally feasible to consider forecasting mesoscale processes a few hours in advance. In order to do so, one must exploit the limited data to their fullest (and perhaps a bit beyond), requiring continuous diagnosis of the data with a wide range of qualitative and quantitative models (see Doswell and Maddox, 1986). A complete and detailed prediction of the storm-scale evolution is a virtual impossibility, which means that one is really incapable of forecasting rainfall isohyets on the storm scale. While a qualitative forecasting approach may make it possible to improve upon the large-scale QPF products, it must be recognized that any QPF product the science of meteorology can produce, now or in the foreseeable future, does not purport to predict actual gage measurements. Nevertheless, we believe that isohyets which represent mesoscale averages are possible, as are estimates of the absolute maximum precipitation within that mesoscale area. Under the right conditions (see Doswell, 1986), mesoscale diagnosis and prognosis can be used successfully to identify mesoscale areas of high flash flood threat (when combined with hydrological input, of course), but one must recognize that the meteorology may put the greatest threat one drainage basin over from where it actually occurs. Perhaps the meteorology leads one to put the threat area into two basins, whereas the event materializes in one basin and not the other. Even the most diligent forecaster is unlikely to hit every such mesoscale "QPF" with enough accuracy and lead time to satisfy the hydrologist's needs. To ask for mesoscale QPF which provides accurate isohyets predicting actual gage measurements is simply beyond the capacity of meteorological science, no matter how desirable it is to have such predictions.

A concept of some interest to mesoscale convective QPF is the *precipitation efficiency*. This usually refers to individual convective cells, although it could be applied to larger, mesoscale entities. It may be possible to estimate the current amount of water substance within a volume rather easily and, with some effort, to estimate the net flux of moisture into that same volume. The important issues about how much of that moisture gets converted into precipitation, over what space and time it will fall, etc. are rather difficult to forecast. Precipitation efficiency can range from zero to over 100% and it is hardly straightforward to forecast it from case to case, or even from time to time within the same event.

IV. Centralized QPF Guidance

Much of the actual QPF available today is produced centrally. This is the result of the lack of dispersion of resources within the operational forecasting system. QPF may represent the single most challenging task confronting a forecaster, and it seems apparent that the forecasting system has, by choice or by accident, put most of the resources for addressing the QPF problem into a few specialized offices. We hope to indicate why this approach may not be the optimum strategy.

The current generation of numerical weather prediction (NWP) models, as well as the next generation, are essentially large-scale models. The convective process, which is the primary mechanism for producing heavy precipitation, is *parameterized* in NWP models rather than being calcuated explicitly. That is, the contribution of convection to model-generated precipitation forecasts is derived from large-scale processes. Thus, those forecasts are most appropriately thought of as large-scale, area-averaged precipitation and not what one would observe with a dense network of gages. Particularly when convection is involved, the local observations of precipitation will depart substantially (by one or more orders of magnitude) from model-generated values. To the extent that the parameterizations are successful in predicting the rainfall input from convection, the model forecasts may be rather good, in the limited sense just described. The problem is that the models are unlikely to perform consistently well (in a quantitative sense) when truly unusual convective events are happening. That is, the models are least likely to have captured the magnitude of the threat from heavy precipitation at just those times when it is most important.

Besides parameterization, another strategy for QPF has evolved to go from large-scale models to actual sensible weather events. This is the *statistical*

approach, with the so-called Model Output Statistics (MOS) being the most common statistical technique used in operations today. This paper is not an appropriate forum for a detailed treatment of MOS (see Glahn and Lowry, 1972), but we can generalize by saying that there is always some important residue of real events which remains untreatable via statistical methods. Once again, this residue is mainly composed of events which are not typical in a statistical sense. As with direct model output, the likelihood that the objective forecasts from MOS will be seriously inadequate is greatest when the magnitude of the event is unusually high; i.e., when the forecaster needs the most help. Note that objective statistical methods are usually cast in terms of probabilities, rather than the apparently desirable isohyets. This is not necessarily bad.

V. Qualitative Methods

If one accepts the idea that large-scale model-generated objective guidance is inadequate for truly important heavy convective precipitation events, the continuing need for QPF must be met by subjective methods. However, the tough task of QPF may be overlooked or given less than full attention in the local office. As with severe thunderstorms, it can be argued that a specialized team at a central location (i.e., the Heavy Precipitation Branch, or HPB, at the National Meteorological Center), concerned only with a single forecasting problem, can be more effective at that task than a local forecaster. That this argument can be disputed is not important in this paper. However, it is clear that a subjective HPB product is not intended to provide the detailed isohyets on the tributary watershed scale that seems desirable. While one might want to have some additional focusing done at the HPB level, they themselves do not claim to be attempting what we already have said is not feasible. Given the data and analysis tools at their disposal, it is unlikely that the subjective QPF guidance provided by HPB will become much more detailed than it currently is.

We have asserted that local QPF is difficult, resource-intensive, and may require more time than is available (as in a combined heavy precipitation and severe weather event). In spite of these problems, some local offices have made serious attempts to refine their QPF products (e.g., Belville *et al.*, 1978). Such efforts entail considerable cost to the local offices, in that they are not given formal support within the organization. The work has to be taken "out of hide", which necessarily limits its scope and rigor. To the extent that these programs have contributed positively to the office's forecasting effort, that cost may be worthwhile. However, the cost factor virtually ensures that detailed validation and documentation of the local QPF techniques will not be done expeditiously, if at all. Thus, if some local office develops a QPF scheme, that scheme may never be given a *rigorous* test. Documentation of essentially unvalidated work can stimulate interest in the schemes outside of where they were developed, but it is not obvious that one office's technique can be transferred as is to another office. Further, successful schemes should manifest themselves by improved verification, but even this (by itself) does not provide the detailed validation that one needs. For instance, a scheme may work better in some situations than in others and those who wish to employ that scheme at another location need to know about such aspects of the technique.

VI. Prospects for the Future

Although the current era is one of great technological and scientific change, it is not clear that this turmoil has resulted in any fundamental change in the way forecasters go about their business. The means of accomplishing the desired ends are rapidly moving out of the "pencil and paper" phase (in which modern meteorology has its roots), and into one where computers are heavily employed. New remote sensing systems are emerging from the laboratories and into testing and evaluation for eventual operational implementation. The science of meteorology is gaining new insights into the processes which produce precipitation, in no small way through using these new technologies.

However, it is not yet obvious how to proceed with the operational employment of all this new hardware, data, and knowledge. Reasons for this situation are rooted in the notion of the "learning curve". That is, new tools require new modes of thought, which must somehow be integrated into older, traditional approaches -- products must still go out while the transition is taking place. Training and education of forecasters have not kept pace with this explosive growth in science and technology, exacerbating the conflict between old and new. Implementation of new tools requires experimenting with different strategies and validating the results of the experiments. This trial-and-error process requires time and resources, both of which are in short supply in today's operational environment. Large capital outlays for nationwide application of new technologies are rather intimidating. The upshot of all of this is that we do not see new science and technology leading to immediate and noticeable increments in QPF skill now or in the near future, regardless of the ultimate value of those new tools.

We can anticipate only modest improvements in the large-scale NWP models until such a time that the new data collection systems provide a usable and more detailed large- to medium-scale data base.

Perhaps of greater interest are the so-called mesoscale NWP models. The most likely immediate impact of mesoscale NWP is an enhanced scientific understanding of the mesoscale processes which focus and initiate heavy convective precipitation events. Without intending to denigrate the potentially valuable new guidance that may one day come from mesoscale NWP models, they have several problems which must be dealt with before operational implementation can begin. First of all, whether mesoscale NWP models can produce valuable guidance without a mesoscale *data base* has to be determined. Operational data collection is going to remain at roughly its current state for at least five years, so this is a crucial question. If it turns out that mesoscale NWP models have to have mesoscale data, it is hard to see how a truly substantial increase in NWP forecast skill is going to come from mesoscale models, except perhaps in some special situations.

Second, the computational cost of such models virtually precludes their use in our resource-limited local offices. This means that the early operational mesoscale NWP models will be run at a few centralized locations (or at *one* location). The real value of a centrally-produced mesoscale NWP model in providing help to local offices is not at all obvious to us. There are a host of issues in this regard that have never been satisfactorily addressed vis-a-vis the *large-scale* models.

Third, considerable scientific progress is required before we can be assured that the cost of such models is paid for in quantitative improvement of forecast guidance. We are only now at the threshold of insight into mesoscale processes, especially with regard to interaction with processes operating at scales above and below the mesoscale. We are not saying that progress has not been made, only that it appears that mesoscale models may not make progress as rapidly as the large-scale models, and we still seem to have a long way to go.

Since the issue of mesoscale data sets is of concern, we think we are safe in saying that *in situ* measurement systems (e.g., surface sites and rawinsondes) are not likely ever to attain mesoscale density on an operational basis, for a variety of reasons. It is probably also safe to state that remote sensing techniques require considerable developmental improvement before becoming operational. The new systems provide incredibly high "information rates" but it is not the same sort of information to which we meteorologists are accustomed (i.e., temperature, humidity, pressure, and wind at well-defined points in space and time). Instead they measure such things as returned radiation (for active sensors, which emit radiation in measured amounts), emitted radiation (for passive sensors), Doppler phase shifts, etc. To go from such measurements to more conventional data requires substantial effort and it may well be that we should contemplate reshaping our meteorological thinking to correspond more directly with what the new systems actually measure, rather than forcing the new data to look like our old data.

In any event, considerable data processing is required to assimilate the high information rate of the new observing technologies. It may turn out that while the data flow has increased, its *value to us* as meteorologists has not increased commensurately. We think it would be a tragic mistake to take it as given that new systems should replace the more traditional technology (a rawinsonde is, after all, a product of technology!) of meteorological measurement. The strategy most likely to yield success, in our opinion, is one in which new data will *supplement and enhance*, rather than replace, old data.

Moreover, if forecasting is to benefit from new scientific insights, new paths must be explored for dealing with old problems. However, computer systems which have reached the field (or are currently envisioned for the field) are not truly interactive -- decisions have been made for the field user as to what products will be available, and how they will be displayed. Human input is limited to selecting from what has been offered. Such systems are not interactive; rather, they are computerizations of what was done with teletype and facsimile. Rather than innovation, these systems are old approaches cast in a new form. If field offices are to retain a role in the "information age", they must have access to the information and the capacity to develop their own products, to manipulate data for their own ends, and to adapt the system's capability to satisfy their own requirements.

Regarding QPF, this sort of local capability would offer the chance to begin validation and documentation of local techniques for QPF, an opportunity heretofore unrealized owing to lack of local resources. Each office could experiment with different strategies, seeking what works on the local level. In fact, this would be a real boon to progress in learning how to cope with the new technological tools, because the range of experimentation would be widened automatically. We do not believe that the learning curve challenge can be overcome only by centralized research and development.

VII. Some Suggested Strategies

We have discussed the current situation with regard to QPF and indicated that in the near term, there is little reason to believe that the situation will change much. It is not our intent, however, to foster a defeatist attitude. There are some approaches which we think

may offer some improvement in service to users of QPF.

Although this paper does not provide a rigorous demonstration for it, we have made the case that mesoscale processes are the key to QPF. Mesoscale research continues to remain active and the new technologies are helping to keep this a vital part of meteorological science. In lieu of having mesoscale NWP models at the forecaster's disposal, physical (or conceptual, qualitative) models are all that is available. Such models do not provide a basis for prediction of accurate observed isohyets. Rather, they give a framework within which it becomes possible to anticipate the mesoscale evolutions so crucial to QPF. It seems to us that it would be a fruitless exercise to try to employ these qualitative models for the the purpose of producing isohyets. Instead, it might be a substantial improvement in service to QPF users if physical models can be used successfully (a) to refine estimates of when and where precipitation probabilities are enhanced or diminished, or (b) to suggest the likelihood (again, probabilistically) of precipitation reaching significant thresholds. There already exists ample evidence that forecasters can use qualitative models to improve upon objective guidance, when they have the conceptual models at their disposal.

There is an urgent need for local data processing capabilities, which is independent of the new data sources. Much of this need can be addressed immediately with microcomputer techology available at low cost "off the shelf". Having local data processing resources independent of the fragile communications system can help smooth the transition to more sophisticated systems. Moreover, this offers a chance for local creativity and experimentation without the immense capital outlays for complex new technological systems. We do not say that microcomputers will solve the QPF problem, but they can help define more clearly what the new systems must be able to do and how they can be used most effectively. For the time being, at the field office level, these requirements remain mysterious and ill-defined.

It is important to emphasize what are realistic expectations. Deciding that predicted isohyets are the ultimate goal serves little purpose, and leads to an attitude of despair, since there is no valid reason to think that such a goal is attainable in the near future. If one accepts the hypothesis that human intervention is worthwhile in producing QPF (or any other forecast product, for that matter), then forecasting services of the future must develop an effective "human-machine mix" which allows forecasters to be meteorologists. More interaction with users of QPF should take place, beginning with the recognition that accurate predicted isohyets are a dream, relegated to some distant future. This interaction can lead to the design of new QPF products which fill the void between our current output and the unattainable ideal. We do not pretend to know what those products must be, but we think assuming that answers can come *only* through centralized, objective approaches is likely to lead to "answers" which are less valuable than what is possible.

References

Belville, J, G.A. Johnson, and J.D. Ward, 1978: A flash flood aid -- The limited area QPF. *Preprints, 1st Conf. Flash Floods* (Los Angeles, CA), Amer. Meteor. Soc., 21-28.

Doswell, C.A. III, 1986: The human element in weather forecasting. *Preprints, 1st Workshop on Operational Meteorology* (Winnipeg, Man), Atmos. Env. Service and Can. Meteor. and Oceanogr. Soc., 1-25.

Doswell, C.A. III, and R.A. Maddox, 1986: The role of diagnosis in weather forecasting. *Preprints, 11th Conf. Weather Forecasting and Analysis* (Kansas City, MO), Amer. Meteor. Soc, in press.

Glahn, H.R., and D.A. Lowry, 1972: The use of Model Output Statistics (MOS) in objective weather forecasting. *J. Appl. Meteor.*, **11**, 1203-1211.

AN AUTOMATED QPF VERIFICATION PROGRAM WHICH PROVIDES BOTH REAL-TIME AND LONG-TERM STATISTICAL SCORES IN A USER-FRIENDLY ENVIRONMENT

Christopher D. Hill
National Weather Service Forecast Office
Boise, Idaho

and

Mark A. Mathewson
National Weather Service/SSD
Salt Lake City, Utah

1. INTRODUCTION

A true measure of the value of a quantitative precipitation forecast (QPF) is how well the receiving hydrologic model verifies. However, hydrologic models are often designed around known or perceived limitations in the meteorological input. As a result, models rarely make optimum use of exceptionally good QPF's. When a new QPF technique is introduced, the meteorologist needs to assess its performance. Knowledge of QPF improvements can also aid the hydrologist in the design of better hydrologic models through the incorporation of greater sensitivity to meteorological input. These requirements are reason enough to expend resources on QPF verification. Added impetus is provided by the fact that a properly designed verification program can also improve existing QPF techniques by pointing out individual forecaster or staff weaknesses. Experience has shown that to be effective, a verification program must require minimal effort by forecasters, provide rapid feedback to forecasters, and give long term statistics to researchers and managers.

Common to all of the above uses for QPF verification is the need to answer the basic questions:

1) How well are precipitation events detected?
2) How well are peak precipitation intensities detected?
3) What is the skill in forecasting precipitation amounts?

Unfortunately, these same questions regarding detection of precipitation, timing of peaks, and determining quantities also apply to observational networks. This is especially true in the western United States where the network is extremely sparse, and many river basins lack even a single observation point. The number of usable observations is reduced even further if periods shorter than twenty-four hours are to be verified. Thus the observational network often places considerable constraints on the forms the verification program can assume.

The remainder of this paper will discuss first how a useful verification program was developed for the very data sparse northwest United States. Second, it will be shown how the program has been automated and couched in a very user-friendly environment.

2. THE NORTHWEST UNITED STATES QPF PROGRAM

National Weather Service Forecast Offices (WSFO's) in Montana, Idaho, Washington and Oregon provide daily QPF's to the Northwest River Forecast Center (NWRFC) at Portland, Oregon, for input to hydrologic models. The area covered by these forecasts extends from the Continental Divide in Montana and Idaho, west to the Pacific Coast of Oregon and Washington. Most of this region is mountainous, and many river basins are characterized by significant variations in elevation. Reporting stations are almost all in valley locations, however, and, except for sites west of the Cascades, the large rainfall totals measured east of the Rocky Mountains are rarely reported. The mountains surrounding these reporting stations do receive heavy precipitation more frequently. Storm run-off is greatly complicated because some precipitation may be locked in snow fields. At other times, snowmelt may be the major source of run-off. As a result, QPF's prepared by the WSFO's consist of more than just forecasts of precipitation amounts. Figure 1 is an example of a QPF "package". The first portion of the "package" relays forecasts of precipitation totals for days 1, 2 and 3 in terms of "percent of a normal storm". For example, if a site has a 30-year normal annual rainfall total of 20 inches, the site would receive .2 inches of precipitation from a one percent storm. A five percent storm would produce one inch of precipitation. For day 1 and day 2, the forecast is also divided into six-hour amounts.

The second portion of the package consists of forecasts of the height of the freezing level for each six-hour period for day 1 and day 2. The last portion contains maximum and minimum temperature forecasts for days 1, 2 and 3. During the spring snowmelt season, the temperature forecasts are extended through days 4 and 5.

As discussed by Orwig and Peck (1982), the use of percent of normal storm in the QPF incorporates and simplifies: (1) the variation of rainfall patterns due to topographic effects, (2) representation of basin boundaries, (3) transmission of detailed forecasts, and (4) presentation of a meteorologically-consistent precipitation forecast package.

Also noted by the above authors is the importance of the temporal distribution of precipitation. Figure 2 illustrates the difference in the resulting hydrographs when one inch of rain falls in a 24-hour period versus a six-hour period. In the first case the streamflow rise would only cause minor inconvenience to local residents. The more intense rainfall would produce a flood of serious proportions. In a short study, Kuehl (1981) concluded that in the northwestern United States, one six-hour period in twenty-four hours usually receives 40 percent or more of the total precipitation. He also found that one of the six-hour periods usually receives 10 percent or less of the twenty-four hour total. As can be been from figure 2, these "peaks" and "lulls" in the precipitation intensity are of extreme importance to the hydrologic model.

3. OBSERVATION NETWORK LIMITATIONS

The network of operationally available weather observations dictates, to a large degree, the forms a verification program can assume. The northwest United States is very data sparse, especially if one is concerned with observation periods shorter than twenty-four hours. The complex terrain yields many river drainage basins, most of which lack even a single observation point. Even the data from basins that do have observations can produce erroneous pictures of precipitation events.

Figure 3 depicts some of the problems inherent in attempts to observe basin precipitation. In Figure 3a, the actual area of precipitation during the verification period encompasses 50 percent of the basin with an average point accumulation of .12 inches. Thus, the average basin catch was .06 inches. Due to attenuation, terrain blocking, etc., weather radar indicated thirty percent coverage at .10 inches. Radar observations then yield a basin average of .03 inches, one-half the true basin catch. The surface observation network indicated no precipitation fell on the basin during the verification period.

```
BOIQPSBOI
TTAA00 KBOI 101705
BOI17
QPF
YMDZ 85100112
A FPA0ZM

PTHI D0.5/2/2/3/3/D1.0/5/4/1/0/D0.0
SOG  D0.5/2/2/3/3/D1.0/4/4/2/0/D0.0
S80  D0.5/2/2/3/3/D1.0/4/4/2/0/D0.0
MYL  D0.5/0/3/3/4/D0.5/4/3/3/0/D0.0
LWS  D0.5/2/2/3/3/D1.0/4/4/2/0/D0.0
BOI  D0.0/0/0/0/0/D1.0/3/4/3/0/D0.0
SMN  D0.0/0/0/0/0/D0.0/0/0/0/0/D0.0
TUF  D0.0/0/0/0/0/D0.0/0/0/0/0/D0.0
PIH  D0.0/0/0/0/0/D0.0/0/0/0/0/D0.0

END QPF


HZIQ
YMDZ 85100112
E HZA0ZMD
BOI  09.4/09.2/07.9/07.3/06.0/06.5/06.4/06.4/
LWS  06.7/07.1/06.6/06.5/06.4/05.9/05.9/06.0/

END HZIQ

TFXN
YMDZ 85100112
E TAAIXM/TAAINM

S80 52/30/49/27/50/24
SMN 51/28/51/27/46/25
BOI 57/36/37/35/54/32
TUF 56/33/58/25/53/30
PIH 54/33/54/27/53/20


END TFXN

END USFO BOI
```

Figure 1: Example of QPF product issued daily by NWS WSFO's in the northwest U.S.

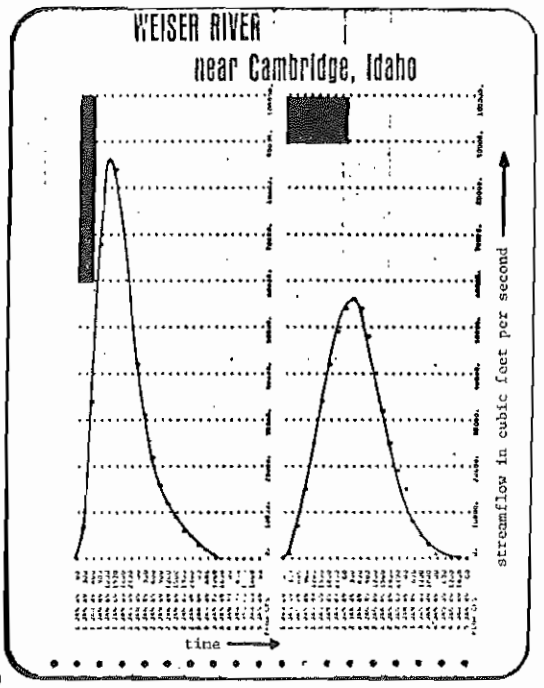

Figure 2: Resulting hydrographs from rainfall of different intensities. The left-hand hydrograph resulted from one inch of rain in six hours. The right-hand hydrograph from one inch in 24 hours (from Orwig and Peck, 1982).

In Figure 3b, actual rainfall was .10 inches over ten percent of the basin for an average basin catch of .01 inches. Radar detected no precipitation in the basin. Surface observations measured .10 inches at one site and no precipitation at the other. If both sites carry equal weight in the basin model, then the observations indicate a basin average of .05 inches, five times the actual amount received.

The cases presented in Figure 3 are somewhat extreme. However, they do point out some of the problems associated with attempts to observe basin precipitation. Radar is, of course, a better determination tool in many respects, since it samples a much larger area than an eight-inch raingage or two. Also, manually digitized radar (MDR) values lend themselves to automated objective accounting methods. Weather radar coverage in the western United States is very limited, however, and a MDR program is not available to most areas. Thus, the surface observation network is sparse, and in many instances, not representative of basin catch; but it must serve as the basis for an objective verification program. To minimize the chances of drawing erroneous conclusions, the limitations of the network must be acknowledged. For example, a synoptic scale storm will generally produce precipitation over an entire basin. The surface observations will be representative of the spatial and temporal nature of the storm. However, precipitation amounts will often vary considerably in different portions of such storms. Thus the network will be the least representative with respect to precipitation amounts. For the spotty convective-type precipitation episodes which frequent the western United States during the spring and summer, the surface observation network will, at times, be unrepresentative in all respects (e.g., amounts and the spatial and temporal characteristics of the precipitation episode).

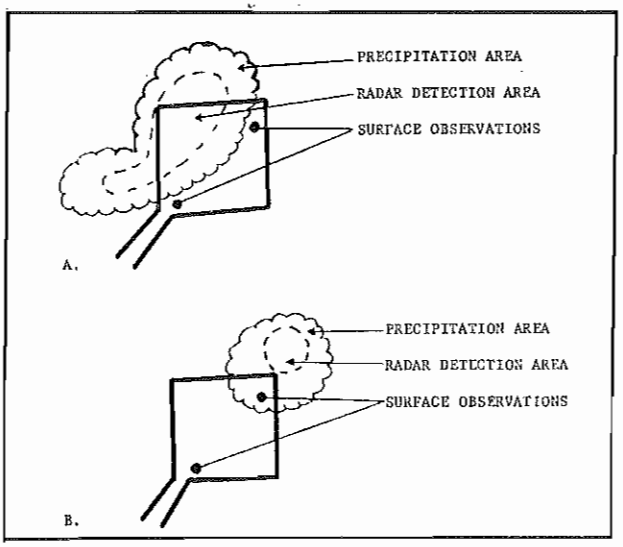

FIGURE 3: Examples of problems in observing basin catch.

4. VERIFICATION PROGRAM DESIGN

The above discussion suggests that there is little hope for a verification system which produces useful information since we cannot even observe the precipitation accurately! However, if QPF's are to improve, and if hydrologists are to capitalize on these improvements; present skill levels must be established to serve as a baseline.

Utilization of a number of statistical scores to profile skills in the area of:

1. Detecting precipitation events
2. Timing peak rainfall periods
3. Forecasting precipitation amounts
4. Detecting major temperature changes

can overcome some of the known observational network limitations and provide the forecaster and hydrologist with useful information. The key is to make use of more than just a single score to obtain such "performance profiles". This profiling is important because as pointed out by Woodcock (1976), compressing data into a single verification score causes a loss of information. To gain insight into forecast skills, standard statistical scores are easily computed from a two by two contingency table:

TABLE 1

		FORECAST Yes	FORECAST No
observed	Yes	a	b
	No	c	d

These standard scores include:

Probability of detection
(POD) = a/(a+b)

Threat Score
(TS) = a/(a+b+c)

False Alarm Ratio
(FAR) = 1 - (a/(a+c))

Bias
(BIAS)= (a+c)/(a+b)

Percent Correct
(PC) = (a+d)/(a+b+c+d)

Frequency
(S) = (a+b)/(a+b+c+d)

Table 2 can be used to illustrate performance profiling. The data is for two different techniques used for forecasting measurable precipitation events during a twelve-hour period at ten forecast points. The scores are based on a total of 1400 forecasts by Technique A and 1050 forecasts by Technique B.

Table 2

	S	PC	BIAS	FAR	POD	TS
A	.15	86	.72	.46	.39	.30
B	.20	86	.95	.32	.65	.49

From Table 2 note that both techniques experienced the same number of rainfall events and both scored the same percent correct (also referred to as the ratio test) of 86. Technique B displayed practically no bias while A displayed a somewhat dry bias of .72. This, plus the percent correct and frequency of rainfall events suggests Technique A may not be forecasting rainfall often enough. However, the false alarm ratio is quite high, and the threat score low. At the same time the probability of detection is not very good. Thus the profile of Technique A indicates the method's major shortcoming is not that it simply does not forecast rain events, but rather that it does a poor job of discriminating between rain/no rain events.

The above scores can be used in a straight forward manner to profile the ability to detect precipitation occurrence. To use these scores to gain insight into skill at forecasting peak rainfall periods, the definition of a "peak" must be established. Drawing on the work of Kuehl cited earlier, a "climatological peak" can be defined for the northwest United States as a six-hour period in which the precipitation total is equal to or greater than the sum of the next two highest period amounts, e.g., at least 40 percent of the twenty-four hour total falls in one six-hour period. If no six-hour period meets this criteria, the precipitation curve (observed or forecast) is flat by definition. With the definition of "peak", a yes/no contingency table can be used to profile temporal skill in QPF's.

As discussed earlier, limited point observations can sometimes be very unrepresentative of actual basin precipitation, especially in the mountainous western United States. Thus verifying actual amounts runs a significant risk of drawing erroneous conclusions. Comparisons of forecast to measured amounts categorically is one means of minimizing the risk of extracting false information from the observations. In addition, utilization of the same categories as NWS MOS guidance provides the opportunity to compare forecaster to model performance.

5. AN AUTOMATED SYSTEM ... PHASE I

Automation of verification of QPF's prepared for the northwest United States has been a joint effort between the forecast offices at Boise, Portland, Seattle and Great Falls, the NWRFC and the Scientific Services Division of the NWS Western Region Headquarters.

Principal goals are to develop a system which provides rapid feedback to forecasters on a daily basis, long-term statistics for research and automatic quality control of data, all in a very flexible and easy to use interactive format. The initial phase of this project has been completed and is operational on a multi-tasking computer system at WSFO Boise.

QPF packages as illustrated in Figure 1 are transmitted on the AFOS network to the NWRFC daily by each of the four WSFO's. These QPF's are also received by the Boise AFOS and automatically transferred to the Boise applications computer. There, the QPF decoder automatically processes each and attempts to decode the available data. If a data decode error is encountered, the program composes a message which describes the problem. No data is stored in the data file unless the product is successfully decoded.

The decoder always sends a message back to the QPF originator (via AFOS), indicating that the product was either successfully decoded or that an error was detected as illustrated in Figure 4.

```
PDXADAPDX
TTAA00 KBOI 041556
** QPS VERIFICATION MESSAGE **      SYSID=NWS_BOI_CP
MESSAGE RECEIVED AT: NOV0485_1555
THE AOS CENTRAL PROCESSOR WAS UNABLE TO PROCESS
YOUR QPS FILE DUE TO THE FOLLOWING REASON:
        DIFFERENT DATES IN SAME PRODUCT
SITE ID = SO6
THE ERROR OCCURRED IN THIS LINE:
YMDZ 85110412
PLEASE CORRECT AND RE-TRANSMIT MESSAGE
```

Figure 4. Error message automatically generated by Boise applications computer and sent to appropriate WSFO.

The program currently verifies forecasts for four locations in each WSFO's forecast area. Observational data from these sixteen sites is automatically collected by computers at the NWRFC and formatted into a bulletin. The bulletin is transmitted on the AFOS network and automatically transferred to the Boise applications computer where it is checked for errors. If a data decode error is detected, a message similar to Figure 5 is composed. All decoded data is stored in the data file except for the site containing the error.

```
PDXADAPDX
TTAA00 KBOI 041556
** RRM VERIFICATION MESSAGE **      SYSID=NWS_BOI_CP
MESSAGE RECEIVED AT: NOV0485_1555
THE AOS CENTRAL PROCESSOR WAS UNABLE TO PROCESS
YOUR RRM FILE DUE TO THE FOLLOWING REASON:
        6HRLY PCPN'S DO NOT ADD TO 24H
SITE ID = SO6
THE ERROR OCCURRED IN THIS LINE:
SO6 /.12/.03/.01/.12/.30/56
PLEASE CORRECT AND RE-TRANSMIT MESSAGE
```

Figure 5. Error message automatically generated by Boise applications computer and sent to NWRFC.

The decoder always sends a message back to NWRFC (via the AFOS network). The message indicates that the product was either successfully decoded or that an error was detected and where the error occurred.

Once the daily QPF's and daily observation bulletins are accepted by the Boise applications computer, the information is archived for later use. The archived data is easily accessed from a remote terminal with a modem.

When the user logs onto the Boise applications computer with his assigned username and password, the QPF verification program is automatically executed. The first option given the user is illustrated in Figure 6. The user can specify the period (a single day, a month, a season, etc.) for which he desires statistics. The user can also specify that the verification be performed on individual or all forecast offices, verification points and individual or collective forecasters.

```
***** QPF VERIFICATION STATISTICS *****
CURRENT DATE/TIME: NOV  4 85  22:23:25   SYSTEM ID: NWS_WRH_CP
..... PREPARE TO SELECT PARAMETERS .....

*** QPF VERIFICATION PROGRAM - PARAMETERS ***
01. START DATE:          OCT 5
02. STOP DATE:           NOV 4
03. SEASON:              8586
04. SELECTED WSFO:       ALL
05. SELECTED SITE:       ALL
06. PCPN DISPLAY MODE:   ALL DAYS
07. FORECASTER NUMBER:    0

VALUE TO CHANGE (0=EXIT,1-7) ? _____
```

Figure 6. MENU to prompt user to select data set upon which verification will be run.

If the data requested does not exist, the message **DATA NOT AVAILABLE** will be displayed. If a second user is logged onto the system and is accessing the same data, the message **WAITING FOR FILE ACCESS** will be displayed and the program will wait until the data becomes available. Also in the "set change parameters" menu, the user specifies whether he wishes statistics for 24-hour or 6-hour periods via the Precipitation Display Mode.

Once the user has specified the who, where and the when he wants verification statistics for, the "Main Menu" is displayed for him. As can be seen from Figure 7, Main Menu options 3 through 13 give the user the choice of what verification statistics will be provided to him.

Menu Option 2 allows for user quality control of the raw data. The user can specify whether the forecast or observed data for a day is displayed. He can then correct erroneous entries or leave the data unchanged and return to the main menu. Other programs, e.g., the AFOS Era Verification System, have shown that the ability to easily quality control the data in an automated system is a very necessary feature if a complete database is desired.

```
****** QPF VERIFICATION STATISTICS *****
CURRENT DATE/TIME: NOV  4 85  22:26:49    SYSTEM ID: NWS_WRH_
00. Exit Program
01. Set/Change Parameters
02. Examine/Change Raw Data
03. Temperature absolute error
04. Temperature average error
05. Temperature change weighted error
06. Precipitation Contingency Table - Catagories
07. Precipitation Contingency Table - Yes/No
08. Precipitation Threat Scores
09. Precipitation Frequency
10. Precipitation probability of detection
11. Precipitation false alarm ratio
12. Precipitation bias
13. Precipitation percent correct
14. Send mail to operator
15. Receive Mail

Enter Choice (0-15) ? _____
```

Figure 7. Verification program MAIN MENU. User selects scores that will be displayed.

Menu options 3, 4, and 5 provide the user with verification scores on the temperature forecasts included in the QPF package. The actual output may be for all forecasters and a single site, or a single forecaster at all sites, etc., depending on what the user specified in Menu Option 1.

```
*** PRECIPITATION CONTINGENCY TABLE ***
START=FEB 1  STOP=JUN30  SEASON=8485  WSFO=BOI SITE=ALL  FCSTR#=
SITE=SO6 DAY=1
                FORECAST-------)
   OBSERVED      0     1     10    26    51    101   250
  ----------|-----|-----|-----|-----|-----|-----|-----|
      0     |  64 |  4  |  2  |  0  |  0  |  0  |  0  |
  ----------|-----|-----|-----|-----|-----|-----|-----|
      1     |  7  |  8  |  5  |  3  |  0  |  0  |  0  |
  ----------|-----|-----|-----|-----|-----|-----|-----|
     10     |  6  |  4  |  6  |  1  |  0  |  0  |  0  |
  ----------|-----|-----|-----|-----|-----|-----|-----|
     26     |  1  |  0  |  2  |  1  |  0  |  0  |  0  |
  ----------|-----|-----|-----|-----|-----|-----|-----|
     51     |  1  |  0  |  0  |  2  |  0  |  0  |  0  |
  ----------|-----|-----|-----|-----|-----|-----|-----|
    101     |  0  |  0  |  1  |  0  |  1  |  0  |  0  |
  ----------|-----|-----|-----|-----|-----|-----|-----|
    250     |  0  |  0  |  0  |  0  |  0  |  0  |  0  |
  ----------|-----|-----|-----|-----|-----|-----|-----|
```

Figure 8. Precipitation category table built and displayed by verification program based on data set chosen via the menu in fig. 6.

Menu Options 6 and 7 provide the user with raw contingency tables. Figure 8 is an example of the precipitation category table which is compiled by the program under option 6. Figure 9 is an example of yes/no contingency tables for the detection of measurable precipitation events upon which statistics provided by menu options 8 through 13 are computed.

```
*** PRECIPITATION CONTINGENCY TABLE (YES/NO)***
START=FEB 1  STOP=JUN30  SEASON=8485  WSFO=BOI SITE=ALL  FCSTHR=  0
SITE=SOS DAY=1
                    FORECAST-------->
        OBSERVED        0     1
          ----------|-----|-----|
             0      |  84 |   8 |
          ----------|-----|-----|
             1      |  15 |  34 |
          ----------|-----|-----|


--- hit return to continue --- or # to abort
SITE=SOS DAY=2
                    FORECAST-------->
        OBSERVED        0     1
          ----------|-----|-----|
             0      |  86 |  10 |
          ----------|-----|-----|
             1      |  20 |  31 |
          ----------|-----|-----|


--- hit return to continue --- or # to abort
SITE=SOS DAY=3
                    FORECAST-------->
        OBSERVED        0     1
          ----------|-----|-----|
             0      |  48 |  20 |
          ----------|-----|-----|
             1      |  26 |  26 |
          ----------|-----|-----|
```

Figure 9. YES/NO contingency tables for the detection of measureable precipitation events. The numeral 1 indicates measureable amounts.

Figure 10 is a composite of the outputs from user chosen menu options 8 through 13. Note that the parameters specified in menu option 1 are also displayed for the user. In Figure 10, the parameters were set for daily scores. Figure 11 is an example of the output format obtained when the precipitation display mode is set for day 1 via main menu option 1. In this mode the scores are computed for each of the 6-hour periods in the day selected.

```
  ** PRECIPITATION THREAT SCORES **
START=FEB 1  STOP=JUN30  SEASON=8485  WSFO=BOI SITE=ALL  FCSTHR=  0
 SITE    DAY1          DAY2          DAY3
       N  ERROR     N  ERROR     N  ERROR
 SOS 119   .62   117   .51   119   .35
 MYL 117   .23   115   .26   117   .21
 PIH 117   .33   116   .17   117   .31
 BOI 120   .43   118   .28   120   .27

  ** PRECIPITATION FREQUENCY SCORES **
START=FEB 1  STOP=JUN30  SEASON=8485  WSFO=BOI SITE=ALL  FCSTHR=  0
 SITE    DAY1          DAY2          DAY3
       N  ERROR     N  ERROR     N  ERROR
 SOS 119  41.2   117  43.6   119  42.9
 MYL 117  12.9   115  15.7   117  14.5
 PIH 117  31.6   115  30.4   117  29.9
 BOI 120  22.5   118  22.9   120  21.7

  ** PRECIPITATION PROB OF DETECTION **
START=FEB 1  STOP=JUN30  SEASON=8485  WSFO=BOI SITE=ALL  FCSTHR=  0
 SITE    DAY1          DAY2          DAY3
       N  ERROR     N  ERROR     N  ERROR
 SOS 119  69.4   117  60.8   119  49.0
 MYL 117  60.0   115  55.6   117  52.9
 PIH 117  41.2   115  22.9   117  42.9
 BOI 120  59.3   118  49.7   120  46.2

  ** PRECIPITATION FALSE ALARM RATIO **
START=FEB 1  STOP=JUN30  SEASON=8485  WSFO=BOI SITE=ALL  FCSTHR=  0
 SITE    DAY1          DAY2          DAY3
       N  ERROR     N  ERROR     N  ERROR
 SOS 119   .15   117   .24   119   .44
 MYL 117   .74   115   .68   117   .74
 PIH 117   .41   116   .68   117   .48
 BOI 120   .30   118   .64   120   .60

  ** PRECIPITATION BIAS **
START=FEB 1  STOP=JUN30  SEASON=8485  WSFO=BOI SITE=ALL  FCSTHR=  0
 SITE    DAY1          DAY2          DAY3
       N  ERROR     N  ERROR     N  ERROR
 SOS 119   .82   117   .80   119   .68
 MYL 117  2.27   115  1.72   117  2.00
 PIH 117   .73   115   .54   117   .83
 BOI 120   .98   118   .89   120  1.15

  ** PRECIPITATION PERCENT CORRECT **
START=FEB 1  STOP=JUN30  SEASON=8485  WSFO=BOI SITE=ALL  FCSTHR=  0
 SITE    DAY1          DAY2          DAY3
       N  ERROR     N  ERROR     N  ERROR
 SOS 119  82.4   117  74.4   119  61.3
 MYL 117  73.5   115  74.8   117  71.8
 PIH 117  72.6   126  67.0   117  70.9
 BOI 120  82.5   118  75.4   120  73.3
```

Figure 10. Composite of output to user when MAIN MENU options 8 through 13 are chosen. In this instance the precipitation display mode specified by the user was for daily scores.

```
  ** PRECIPITATION THREAT SCORES **
START=OCT19  STOP=NOV18  SEASON=8586  WSFO=BOI SITE=ALL  FCSTHR=  0
 SITE    DAY1          PD 1          PD 2          PD 3          PD 4
       N  ERROR     N  ERROR     N  ERROR     N  ERROR     N  ERROR
 SOS  24   .88    13   .69    13   .67    13   .67    12   .63
 MYL  24   .40    23   .30    23   .36    23   .30    23   .22
 PIH  24   .83    23   .40    23   .29    23   .60    23   .33
 BOI  24   .75    23   .60    23   .38    23   .60    23   .25

  ** PRECIPITATION FREQUENCY SCORES **
START=OCT19  STOP=NOV18  SEASON=8586  WSFO=BOI SITE=ALL  FCSTHR=  0
 SITE    DAY1          PD 1          PD 2          PD 3          PD 4
       N  ERROR     N  ERROR     N  ERROR     N  ERROR     N  ERROR
 SOS  24  50.3    13  65.8    13  46.2    13  83.8    12  41.7
 MYL  24  47.8    23  21.7    23  26.1    23  21.7    23  21.7
 PIH  24  30.4    23  13.0    23  21.7    23  26.1    23  17.4
 BOI  24  34.8    23  13.0    23  21.7    23  17.4    23   8.7

  ** PRECIPITATION PROB OF DETECTION **
START=OCT19  STOP=NOV18  SEASON=8586  WSFO=BOI SITE=ALL  FCSTHR=  0
 SITE    DAY1          PD 1          PD 2          PD 3          PD 4
       N  ERROR     N  ERROR     N  ERROR     N  ERROR     N  ERROR
 SOS  24 100.0    13 100.0    13 100.0    13  65.7    12 100.0
 MYL  24  64.6    23  60.0    23  66.7    23  83.0    23  40.0
 PIH  24  71.4    23  66.7    23  40.0    23  66.7    23  50.0
 BOI  24  76.0    23 100.0    23  60.0    23  76.0    23  50.0

  ** PRECIPITATION BIAS **
START=OCT19  STOP=NOV18  SEASON=8586  WSFO=BOI SITE=ALL  FCSTHR=  0
 SITE    DAY1          PD 1          PD 2          PD 3          PD 4
       N  ERROR     N  ERROR     N  ERROR     N  ERROR     N  ERROR
 SOS  24  1.14    13  1.14    13  1.60    13  1.14    12  1.60
 MYL  24   .91    23  1.60    23  1.60    23  1.60    23  1.20
 PIH  24   .68    23  1.33    23   .80    23  1.00    23  1.00
 BOI  24   .75    23  2.00    23  1.20    23  1.36    23  1.60

  ** PRECIPITATION FALSE ALARM RATIO **
START=OCT19  STOP=NOV18  SEASON=8586  WSFO=BOI SITE=ALL  FCSTHR=  0
 SITE    DAY1          PD 1          PD 2          PD 3          PD 4
       N  ERROR     N  ERROR     N  ERROR     N  ERROR     N  ERROR
 SOS  24   .13    13   .13    13   .33    13   .25    12   .38
 MYL  24   .40    23   .63    23   .56    23   .63    23   .67
 PIH  24   .17    23   .60    23   .50    23   .33    23   .60
 BOI  24   .00    23   .50    23   .60    23   .40    23   .67

  ** PRECIPITATION PERCENT CORRECT **
START=OCT19  STOP=NOV18  SEASON=8586  WSFO=BOI SITE=ALL  FCSTHR=  0
 SITE    DAY1          PD 1          PD 2          PD 3          PD 4
       N  ERROR     N  ERROR     N  ERROR     N  ERROR     N  ERROR
 SOS  24  91.7    13  92.3    13  76.9    13  76.9    12  75.0
 MYL  24  60.9    23  69.6    23  69.6    23  60.8    23  69.6
 PIH  24  87.0    23  87.0    23  78.3    23  82.6    23  82.6
 BOI  24  91.3    23  87.0    23  70.3    23  87.0    23  87.0
```

Figure 11. Same as fig. 10 except in this case the user specified that scores be output for 6-hour periods instead of 24-hour periods.

6. SUMMARY

The terrain of the Northwest United States necessitates Quantitative Precipitation Forecast guidance which consists of surface temperatures and freezing level forecasts as well as forecasts of rainfall amounts. The lack of a dense reporting network places great constraints on the design of a verification program for assessing these forecast packages.

It has been found that utilization of a battery of statistical scores overcomes some of the observational network deficiencies by producing performance profiles which yield useful information about spatial, temporal and quantitative precipitation forecasting skills. This encouragement has led to the development of an automated QPF verification system for the northwest states. From the onset this system is being designed to be extremely user-friendly for ease of use by forecasters and researchers. A series of menus leads the user through the program and also helps the user make optimum use of the program's flexibility.

The initial phase of this program has been completed and runs on an applications computer at WSFO Boise. The system automatically collects forecast and observational data. The program provides verification scores on temperature forecasts and provides statistics for profiling the skill at forecasting the spatial characteristics of precipitation events for both 6-hour and 24-hour periods. The next phase of the program will profile skill at forecasting peaks in the rainfall curve.

REFERENCES

Kuehl, Donald W. (1981): Climatology of 24-Hour Distribution of QPF. Unpublished Weather Service Manuscript.

Orwig, C.E. and Peck, P.A. (1982): Use or Misuse of QPF. AMS 9th Conference Weather Forecasting and Analysis, Seattle, WA PREPRINTS.

Woodcock, F. (1976): The Evaluation of Yes/No Forecasts for Scientific and Administrative Purposes. Mon. Wea. Rev. 104, 1209-1214.

A CLOSER LOOK AT THE NESTED GRID MODEL QPF

Frank C. Brody

National Meteorological Center
Camp Springs, Maryland

1. INTRODUCTION

The National Weather Service recently implemented the Nested Grid Model (NGM) as part of the new Regional Analysis and Forecast System (Hoke and Phillips, 1985). The NGM Quantitative Precipitation Forecast (QPF) has occasionally displayed a remarkable consistency from one model run to the next on the placement, shape, and maximum amount of precipitation forecast during a particular 12-hour period. The associated vertical velocity forecasts on these occasions were also very consistent. This was especially true during the late winter and early spring of 1985. While usually not verifying exactly, the NGM runs which displayed this QPF consistency were normally much better than the corresponding LFM QPFs. In some cases, the NGM mostly "missed" the observed precipitation area; yet it could still be considered a superior forecast since the NGM at least suggested big rainfall amounts fairly close to the observed area, while the LFM did not. During the summer, the NGM vertical velocity forecasts occasionally showed the same type of consistency as the winter QPFs did. This proved to be quite helpful in forecasting areas of convective development.

2. EXAMPLES

Table 1 and Figures 1 through 4 illustrate some of the more dramatic cases of this NGM QPF consistency.

In Figure 1, the NGM forecasts were very consistent with both the area of measurable ($\geq$ .01 inch) precipitation and the maximum precipitation amount for the 12-hour period ending 12Z February 20, 1985. Comparable LFM runs were much less consistent with the measurable and maximum precipitation areas. The maximum observed precipitation for this period was 0.97 inch at Columbia, South Carolina. Although the NGM QPFs were somewhat deficient with this maximum amount, they were still clearly superior to the LFM runs leading up to this event.

Figure 2 shows that the NGM forecasts were remarkably consistent with the location, shape, and maximum amount of precipitation forecast for the 12-hour period ending 12Z February 27, 1985. LFM QPFs were neither as consistent nor as accurate with the maximum amounts. Although the NGM forecasts were centered a bit too far northeast and were slightly overdone, they still provided much better QPF guidance than the LFM, especially for southeast Texas.

In Figure 3, the LFM actually did "better" than the NGM at 48-hours, by virtue of forecasting at least some measurable precipitation in the correct area of the Gulf Coast region. By 36- and 24-hours, though, the NGM was far more consistent and successful than the LFM in forecasting heavy rains across northern Florida, southern Alabama, and southern Georgia.

Figure 4 shows a summertime case where the NGM vertical velocity forecasts were more consistent and accurate than the LFM. Successive NGM vertical velocity forecasts were emphatic that a band of significant upward motion would occur across Kansas into southwest Iowa at the valid time of 00Z August 10, 1985. Corresponding LFM forecasts were much less specific. The verifying radar summary for 0035Z August 10 shows a narrow band of strong thunderstorms from the Texas panhandle northeast across Kansas into southwest Iowa. This matches the axis of the NGM vertical velocity forecasts quite well.

3. SYNOPTIC CONDITIONS

An attempt was made to relate synoptic conditions to this pattern of consistent NGM QPFs. A comparison of surface analyses revealed no clear-cut pattern common to the cases listed. However, 500mb patterns did show some similiarities. Each case occurred in response to the approach of a weak to moderate short wave trough and associated PVA. All but one case occurred in the PVA region south or southeast of the track of the vorticity maximum. This is a favored region for convection, given the existence of adequate moisture and instability. Since all the cases listed in Table 1 involved convective rainfall to some extent, the NGM apparently reacted more forcefully than the LFM to the convective rainfall potential in these situations.

4. DISCUSSION

The cases presented show that when the NGM QPF is very consistent from one model run to the next, it is likely to be superior to the LFM QPF. However, the NGM rarely displayed this consistency characteristic from late April through September 1985. A characteristic the NGM did show during the warm season was a tendency to be overly specific with the convective QPF, often with poor results, especially when compared to the LFM QPF. The NGM vertical velocity forecasts were often more useful in summer than the NGM QPFs, as demonstrated in Figure 4.

Despite the apparent seasonal limitation, there seems to be enough evidence to this NGM QPF characteristic to warrant close attention by operational forecasters. In practice, this means emphasizing the comparison of previous NGM runs to the current one, in addition to comparing the latest versions of all the models. This characteristic can be useful in improving manually-produced QPFs as well as general rainfall forecasts, including probability of precipitation forecasts. In extreme cases, this NGM characteristic may help in the decision making process leading up to the issuance of an excessive rainfall forecast or flash flood watch.

5. SUMMARY

The Nested Grid Model QPF has occasionally displayed remarkable consistency on the placement, shape, and maximum amount of precipitation forecast during a particular 12-hour period. NGM vertical velocity forecasts also showed this consistency. This was especially true during the late winter and early spring of 1985. The NGM was almost always superior to the LFM in these situations. All cases involved convective rainfall to some extent, and all were related to the approach of a weak to moderate short wave trough at 500mb. Although this may prove to be a seasonally limited model characteristic, awareness of it can be quite useful to operational forecasters.

6. ACKNOWLEDGEMENTS

The author would like to thank the following for their helpful suggestions: Ron McPherson, Wes Junker, Brian Korty, John Sokich and Dennis Haller. Special thanks to Donna Thomas for skillful preparation of the manuscript.

7. REFERENCES

Hoke, James E., 1985: The Regional Analysis and Forecast System (RAFS). National Weather Service Technical Procedures Bulletin, Series No. 345.

Phillips, Norman A., 1985: Pre-Implementation Results from the Regional Analysis and Forecast Systems (RAFS). National Weather Service Technical Procedures Bulletin, Series No. 350.

TABLE 1

COMPARISON OF NGM AND LFM QPFS AND OBSERVED PRECIPITATION

ALL PRECIPITATION VALUES IN INCHES

12 HOUR PERIOD ENDING	MAX NGM QPF	MAX LFM QPF	OBSERVED 12 HR PCPN
12Z 2/20/85	48 HR .20 36 HR .25 24 HR .34	48 HR 0 36 HR .14 24 HR .07	.20 TO 1.0 NC AND SC
12Z 2/27/85	48 HR 1.25 36 HR 1.60 24 HR 1.27	48 HR .06 36 HR 0 24 HR .22	.20 TO 1.0 SERN TX
12Z 3/1/85	48 HR .50 36 HR 1.60 24 HR 1.10	48 HR .43 36 HR .23 24 HR .35	.50 TO 1.5 SERN TX AND SRN LA
12Z 3/14/85	48 HR 1.15 36 HR 1.03 24 HR 0.56	48 HR .50 36 HR .50 24 HR .30	.50 TO 3.0 EAST CNTRL TX
00Z 3/15/85	48 HR .60 36 HR .87 24 HR .94	48 HR .08 36 HR .49 24 HR .48	1.0 TO 4.0 SERN TX
00Z 3/17/85	48 HR .01 36 HR 1.88 24 HR 1.17	48 HR .19 36 HR .38 24 HR .30	.80 TO 2.0 SWRN GA/FL PNDL/ SERN LA
12Z 4/10/85	48 HR .17 36 HR .19 24 HR .56	48 HR .07 36 HR 0 24 HR .08	.20 TO .85 CNTRL KS TO SWRN MO
00Z 4/16/85	48 HR 2.22 36 HR 1.40 24 HR 2.80	48 HR .05 36 HR .02 24 HR .50	.40 TO 1.2 SRN FL

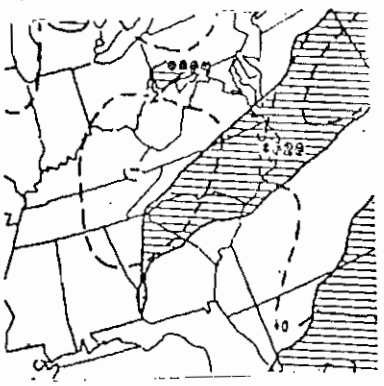

48 HR NGM QPF

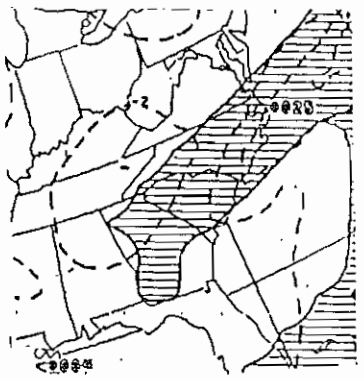

36 HR NGM QPF

24 HR NGM QPF

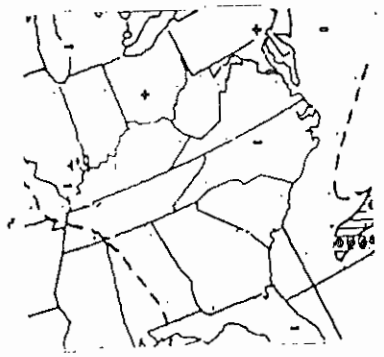

48 HR LFM QPF

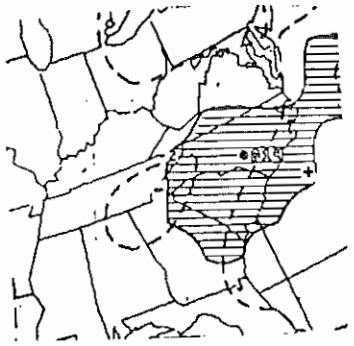

36 HR LFM QPF

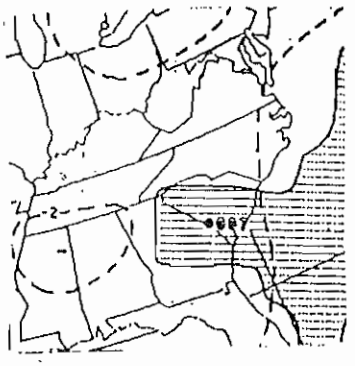

24 HR LFM QPF

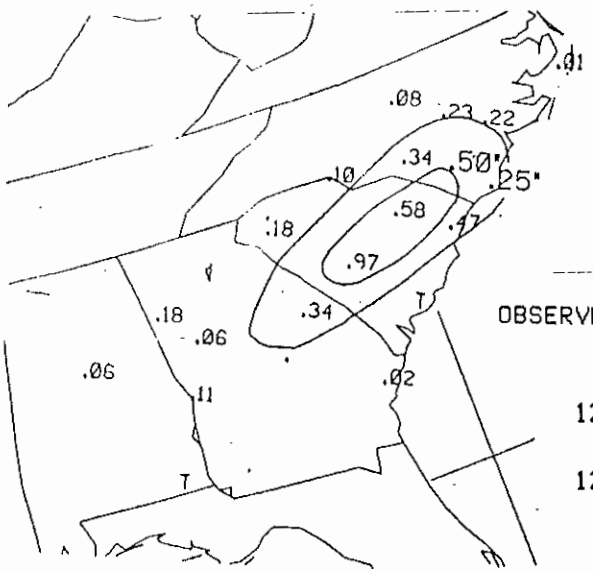

OBSERVED PRECIPITATION (INCHES)

12 HOURS ENDING

12Z FEB 20, 1985

FIGURE 1. NGM VS. LFM QPFS FOR 12 HOUR PERIOD ENDING 12Z FEB. 20 1985 AND OBSERVED PRECIPITATION FOR SAME 12 HOUR PERIOD

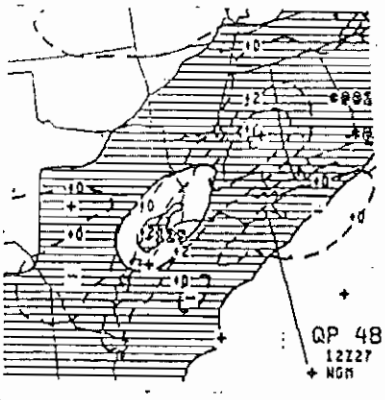

48 HR NGM QPF

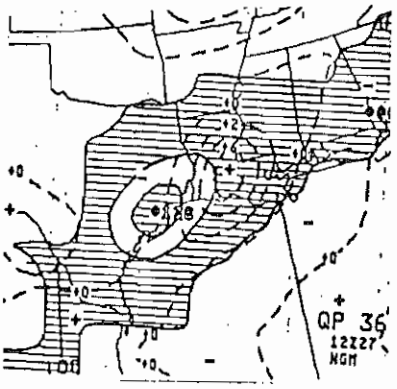

36 HR NGM QPF

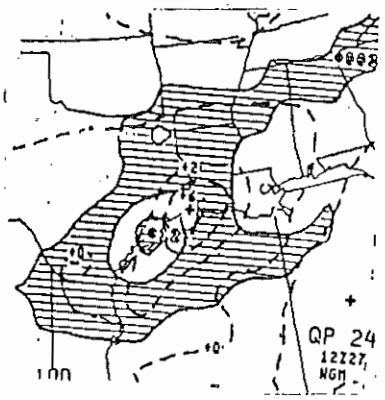

24 HR NGM QPF

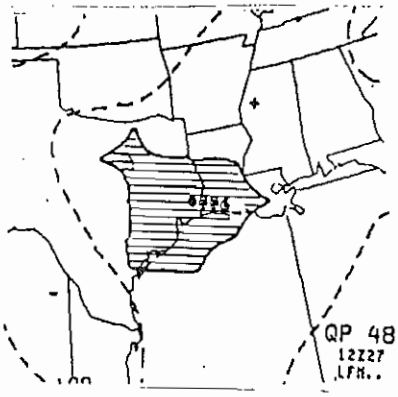

48 HR LFM QPF

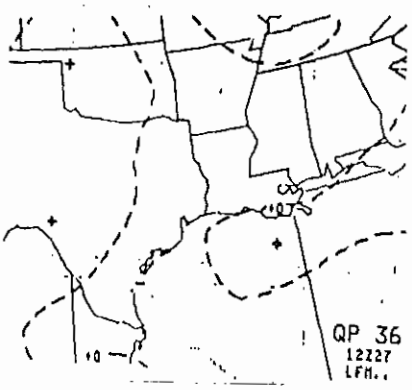

36 HR LFM QPF

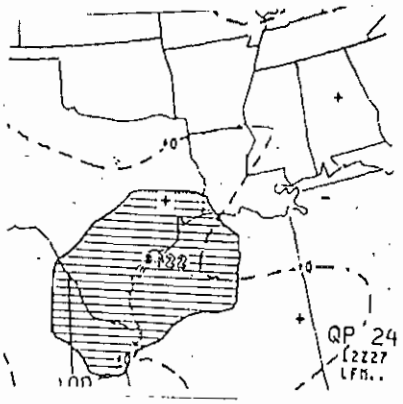

24 HR LFM QPF

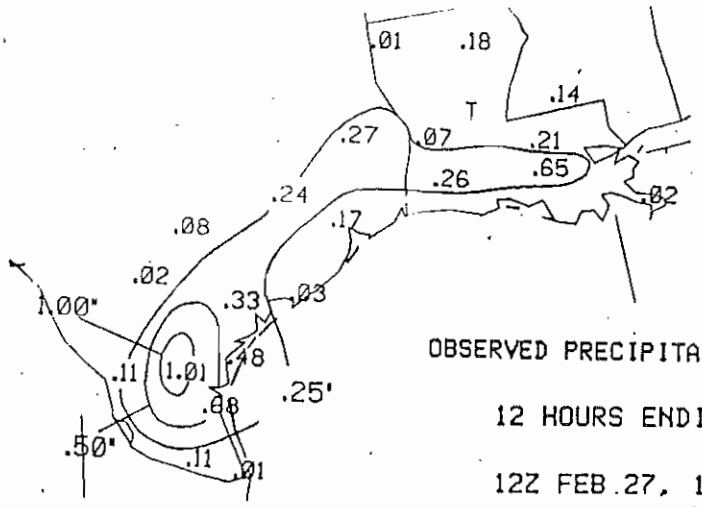

FIGURE 2. NGM VS. LFM QPFS FOR 12 HOUR PERIOD ENDING 12Z FEB. 27 1985 AND OBSERVED PRECIPITATION FOR SAME 12 HOUR PERIOD

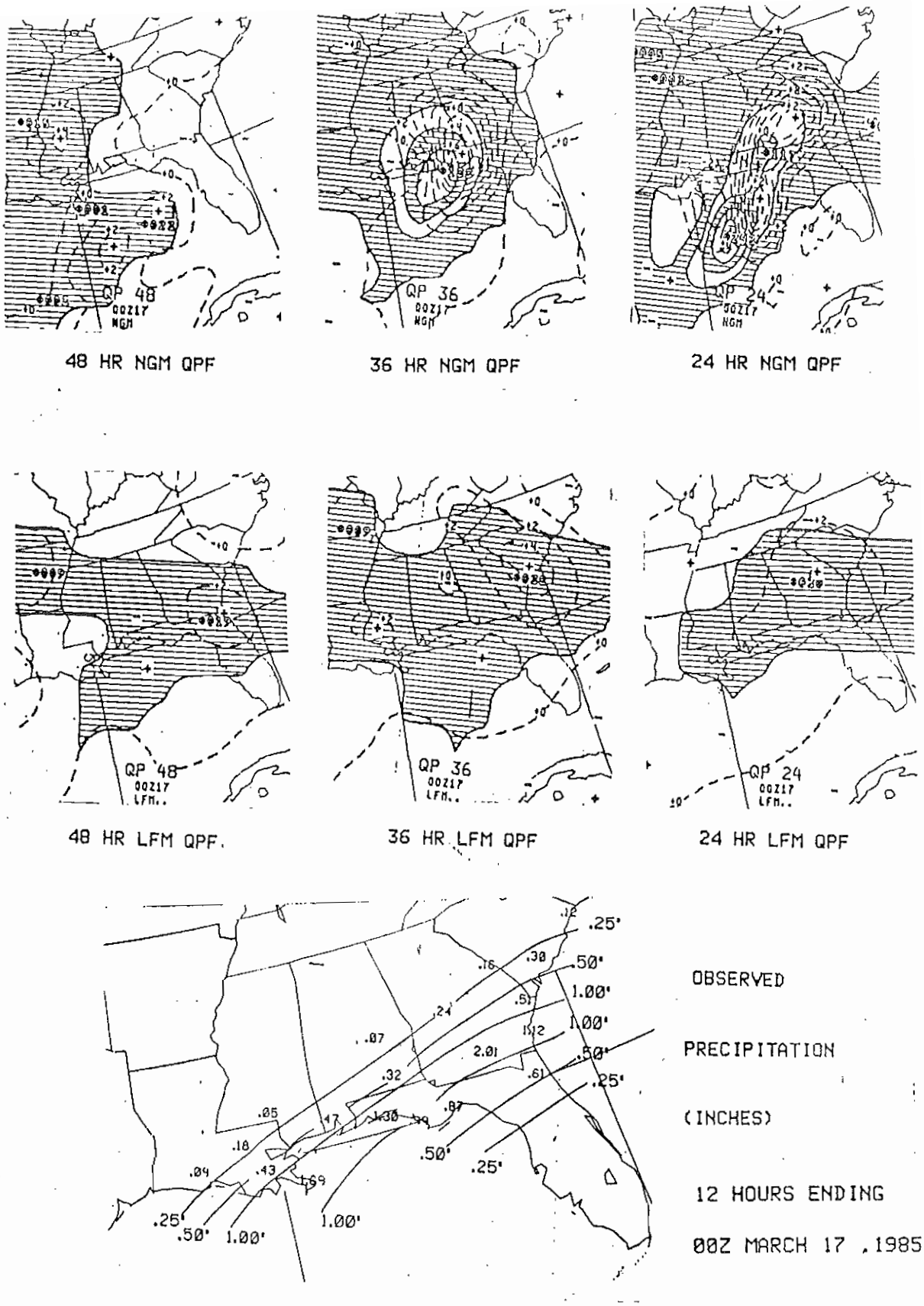

FIGURE 3. NGM VS. LFM QPFS FOR 12 HOUR PERIOD ENDING 00Z MARCH 17 1985 AND OBSERVED PRECIPITATION FOR SAME 12 HOUR PERIOD.

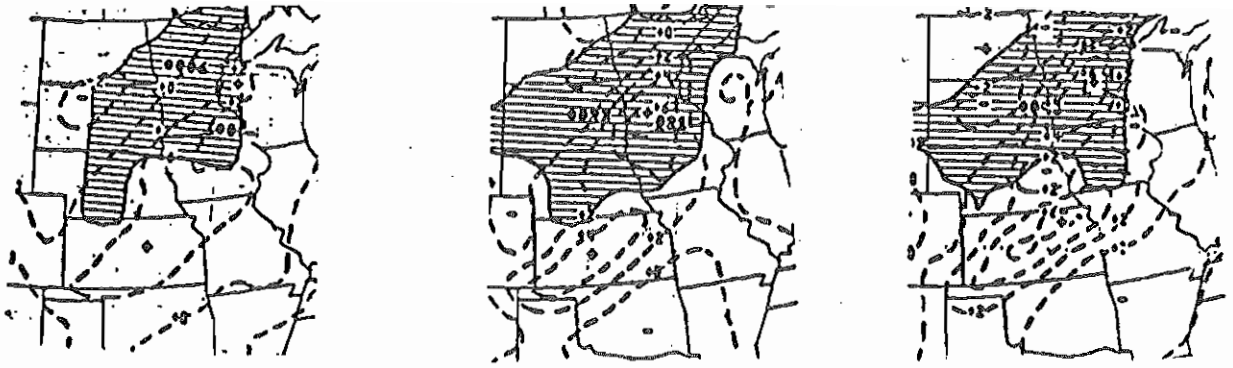

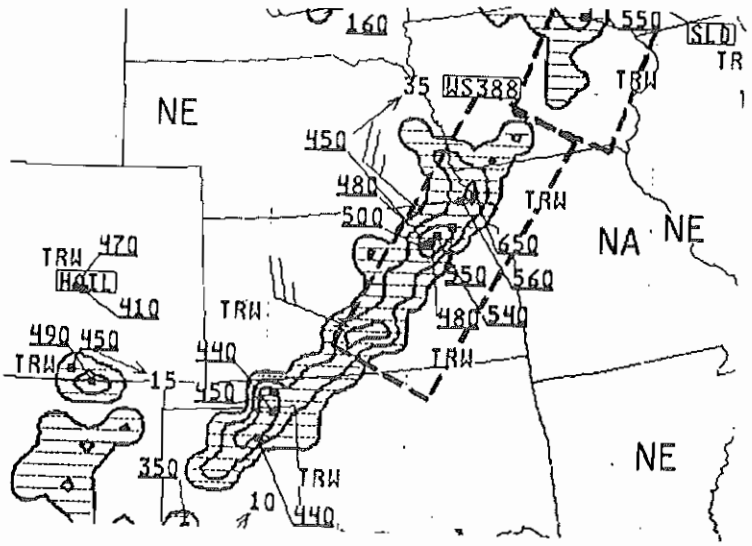

RADAR SUMMARY 0035Z AUG 10 1985

FIGURE 4. NGM VS. LFM VV FCSTS VALID 00Z AUG 10 1985 AND RADAR SUMMARY FOR 0035Z AUG 10 1985

VERIFICATION RESULTS FOR NMC 24-HOUR QPFs

Robert E. Bell

National Meteorological Center
Forecast Branch/Heavy Precipitation Unit

The Forecast Branch of NMC uses all available analysis data and numerical model output to produce manual QPFs each day for 24-hour Day 1, Update, and Day 2 periods. Over the United States, east of the Rockies, areally verified threat scores are calculated. The accompanying figures show percent improvement of manual threat scores, by month, over scores of the LFM and NGM output for .50" and 1.00" forecast areas. Day 1 and Update periods are shown. NGM scores were available for the months of April through December only.

Threat Score (TS) is defined as

$$\frac{A}{B + C - A}$$

Where

A = Area Correctly Forecast
B = Area Forecast
C = Area Observed

If the area forecast matches the area observed, then TS = 1, the maximum possible.

Comparison of manual and model scores for 1985 QPFs shows a very large percentage improvement by forecasters during summer months and a more modest improvement during the remainder of the year. Manual improvement to the NGM output was greater, reflecting the consistently higher LFM threat scores. Note that the graphs do not reflect actual threat scores, which in some cases were quite low. For example, .50" forecasts for the Day 1 periods in July had scores of .268 and .102 for manual and LFM forecasts, respectively.

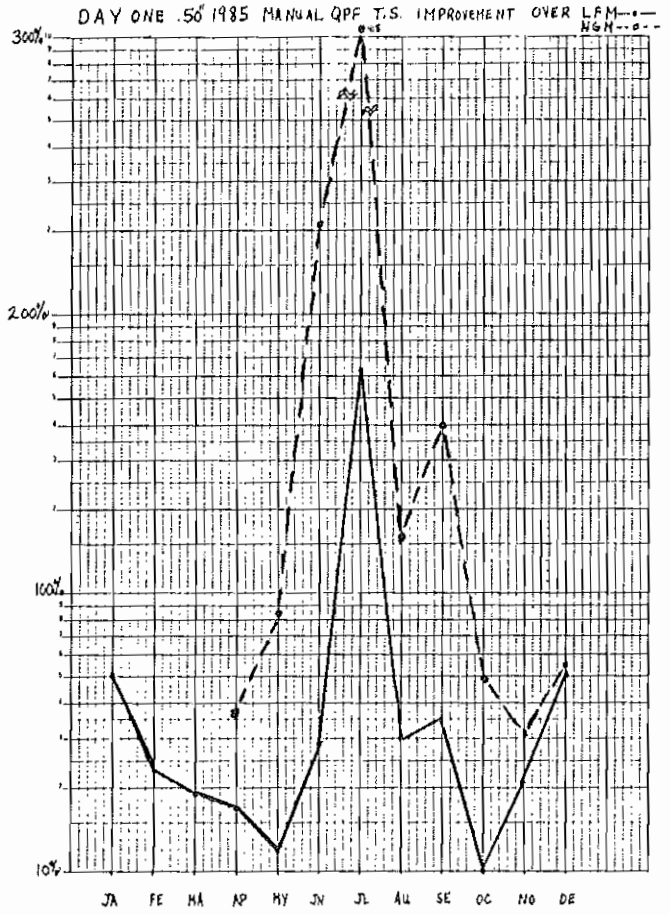
DAY ONE .50" 1985 MANUAL QPF T.S. IMPROVEMENT OVER LFM
NGM
300%
200%
100%
10%
JA FE MA AP MY JN JL AU SE OC NO DE

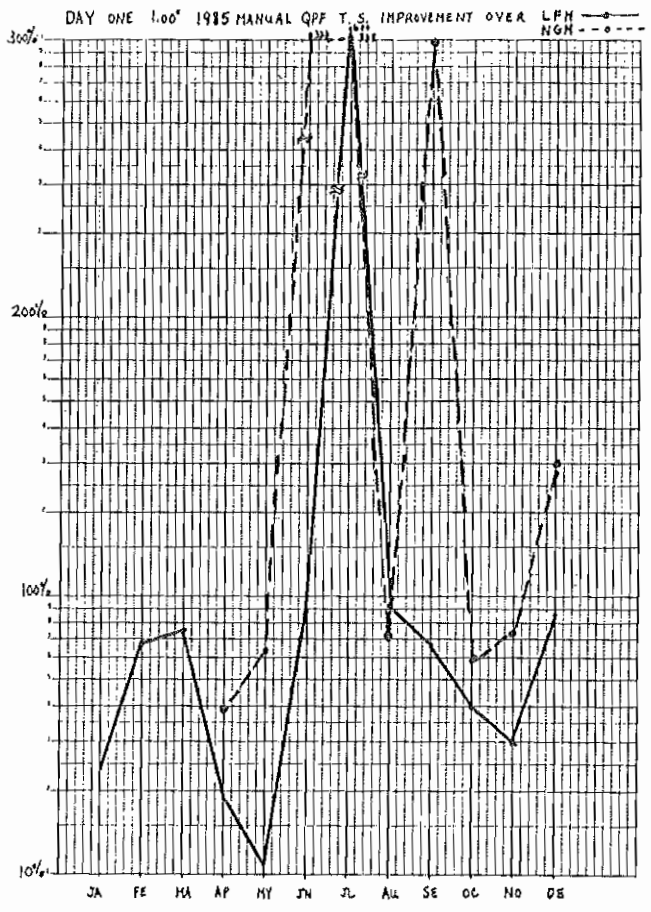
DAY ONE 1.00" 1985 MANUAL QPF T.S. IMPROVEMENT OVER LFM
NGM
300%
200%
100%
10%
JA FE MA AP MY JN JL AU SE OC NO DE

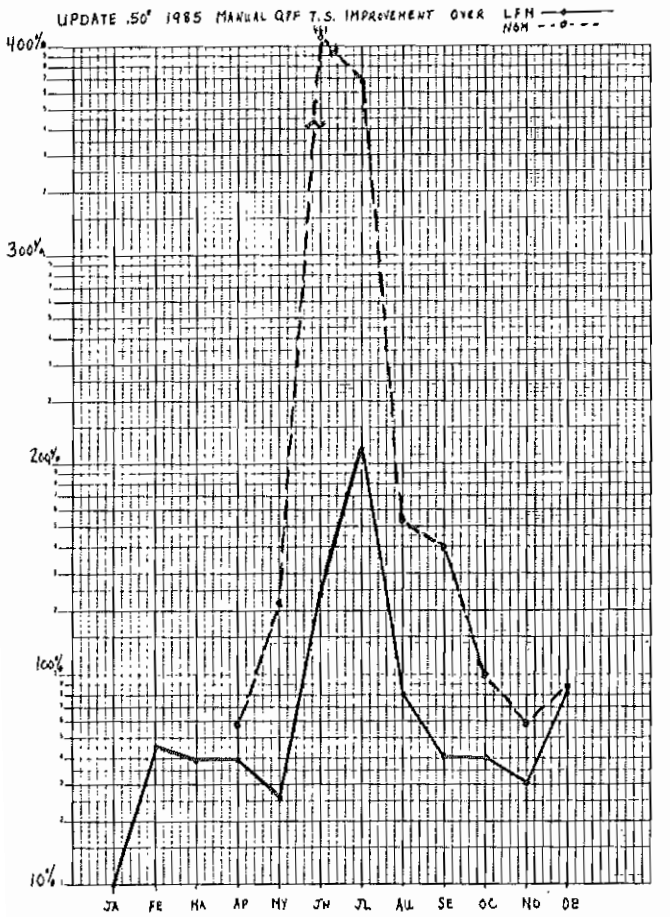
UPDATE .50" 1985 MANUAL QPF T.S. IMPROVEMENT OVER LFM
NGM
400%
300%
200%
100%
10%
JA FE MA AP MY JN JL AU SE OC NO DE

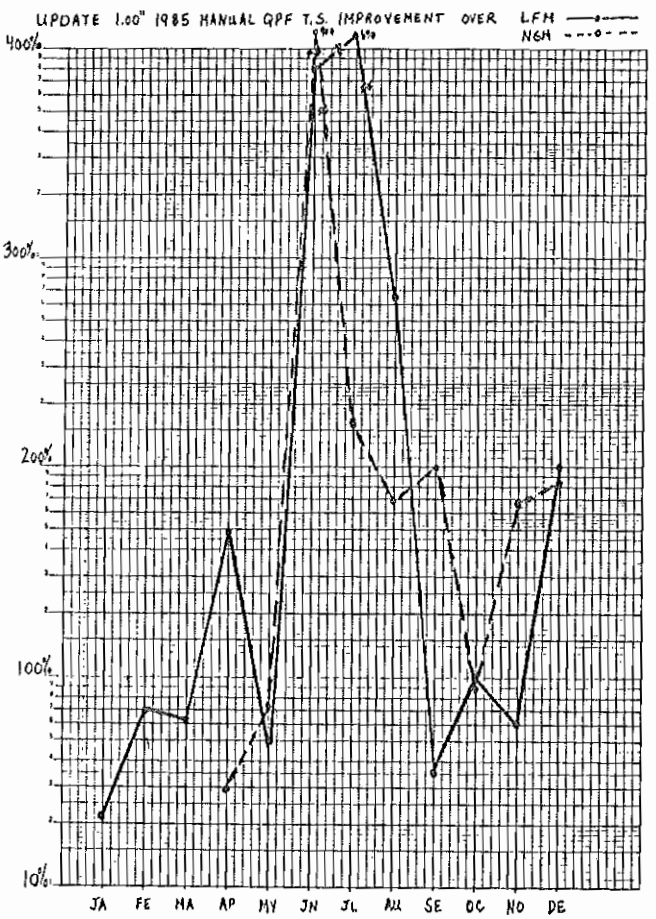
UPDATE 1.00" 1985 MANUAL QPF T.S. IMPROVEMENT OVER LFM
NGM
400%
300%
200%
100%
10%
JA FE MA AP MY JN JL AU SE OC NO DE

SATELLITE-DERIVED PRECIPITATION ESTIMATES

DURING THE 1985 TROPICAL STORM SEASON

Dane Clark

Synoptic Analysis Branch
National Environmental Satellite, Data, and Information Service
Washington, D.C.

1. INTRODUCTION

Satellite-derived estimates of precipitation were produced operationally by the Synoptic Analysis Branch of NESDIS for eight tropical systems during the 1985 Hurricane Season. The estimates were disseminated in real-time via AFOS to NWS forecast offices as guidance information for flash flood watches and warnings. The estimates were derived on the Interactive Flash Flood Analyzer (IFFA) using a modified tropical cyclone precipitation estimation technique. This paper presents the results of this effort during the 1985 Hurricane season.

2. HURRICANE BOB

Heavy rains associated with Bob first affected the southwest Florida Coast on July 22, as the storm began to organize and move slowly eastward across Florida. Operational estimates reached 15 inches for a 24-hour period. Spotty observations generally ranged from 7 to 11 inches with one report as high as 21 inches. As the storm moved into the Atlantic it began to move northward and strengthen, finally reaching landfall in the Carolinas on July 25 (fig. 1). Two-day rainfall estimates and rainfall observations are shown in figures 2a & 2b. Observations and estimates agree very well. The dashed lines on figure 2b indicate areas where observations were not available due to evacuations.

Hurricane Bob was a well behaved, minimal hurricane that moved on a steady course through the Carolinas and had no major interactions with baroclinic systems. The estimate technique worked effectively with Hurricane Bob.

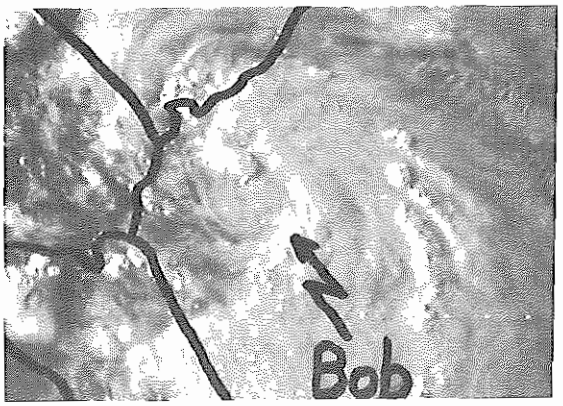

Figure 1. Visible satellite image of Hurricane Bob approaching the South Carolina coastline at 2300Z, July 24, 1985.

3. HURRICANE DANNY

Hurricane Danny moved inland on August 15, spreading heavy rains inland along coastal waters (fig. 3). As the storm moved further inland that night (fig. 4), IR cloud tops warmed significantly reducing definition of the heavy rain bands associated with the storm. Estimates and observations over Louisiana and Mississippi generally agreed, but there were some differences. One striking difference was 10-15 inch estimates produced in the vicinity of landfall compared with only one observation of 5-6 inches along the entire coastline. The evacuation of this area probably led to the poor observations from this area.

As Danny moved slowly northeastward over the next four days, heavy rains spread over the Tennessee Valley and into the Carolinas. Estimate - observation totals were in very good agreement with the exception of orographically enhanced rainfall in the Virginia and North Carolina Mountains.

Figure 2a. Satellite precipitation estimates for Hurricane Bob from 1300Z, July 24 to 0200Z, July 26, 1985.

Figure 2b. Observed precipitation for Hurricane Bob. Dashed lined indicate no observations were available.

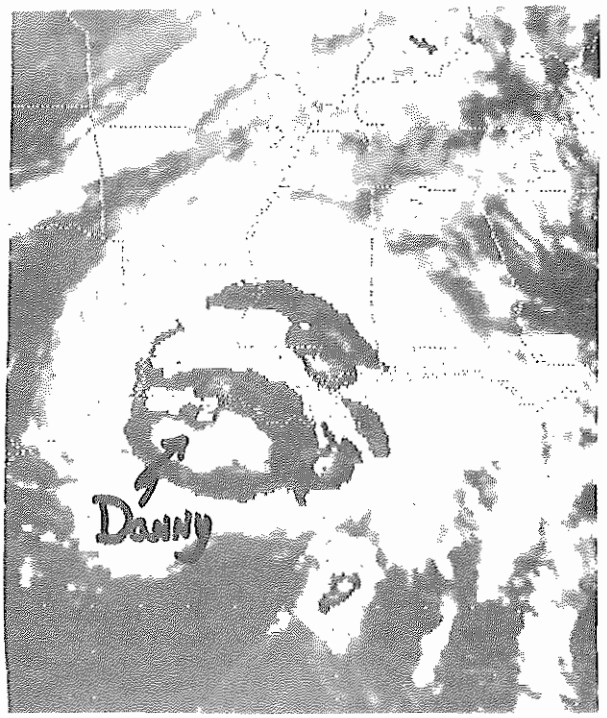

Figure 3a. Enhanced IR satellite image of Hurricane Danny approaching the Louisiana coastline at 1300Z, August 15, 1985.

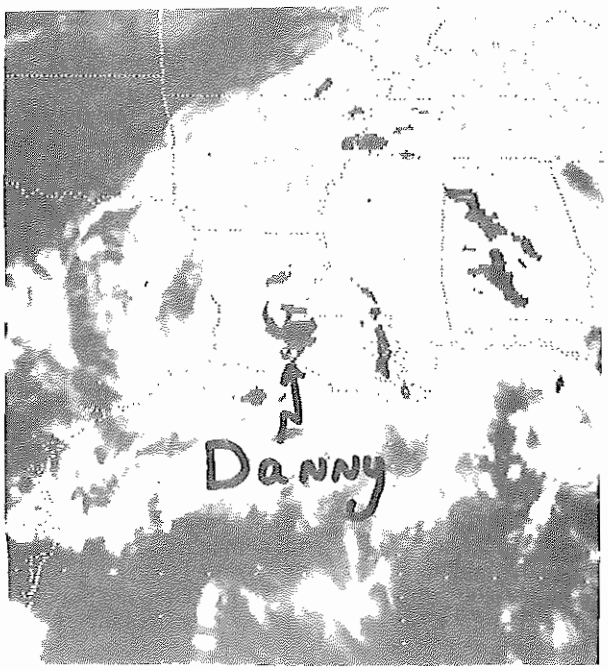

Figure 3b. Enhanced IR satellite image of Hurricane Danny inland over central Louisiana at 0000Z, August 16, 1985.

4. HURRICANE ELENA

Hurricane Elena brought heavy rains to much of the Central and Eastern Gulf Coastal areas as the storm moved erratically, and slowly through the northeastern Gulf (fig. 4) and finally inland over coastal Mississippi on September 2. Again coastal evacuations resulted in very little coastal data which made it difficult to verify estimates. One estimate of 13 inches near Apalachicola verified well when one 10 inch and another unofficial 16 inches were reported. Another estimate of 16 inches near Cedar Key was never verified due to lack of observations.

5. HURRICANE GLORIA

Even though Gloria was a strong storm, its rapid movement reduced potential heavy rains. One exception was over the Middle Atlantic States where the circulation from Gloria interacted with a strong vorticity center approaching from the west creating a north-south band of heavy precipitation (fig. 5). Estimates and observations were in very good agreement from North Carolina to Maryland. Estimates were generally too low in the warmer tops over Pennsylvania.

6. TROPICAL STORM ISABEL

A tropical wave, which later became tropical storm Isabel, enhanced dramatically over Puerto Rico on October 5-6 and dumped record rains over most of Puerto Rico (fig. 6). Estimates with the system reached 17 inches, even though satellite outages prevented several hours of estimates. This compared very favorably with reports of near 20-25 inches.

7. HURRICANE JUAN

The slow and erratic movement of Juan caused very heavy rains of 10-15 inches across the Central Gulf Coast over a 3-4 day period. Satellite data (enhanced IR) revealed a drastic change in the cloud top temperatures between the time the storm neared the coast on October 28 (fig. 7a) and after the storm moved inland on October 29 (fig. 7b). This dramatic warming of cloud tops resulted in some under-estimates especially on October 29 and 30.

8. HURRICANE KATE

Hurricane Kate (fig. 8) was a well behaved, steady moving storm similar to Bob. And like Bob, estimates with Kate were excellent (figs. 9a and 9b).

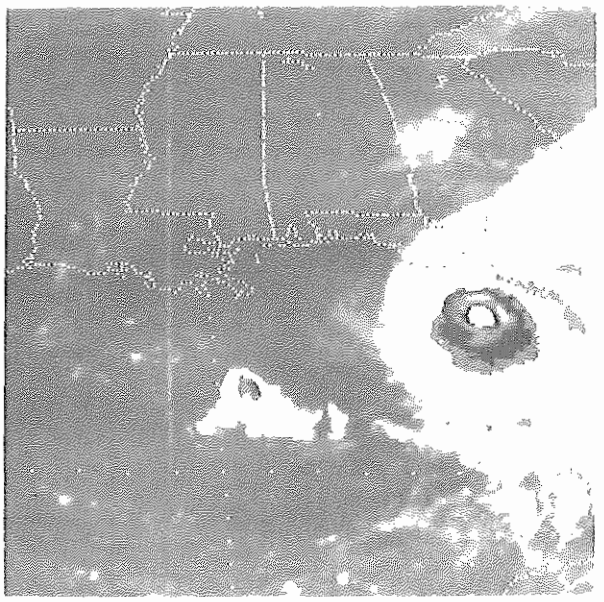

Figure 4. Enhanced IR satellite image of Hurricane Elena at 1200Z, September 1, 1985.

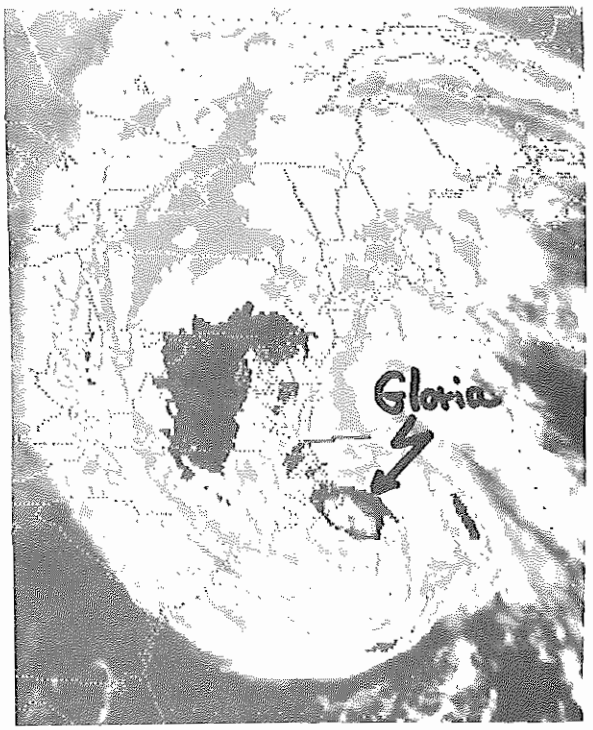

Figure 5. Enhanced IR satellite image of Hurricane Gloria at 0400Z, September 27, 1985.

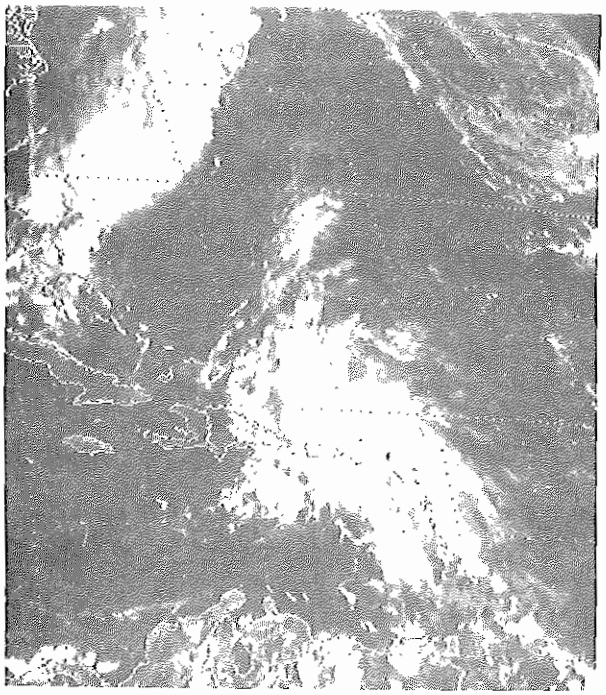

Figure 6. Visible satellite image of an intense rain event over Puerto Rico at 1530Z, October 6, 1985.

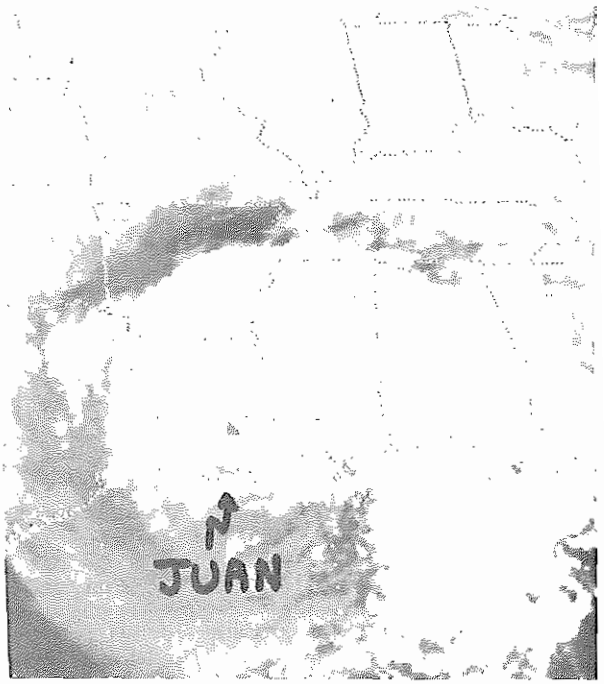

Figure 7b. Enhanced IR satellite image of Hurricane Juan at 2000Z, October 29, 1985.

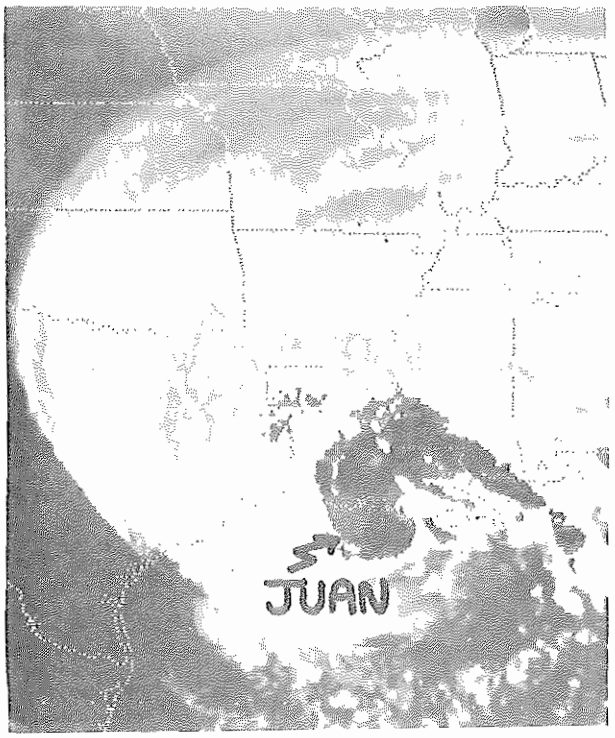

Figure 7a. Enhanced IR satellite image of Hurricane Juan at 0330Z, October 28, 1985.

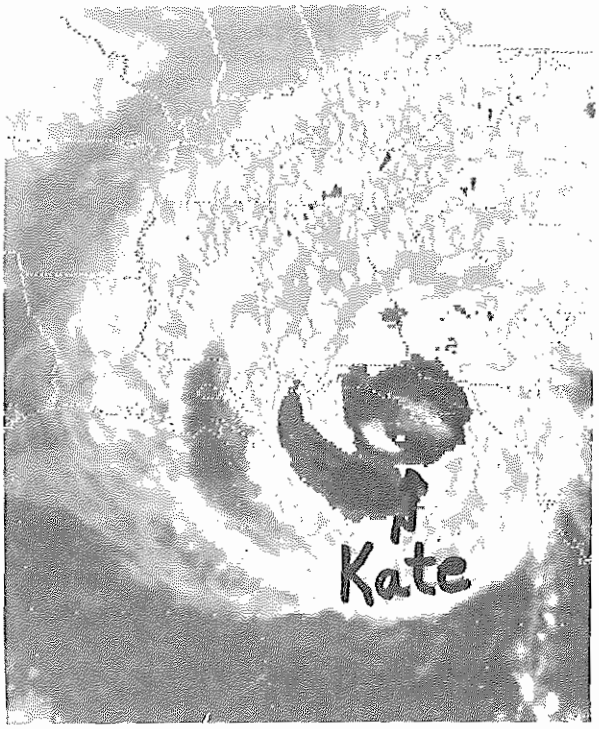

Figure 8. Enhanced IR satellite image of Hurricane Kate at 1900Z, November 21, 1985.

Figure 9a. Satellite precipitation estimates for Hurricane Kate from 0300Z, November 21 to 0000Z, November 23, 1985.

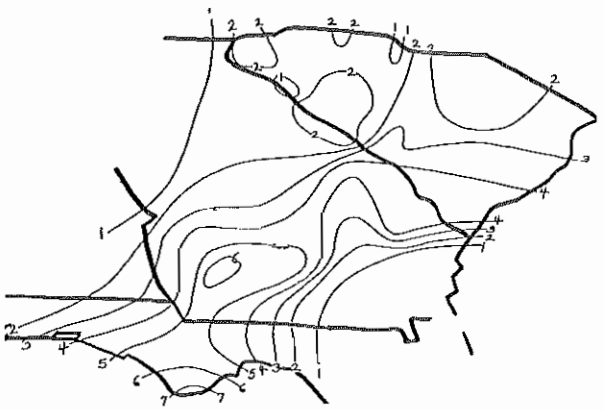

Figure 9b. Observed precipitation for Hurricane Kate.

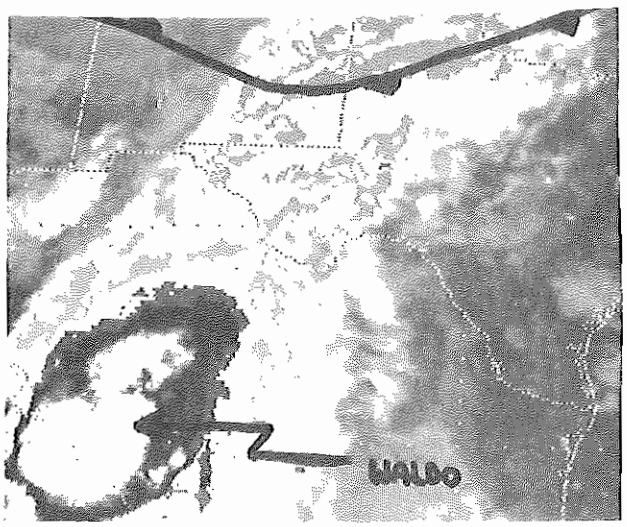

Figure 10. Enhanced IR satellite image of Hurricane Waldo crossing Old Mexico at 1230Z, October 9, 1985.

9. HURRICANE WALDO (EAST PACIFIC)

Hurricane Waldo was a strong East Pacific Hurricane that crossed Old Mexico (fig. 10), and interacted with a baroclinic zone over the southern plains to produce widespread heavy rains. Estimates were excellent over west Texas but as the remnants of Waldo continued to move northeastward, cloud tops warmed and under-estimates resulted over Oklahoma and Kansas.

10. CONCLUSIONS

The 1985 Hurricane Season was an extremely busy one at the Synoptic Analysis Branch. Several hundred hours of estimates were performed on tropical systems alone. The estimate techniques worked well with steady moving storms (Bob and Kate) but were inconsistent with erratic moving and rapidly warming (IR - enhancements) ones. Field's and Kusselson's (1986) work on precipitation verification of four 1985 Hurricanes presents a more detailed look at the comparisons, techniques, and recommended changes to the estimate program.

11. ACKNOWLEDGEMENTS

The author would like to thank Glenn Field and Sheldon Kusselson for the use of several figures from their recent paper on precipitation verification. I would also like to thank Joy Burke for typing the manuscript.

12. REFERENCES

Field, Glenn A. and Sheldon Kusselson, 1986: Verification of NESDIS's Operational Satellite Precipitation Estimates for four Hurricanes affecting the U.S. during 1985. Eleventh Conference on Weather Forecasting and Analysis, June 17-20, 1986, Kansas City, Missouri.

Spayd, LeRoy E., Jr. and Roderick A. Scofield, 1984: A Tropical Cyclone Precipitation Estimation Technique Using Geostationary Satellite Data. NOAA Technical Memorandum NESDIS-5, Washington, D.C., July 1984, 36 pages.

TECHNIQUES AT THE NATIONAL HURRICANE CENTER FOR ESTIMATING MAXIMUM RAINFALL FROM TROPICAL DISTURBANCES

by

James S. Lynch and James B. Lushine
Tropical Satellite and Analysis Center
National Hurricane Center
Miami, FL

1. INTRODUCTION

Tropical cyclones are typically accompanied by one or more hazardous phenomena, including: storm surge, high winds, tornadoes, and excessive rainfall. Each of these phenomena can produce devastating and potentially lethal consequences. The National Hurricane Center (NHC) attempts to forecast these features using a variety of methods and techniques.

Three techniques to estimate the rainfall potential from tropical cyclones and disturbances are in day-to-day use at the NHC. A rule of thumb, developed in the 1960s, is used as a quick estimate of rainfall potential. A second method utilizes infrared satellite data to estimate the maximum rainfall normally located near the inner core of a tropical cyclone. A third technique describes the spatial distribution of rainfall at/near the coastline normal to the track of a disturbance or cyclone.

2. RULE OF THUMB

The NHC rule of thumb was developed by Kraft in the 1960s. The scheme was originally intended to forecast the maximum rainfall for hurricanes affecting the U.S. Gulf of Mexico coast, but has been operationally applied to other Atlantic tropical systems. The technique was the basis for maximum rainfall estimates in public advisories issued by the NHC for many years. The original formula takes the form:

$$R = 100/S,$$

where R is the expected cumulative total rainfall (inches) and S is the disturbance's speed of translation (knots).

To test the rule of thumb, 230 cases of tropical storms and hurricanes are examined for the period 1900 to 1984. Two of the cases affected only the Caribbean Sea, while the remainder affected the U.S. coast of the Gulf of Mexico and/or Atlantic. The speed of translation is calculated from "best track" data by averaging the speed over a 24 hour period, from 12 hours prior to landfall to 12 hours after the cyclone center made landfall. The cases are stratified by intensity and geographic location of landfall (see Table 1).

For the 230 cases examined, the formula representing the "average" cyclone is:

$$R = 111/S.$$

Comparing tropical cyclones of hurricane versus tropical storm intensity, the 131 hurricane cases are slightly wetter than the 99 tropical storm cases, with respective numerators of 114 and 107. The stratification based upon geographic region of landfall suggests that the Gulf of Mexico cyclones produce more onshore rainfall than their Atlantic coast counterparts, with numerators of 122 and 105 respectively.

3. CORE RAINFALL

A technique to estimate the "core" rainfall, representing the maximum rainfall normally located near the inner core of a landfalling tropical cyclone, was developed by Woodley and Griffith (Griffith, et al., 1973, 1976, and 1978; Woodley, et al., 1971). The technique is based on the concept that colder (brighter) cloud tops detected with 11.6um infrared satellite data yield higher rainfall rates. The technique was tested against radar and rainguage measurements over south Florida.

The technique uses the infrared satellite data to produce an area average rainfall for tropical cyclones (Waters, et al., 1977). The scheme was modified (Woodley, et al., 1975) to adjust the rainfall so that 50% of the total rainfall from a cyclone occurs in the coldest (highest) 10% of the cloud area. The technique is used operationally at the NHC using digital satellite data to estimate the maximum rainfall potential for hurricanes and tropical storms within 36 hours of landfall.

4. MAXIMUM AREAL RAINFALL

The original Woodley-Griffith technique was modified by Jarvinen and Griffith (1981) to provide a one dimensional profile of rainfall distribution for landfalling tropical cyclones and disturbances. The technique describes the spatial distribution of rainfall at/near the coastline normal to the track of the disturbance. The maximum value on the profile represents the maximum rainfall expected at landfall.

The technique is based on the premise that each cloud top temperature (height) has an associated rainfall rate. An estimate of the rainrate together with information on the size and translational velocity allows for the inference of total rainfall for points in the path of the disturbance. The expected cumulative total rainfall (R) for a station in the path of the disturbance is given as:

$$R = \overline{rr}\ (W/S),$$

where $\overline{rr}$ is the average rainfall rate of each individual cloud top (or PIXEL) passing over the station, W is the width of the disturbance along its translational path relative to the station, and S is the translational speed. The technique is used operationally at the NHC to estimate the maximum rainfall potential for tropical disturbances and depressions within 36 hours of landfall.

5. THE 1985 ATLANTIC HURRICANE SEASON

The 1985 Atlantic hurricane season produced an unusual number of landfalling tropical cyclones on the U.S. coast (see Figure 1), as can be attested to by the residents of Louisiana who experienced three cyclones. Though the total number of eleven named cyclones is not particularly anomalous for the Atlantic basin, eight of the cyclones struck one or more sections of the U.S. coastline. In addition, several days prior to being named Isabel, a slow moving tropical disturbance produced catastrophic floods over Puerto Rico.

The NHC Tropical Satellite and Analysis Center literally prepared several hundred rainfall estimates using the two satellite techniques for the Atlantic basin during the course of the season. In general, rainfall potential estimates were prepared whenever a tropical cyclone or disturbance was within 36 hours of landfall of the nations within and surrounding the Caribbean Sea, the Bahamas, Mexico (both the Atlantic and Pacific coasts), or the U.S. coastline. Because tropical cyclones and disturbances can significantly change their translational velocity and cloud canopy appearance over a 24 to 36 hour period, verification material presented in this section will focus on rainfall potential estimates prepared during the period 6 hours prior to landfall.

Table 1. Rule of Thumb, stratified by cyclone intensity and geographic region of landfall.

Intensity	All Tropical Cyclones	All Hurricanes	All Tropical Storms
Number of Cases	230	131	99
Average Maximum Rainfall (inches)	10.6	11.3	9.6
Standard Deviation Rainfall (inches)	5.8	5.3	6.2
Average Translational Speed (knots)	10.5	10.1	11.0
Standard Deviation Speed (knots)	4.8	4.4	5.2
Revised Formula (R=)	111/S	114/S	107/S

Geographic Region (Hurricanes)	U.S. Gulf of Mexico	Florida	U.S. East Coast
Number of Cases	79	58	52
Average Maximum Rainfall (inches)	12.1	11.2	10.1
Standard Deviation Rainfall (inches)	5.8	4.3	4.0
Average Translational Speed (knots)	10.0	9.9	10.4
Standard Deviation Speed (knots)	4.2	3.9	4.7
Revised Formula (R=)	122/S	111/S	105/S

Figure 1. Track of 1985 Atlantic hurricanes and tropical storms.

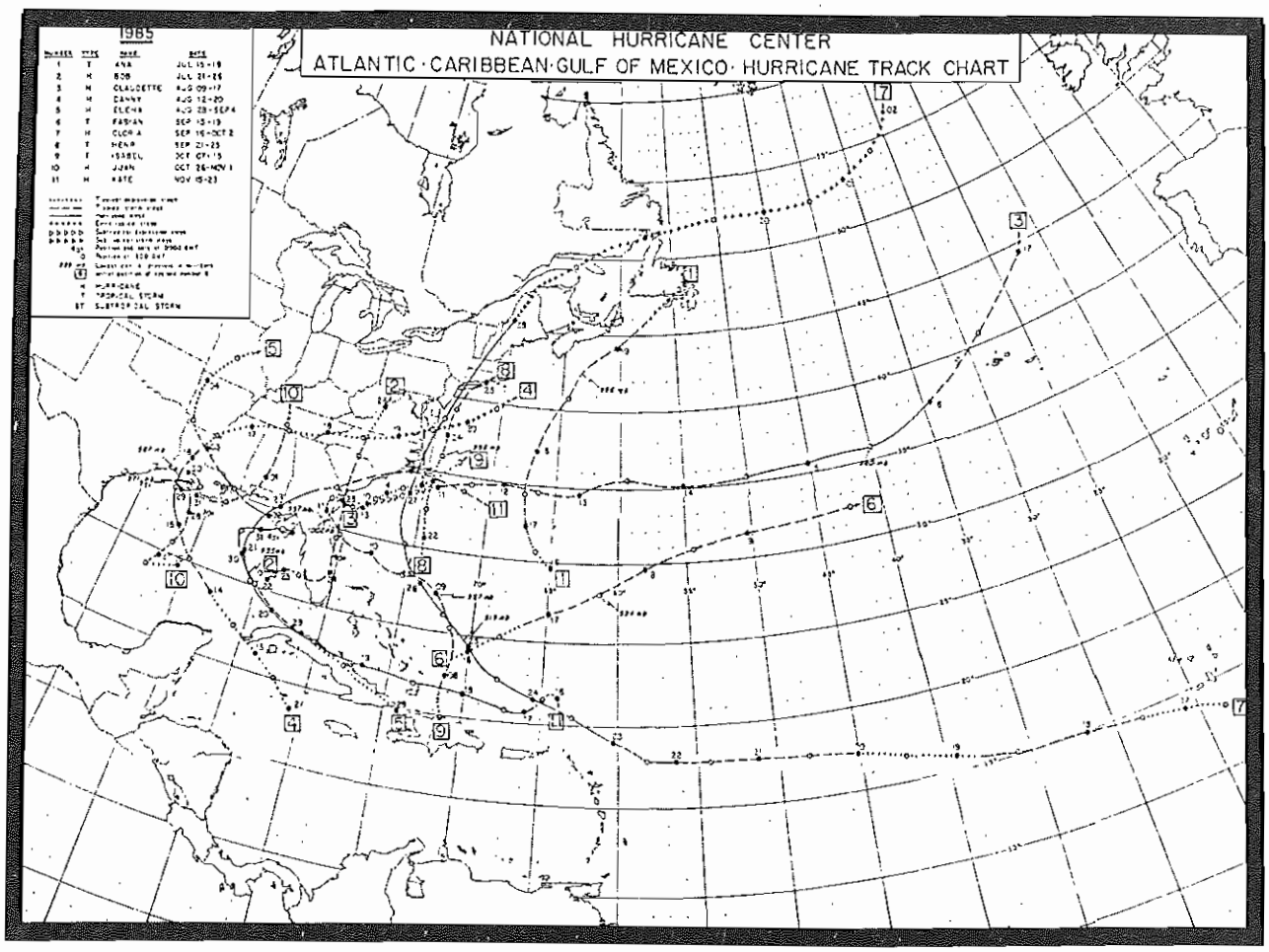

The cumulative rainfall potential forecasts based on the "official" speed of translation (as used in the advisory package) and based on satellite data six hours prior to landfall are presented in Table 2. The average absolute error for the rule of thumb, maximum areal rainfall, and core rainfall were 6.0 inches, 7.8 inches, and 5.3 inches, respectively. At first glance, none of the three techniques appear to show much skill in estimating the total rainfall.

However, re-examination of the speed of translation suggests that the "official" speed six hour prior to landfall does not always concur with the "actual" speed of translation at the time of landfall (defined in Section 2). Based on the "actual" speed of translation the revised rainfall potential estimates are shown in Table 3. The average absolute error for the rule of thumb, the maximum areal rainfall, and the core rainfall become 4.4 inches, 3.2 inches, and 2.8 inches, respectively. This shows the importance of the speed of translation in operationally estimating the maximum rainfall potential for a tropical disturbance.

For three of the cases, all three of the techniques significantly overestimated the maximum cumuluative rainfall. Close examination of Tropical Storms Henri and Isabel reveals that the deep convection associated with each storm "sheared" away from the cyclone in the hours just prior to landfall. Hurricane Juan, on the otherhand, demonstrated more of the characteristics of a subtropical low than that of a "classic" hurricane. None of the techniques take into account these anomalous features (or orographic effects). Removing these cases and assuming the "actual" speed of translation, the average absolute error for 1985 becomes 1.8 inches, 2.6 inches, and 1.6 inches for the rule of thumb, maximum areal rainfall, and core rainfall, respectively.

Table 2. Cumulative rainfall potential forecasts based on "official" speed of translation and satellite data 6 hours prior to landfall.

Name (Affected Area)	Landfall Date/Time	Actual Transl. Speed	Official Transl. Speed	Maximum Observed Rainfall	Rule of Thumb	Max. Areal Rain	Core Rain
Bob (FL)	7/23/12Z	6kt	5kt	21.5"	20.0"	10.7"	16.6"
Bob (NC,SC)	7 25/00Z	13kt	13kt	7.8"	7.7"	5.9"	7.9"
Danny (MS,LA)	8/15/12Z	11kt	12kt	8.9"	8.3"	6.2"	7.8"
Elena (MS,AL,FL)	9/02/12Z	13kt	8kt	7.1"	12.5"	11.1"	10.5"
Gloria (NC)	9/27/06Z	25kt	20kt	7.1"	5.0"	5.1"	5.4"
Gloria (NY,CT,VT,NH)	9/27/18Z	33kt	30kt	6.0"	3.3"	2.1"	2.6"
Henri (NY,CT)	9/25/00Z	13kt	12kt	0.5"	8.3"	2.9"	5.2"
Pre-Isabel (PR)	10/07/12Z	5kt	10kt	22.2"	10.0"	10.9"	11.0"
Isabel (FL,GA)	10/10/18Z	6kt	12kt	0.6"	8.3"	3.0"	3.0"
Juan (LA,MS)	10/29/00Z	4kt	3kt	15.0"	33.3"	12.0"	30.4"
Kate (FL)	11/22/00Z	15kt	7kt	6.0"	14.3"	16.1"	17.0"
			Average Absolute Error:		6.0"	7.8"	5.3"

Table 3. Cumulative rainfall potential forecasts based on actual speed of translation at the time of landfall and satellite data 6 hours prior to landfall.

Name (Affected Area)	Landfall Date/Time	Actual Transl. Speed	Maximum Observed Rainfall	Rule of Thumb	Max. Areal Rain	Core Rain
Bob (FL)	7/23/12Z	6kt	21.5"	16.6"	12.8"	19.9"
Bob (NC,SC)	7/25/00Z	13kt	7.8"	7.7"	5.9"	7.9"
Danny (MS,LA)	8/15/12Z	11kt	8.9"	9.1"	5.7"	7.1"
Elena (MS,AL,FL)	9/02/12Z	13kt	7.1"	7.7"	6.8"	6.5"
Gloria (NC)	9/27/06Z	25kt	7.1"	4.0"	4.1"	4.3"
Gloria (NY,CT,VT,NH)	9/27/18Z	33kt	6.0"	3.0"	1.9"	2.4"
Henri (NY,CT)	9/25/00Z	13kt	0.5"	7.7"	2.6"	4.8"
Pre-Isabel (PR)	10/07/12Z	5kt	22.2"	20.0"	21.8"	21.9"
Isabel (FL,GA)	10/10/18Z	6kt	0.6"	16.7"	6.1"	6.1"
Juan (LA,MS)	10/29/00Z	4kt	15.0"	25.0"	9.0"	22.8"
Kate (FL)	11/22/00Z	15kt	6.0"	6.7"	7.5"	7.9"
		Average Absolute Error:		4.4"	3.2"	2.8"

6. CONCLUSIONS

The three techniques (rule of thumb, maximum areal rainfall, and core rainfall) are used operationally at the NHC to provide cumulative rainfall potential estimates for tropical cyclones and disturbances. The data are typically incorporated into the NHC public advisories for tropical cyclones approaching landfall on the U.S. coast.

The original rule of thumb, developed in the 1960s, can and does provide useful information. Examination of cyclones by intensity and geographic region of landfall suggests that some improvement can be made by applying specific formulae based on these parameters. Some improvement in skill beyond the rule of thumb is provided by the Woodley-Griffith "core" rainfall technique.

All three techniques are extremely susceptible to errors in translational speed. The "official" speed of translation used in NHC advisories six or more hours prior to landfall frequently is not representative of the disturbance's translational speed at landfall. For accelerating or decelerating cyclones some modification to the "official" speed may be required.

None of the techniques provide representative results when the vertical wind distribution shears the deep convection away from the cyclone in the last few hours prior to landfall. In addition, none of the techniques are designed for hybrid or subtropical cyclones. Furthermore, orographic effects are not accounted for in any of the techniques.

All three techniques, however, do show skill in providing useful and representative information regarding the cumulative rainfall potential when the exceptional cases and actual translational speeds are accounted for.

REFERENCES

Griffith, C.G., and W.L. Woodley, 1973: On the variation with height of the brightness of precipitating convective clouds. J. Appl. Meteor., 12, 1086-1089.

_____, W.L. Woodley, S. Browner, J. Teijeiro, M. Maier, D.W. Martin, J. Stout, and D.N. Sikdar, 1976: Rainfall estimation from geosynchronous satellite imagery during daylight hours. NOAA Tech. Report ERL 356-WMP07, Boulder, CO, 106pp.

_____, W.L. Woodley, P.G. Grube, D.W. Martin, J. Stout, and D.N. Sikdar, 1978: Rain estimation from geosynchronous satellite imagery - visible and infrared studies. Mon. Wea. Rev., 106, 1153-1171.

Jarvinen, B.R., and C.G. Griffith, 1981: Forecasting rainfall in tropical cyclones using digital infrared satellite data. Unpublished Manuscript, National Hurricane Center, 12pp.

Water, M.P. III, C.G. Griffith, and W.L. Woodley, 1977: Use of digital geostationary satellite imagery for real-time estimation of hurricane rain potential in landfalling storms. Preprints, 11th Tech. Conf. on Hurricanes and Tropical Meteor., Amer. Meteor. Soc., 198-203.

Woodley, W.L., and B. Sancho, 1971: A first step toward rainfall estimation from satellite cloud photographs. Weather, 26, 279-289.

_____, A.R. Olsen, A. Herndon, and V. Wiggert, 1975: Comparison of gage and radar methods of convective rain measurements. J. Appl. Meteor., 14, 909-928.

CLIMATOLOGY OF HEAVY RAIN SYNOPTIC PATTERNS IN SOUTH FLORIDA: NOVEMBER THROUGH APRIL

Frank J. Revitte
National Weather Service Forecast Office
Coral Gables, FL 33146

1. INTRODUCTION

The annual south Florida rainfall is quite heavy (fifty-five to sixty inches) mainly due to its southern latitude and geographical location with respect to the Gulf of Mexico and Atlantic Ocean. An ample moisture supply provided by the surrounding warm ocean water combined with mesoscale convergence due to land/sea interaction causes thunderstorms to develop on a daily basis during the summer. The rainfall pattern during the year can be divided into two distinct regimes, wet and dry. Between seventy-five and eighty percent of the annual rainfall occurs from May through October. However, daily rainfall during the "dry season" can occasionally be quite heavy as mid-latitude synoptic systems penetrate into south Florida. Due to the normal dry regime in place over the area, the populace can be quite sensitive to these heavy rainfall events which occur during the "dry season" from November through April.

Much research on forecasting heavy precipitation has been accomplished on a national scale by Maddox (1979) and in the Southern Region of the National Weather Service by Biedinger (1985), Bellville (1983), Goodman (1982), and Grice (1982). The intent of the above mentioned papers was to identify synoptic patterns associated with heavy rainfall. In a similar manner, the aim of this paper is to identify and classify synoptic patterns which immediately precede the onset of heavy rain across south Florida during the months of November through April. Once heavy rain synoptic patterns are recognized, forecasters then can concentrate on sub-synoptic scale features to decide if and where heavy rain is a threat.

2. DATA CRITERIA

Criteria for heavy rainfall in this study was any calendar day in which rainfall equalled or exceeded three inches. If consecutive days of "heavy rainfall " were noted, it was still considered as single heavy rain event resulting in more heavy rain days than heavy rain events.

The area of study was over the Florida peninsula south of 27N, excluding the Florida Keys (Figure 1). The number of stations which reported calender day rainfall during the period of study varied from approximately twenty-five to thirty. The rainfall data were reported in NOAA's Daily Precipitation Totals.

The period of study included heavy rainfall events during the dry season months of November through April from 1948 through 1984, therefore 36 dry seasons were studied.

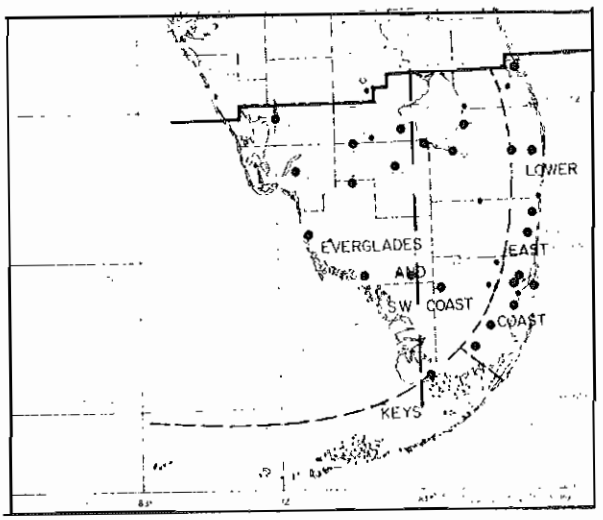

Figure 1. Area included in heavy rain study was the southern third of the Florida peninsula, generally south of 27N, excluding the Florida Keys. Heavy dots denote precipitation reporting stations as of 1984.

3. MONTHLY DISTRIBUTION

During the thirty-six year period, ninety-seven heavy rainfall events occurred over south Florida. Biedinger (1985) found approximately thirty percent more heavy rain events during the same period in a similar heavy rainfall study over north Florida. The occurrence of more heavy rain events over north Florida can be attributed to the fact that rainfall during the November through April period is significantly greater over north Florida than south Florida. For instance, the normal rainfall at Tallahassee

during this period is slightly more than twenty-five inches while at Miami the normal is about fourteen inches. Thirty-five of the ninety-seven (37%) heavy rain events over south Florida had amounts equal to or exceeding five inches. This is a significantly higher percentage than found in north Florida. Biedinger found thirty six of the one hundred thirty-three heavy rain events (27%) with rainfall amounts equal to or greater than five inches.

As shown in figure two, the two months with the greatest number of heavy rainfall events were November and April, with each month accounting for approximately twenty-five percent of the total. The remaining four months of December, January, February, and March made up the remaining fifty percent. In addition, November accounted for the greatest number of events with rain amounts equalling or exceeding five inches over south Florida. Fourteen of the twenty-six rain events in November met this criteria. In contrast, Biedinger found that the months of February, March, and April to have the greatest number of heavy rain events in north Florida.

Several factors would logically suggest why these two months, November and April, account for nearly fifty percent of the total heavy rain events. Both of these months mark the transition from a wet to dry regime or vice-versa. During these months fronts are not as likely to quickly sweep through the south Florida peninsula but rather slow down or become stationary. In a study by DiMego (1976), frontal duration over south Florida during November and April was longer compared with the other dry season months. Interaction of tropical air with the frontal boundary is more likely as fronts linger over south Florida increasing the prospect of heavy rainfall.

Another contributing factor to large number of heavy rain events during November is the relatively warm Atlantic waters off the lower southeast Florida coast. The normal sea surface temperatures in this area during November is the middle seventies. Many heavy rain events in November occur under strong low level east or northeast flow. Relatively cool, dry air brought southward by high pressure centered over the eastern U.S. can rapidly become saturated as it moves over the relatively warm ocean waters.

The four months, January, February, March, and April, account for the remaining fifty percent of the heavy rain events. January and March each contribute about fifteen percent of the total while February and December account for ten percent each.

4. GEOGRAPHICAL DISTRIBUTION

The area of study was divided into an eastern and western part with the dividing line extending from approximately the western shore of Lake Okeechobee southward to near Flamingo (see Figure 1.). During the period of study about eight to ten stations (one third) were located in the western portion of the study area with remaining stations in the eastern portion.

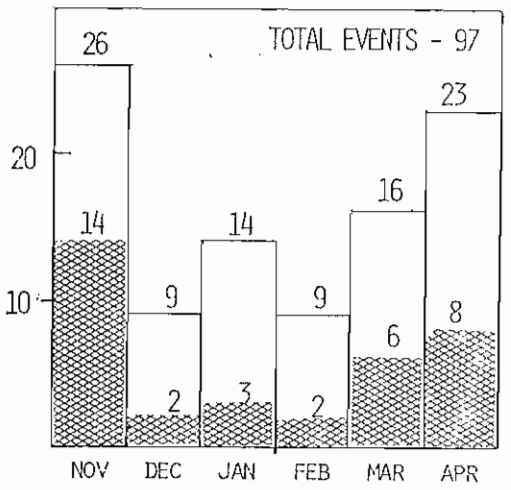

Figure 2. Monthly distribution of heavy rain events. Open bars-rain amounts $\geq$ 3 inches. Hatched bars-rain amounts $\geq$ 5 inches.

Of the ninety-seven heavy rainfall events, sixty-nine (71%) occurred solely on the east side of the peninsula with eleven (11%) on the west side. Seventeen heavy rain events (18%) occurred over both areas. In twenty-five of the sixty-nine heavy rain events over the eastern portion, rainfall totals equalled or exceeded five inches. However, only one of the eleven heavy rain events over the western portion had rain amounts equal to or exceeding five inches.

Even though a significantly greater number of rainfall reporting stations were located over the eastern portion of the peninsula, there appears to be a bias to the occurrence of heavy rain events over the eastern portion of the peninsula compared to the western portion. A contributing factor to this distribution pattern could be the fact that many heavy rain events occurred under strong low level east or northeast flow. As the precipitation moves onshore the Atlantic coast, most of the precipitation falls within the coastal area and is considerably less intense as it moves to the western portion.

5. SYNOPTIC PATTERNS AND DISTRIBUTION

After reviewing the synoptic conditions which produced heavy rainfall across south Florida, four synoptic patterns emerged as the most prevalent heavy rain producers.

5.1 Type I

Type I (Figure 3) was a split flow pattern at 500 millibars (mb) where a closed low or trough was moving through the southern branch of the westerlies. The low or trough was usually located east of 105W with a southwest flow prevailing in the middle layer of the troposphere over Florida and adjacent areas. At the surface, an east/west frontal boundary stretched from the Bahamas across south Florida into the Gulf of Mexico. In many cases the frontal boundary was quasi-stationary. A strong high pressure center was located over or offshore the U.S. Mid-

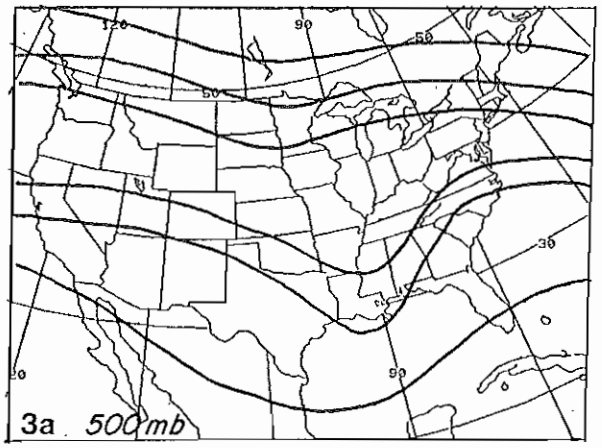

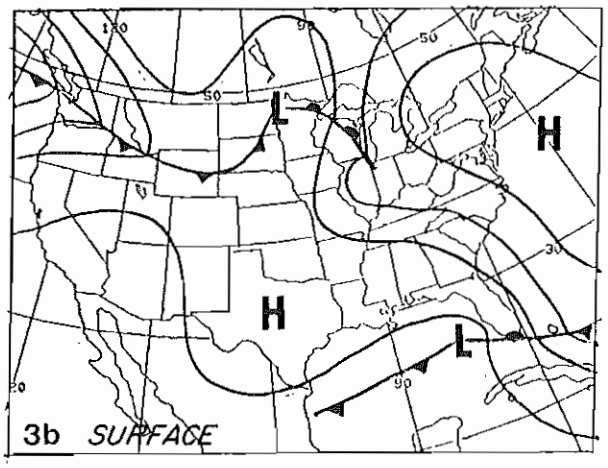

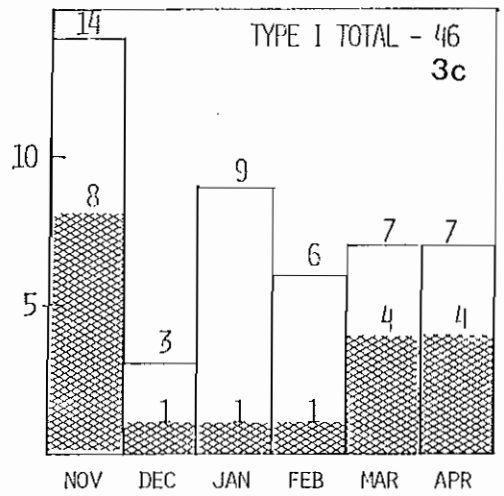

Figure 3. Example of Type I synoptic pattern. (3a) A split flow pattern exists at 500 mb with a short wave moving through the southern branch of the westerlies. (3b) A surface front extends from the Bahamas across south Florida into the Gulf of Mexico with a low developing along the front in the eastern Gulf. (3c) monthly distribution of heavy rain events associated with Type II.

Atlantic coast. The frontal boundary marked the transition between the northeast flow to the north of the boundary and the southeast flow to the south. The trough or low at 500 mb in many cases caused a low or frontal wave to develop on the front over the southeast Gulf of Mexico which enhanced convection over south Florida.

Precipitation in Type I events usually occurred along and just north of the frontal boundary in the east or northeast flow at low levels. In many cases, convective bands lined up perpendicular to the shore, or parallel to the wind flow, and moved onshore with "train" effect over a particular area. Although moisture depth was not examined in this study, from personal experience as a forecaster, moisture depth is often quite shallow with heavy rain falling out of relatively warm cloud tops.

The split flow pattern was the most prolific heavy rain producer, accounting for forty-six of the ninety seven (47%) heavy rain events. Type I was the most significant heavy rain producer in November, the month with the greatest number of events. Type I also accounted for nineteen of the thirty-five events (54%) where rain amounts equalled or exceeded five inches.

5.2 Type II

The zonal pattern, Type II (Figure 4), was somewhat similar to Type I in the fact that a frontal boundary extended from the Bahamas across south Florida into the Gulf of Mexico. Additionally a large high center was normally located over the Atlantic offshore the U.S. Mid-Atlantic coast. A zonal flow existed at 500 mb. In some cases, a minor short wave was detected in the westerly flow over the southern U.S.

Precipitation characteristics in the zonal pattern were also similar to Type I with most of the activity occurring along and just north of the frontal zone with moisture depth being rather shallow.

Type II was the prevailing synoptic pattern in only fifteen of the ninety-seven (15%) heavy rain events. April had the greatest number of Type II events with five.

Type I and II showed similar characteristics to studies completed on rainfall patterns in the neighboring Bahamas and over the island of Hispaniola in the Greater Antilles. Bosart (1980) found that heavy rainfall events in the Bahamas were usually associated with strenthening easterly flow behind a front which was becoming parallel to the upper flow, increased horizontal confluence, and weak lower tropospheric warm advection. Garcia (1978) found winter rainfall in the Dominican Republic also to be associated with strenthening westerlies resulting in increased vertical wind shear. In both Types I and II, moderate to strong east and northeast flow existed behind a frontal boundary, confluence was noted along the front, and strong vertical wind shear was implied as westerlies prevailed above the low level easterly flow.

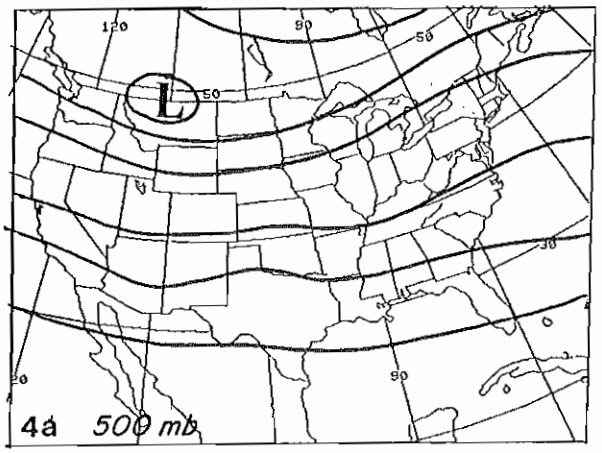

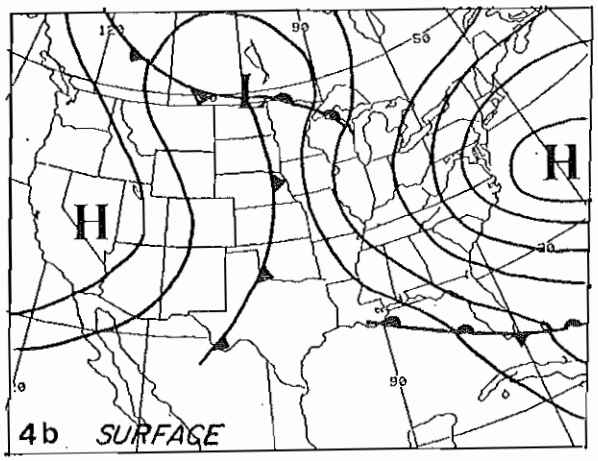

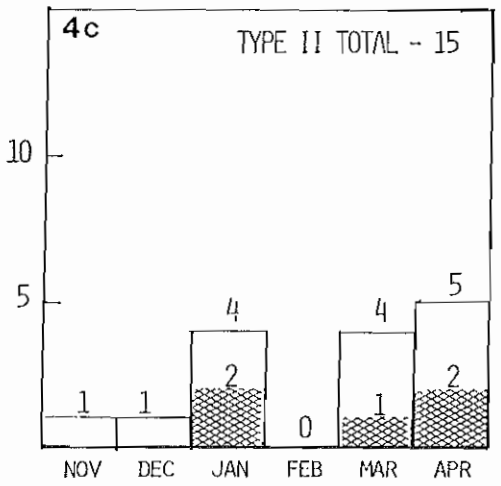

Figure 4. Example of Type II. (4a) zonal flow is present at 500 mb. (4b) stationary front extends across south Florida from Bahamas into the Gulf of Mexico. (4c) monthly distribution of heavy rain events associated with Type II.

5.3 Type III

Type III (Figure 5) was characterized by a full latitude trough at 500 mb usually situated between 85W-100W and extending south of 35N. A vorticity maximum was detected in many cases moving through the southern portion of the trough located over the Gulf of Mexico. At the surface, a slow moving northeast/southwest front was normally located over the eastern U.S. The surface flow was usually from a southerly direction with the upper flow from a southwest direction.

Heavy precipitation occurred with this pattern as convection moved north and northeast out of the southeast Gulf of Mexico or Yucatan Peninsula in advance of the front. Many times the convection was associated with wave development along the front. Rarely did heavy precipitation occur with a pre-frontal squall line moving across south Florida from northwest to southeast.

The full latitude 500 mb trough pattern, Type III, made up twenty of the ninety-seven (20%) heavy rain events in this study. During November, Type II was linked to eight of twenty-four events while in December nearly one half of the events were related to the Type III pattern. Of the twenty Type III events only five had rain amounts equal to or greater than five inches.

5.4 Type IV

Type IV (Figure 5) is similar to the Type III pattern. However, instead of a 500 mb long wave trough in the center of the U.S., a closed 500 mb low was situated north of 35N with a trough extending southward into the Gulf of Mexico. At the surface, a slow moving northeast/southwest cold front was typically located from the southeast U.S. into the eastern Gulf of Mexico.

As in Type III, the cold front was moving slowly in order to produce heavy rain amounts. Also, most heavy precipitation moved into south Florida from the Southeast Gulf of Mexico or the Yucutan Peninsula as a result of wave development along the frontal bounday.

Overall, the closed 500 mb low pattern, Type IV, was linked to only eleven (11%) heavy rain events. Of the eleven events, only four had rain amounts equal to or greater than five inches. The Type IV pattern was most significant in producing heavy rain events in April, accounting for twenty percent of the total.

Types III and IV are similar to the synoptic model as described by Maddox (1979) in his study of heavy rain/flash flood events over the entire U.S. As in the the synoptic model, both Types III and IV involve a moist and ussually deep south and southwest flow through the lower and middle portion of the atmosphere in advance of an approaching cold front and 500 mb trough.

Five of the ninety-seven events were not classified because they did not fit any of the above synoptic types. Of the five events, only two had rain amounts equalling or exceeding five inches.

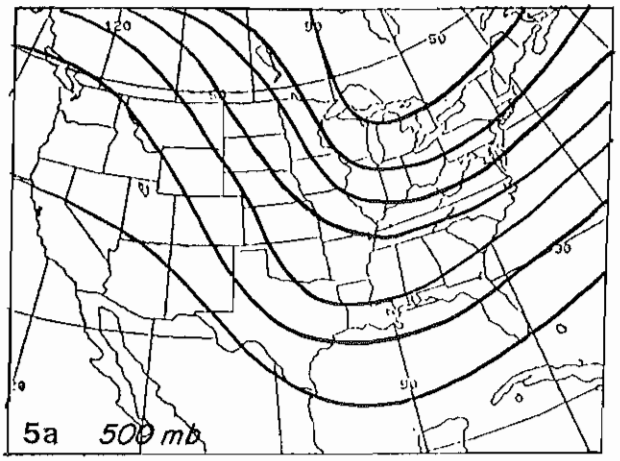

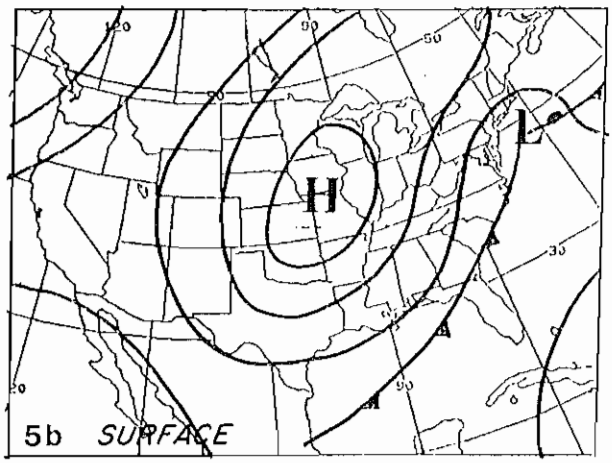

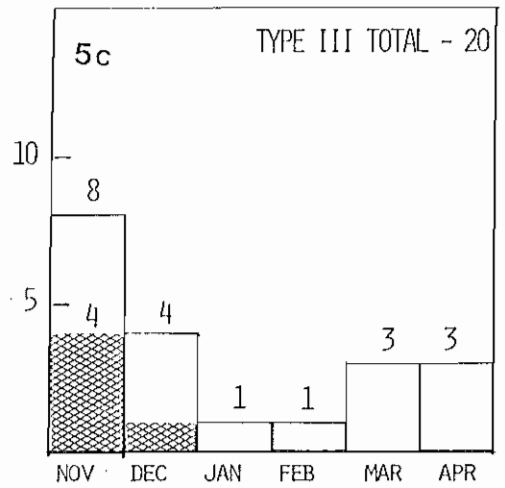

Figure 5. Example of Type III. (5a) a full latitude 500 mb trough extends across the southeast U.S. into the central Gulf of Mexico. (5b) cold front extends across the southeast U.S. into the central Gulf of Mexico. (5c) monthly distribution of heavy rain events associated with Type III.

5.5 Limitations

It should be noted that heavy rain did not always take place over south Florida every time a synoptic pattern described in this paper occurred. This study focused on two important and readily analyzed levels, 500 mb and the surface. However, the classification scheme used in this study has several limitations. The 500 mb and surface pattern were examined prior to the occurrence of heavy rain. Synoptic patterns at 500 mb and the surface can, and in many cases do, undergo changes from when the synoptic pattern was classified and the time the heavy rain events took place. For instance, because of the somewhat crude scale of the 500 mb maps, small vorticity maximas which play significant roles in deepening of troughs were not easily detected. At the surface, changes often occurred with respect to frontal characteristics. In many cases, a front which was stationary at first analysis became a warm front by the time heavy rain occurred or a cold front became stationary during the rain event.

Unfortunately, surface meso-scale features were also not examined in this study because of the time and scale constraints of the maps examined. Like many other significant weather events, heavy rain occurrences are frequently related to meso-scale developments. Many of the heavy rain events over south Florida examined in this study occurred over limited areas, probably as the result of a meso-scale feature developing along the frontal boundary.

Despite these obvious drawbacks and the degree of subjectivity built into the classification scheme, there is great usefulness in using this type of scheme as a first step in forecasting heavy rain the in time period of one to two days. An operational meteorologist can be alerted to begin closely examining additional synoptic and meso-scale data when a synoptic pattern known to cause heavy rain is developing or forecast to develop.

6. CONCLUSION

During the past thirty-six years, ninety-seven heavy rain events occurred over south Florida. In each heavy rain event, at least one station in south Florida reported rainfall amounts equal to or greater than three inches. Two months, November and April, accounted for approximately fifty percent of the heavy rain events.

Nearly ninety-five percent of these heavy rain events were classified according to synoptic patterns at 500 mb and the surface. Four types of synoptic patterns emerged as significant producers of heavy rain over south Florida. The most significant type was a split flow 500 mb pattern with an east/west oriented frontal boundary across south Florida. This synoptic pattern, Type I, was associated with forty-six heavy rain events. The second most significant synoptic type was a full latitude 500 mb trough over the central U.S. and an associated cold front extending from the southeast U.S. into the central Gulf of Mexico. This synoptic pattern, Type III was

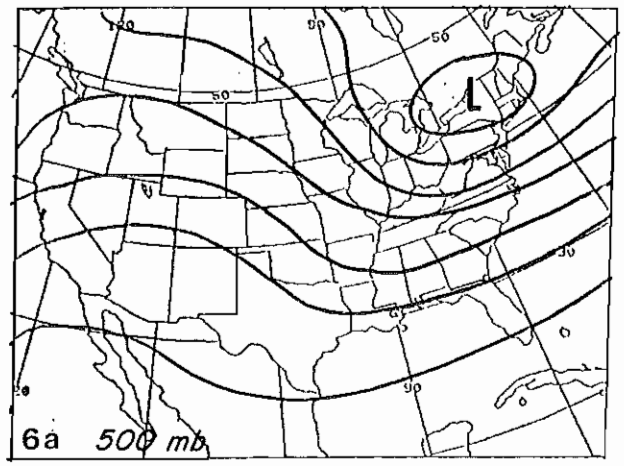

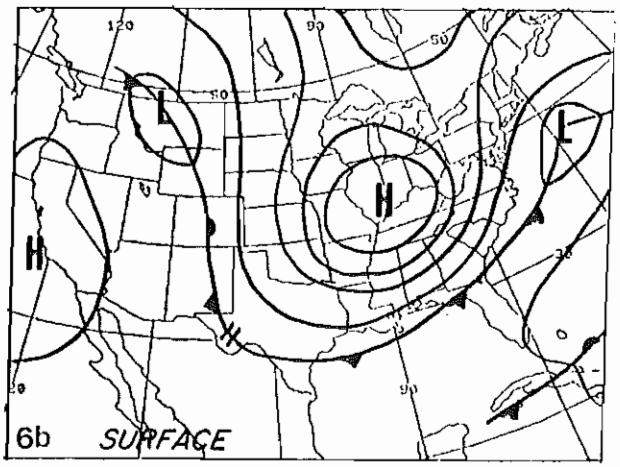

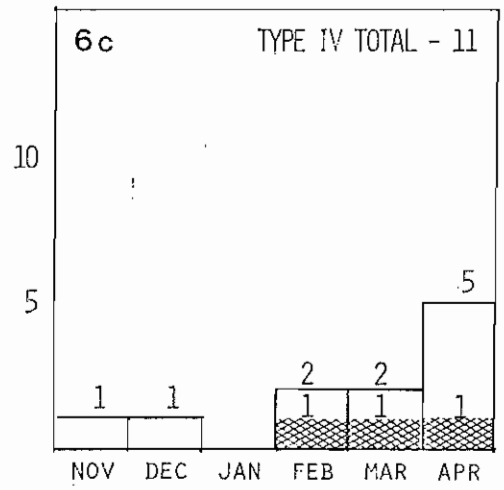

Figure 6. Example of Type IV. (6a) closed 500 mb low is present over southeast Canada with a trough extending south southwest into the lower Mississippi River Valley. (6b) a cold front is located from the Mid-Atlantic states into the northern Gulf of Mexico. (6c) monthly distribution of heavy rain events assoicated with Type IV.

linked to twenty heavy rain events. Type II, a zonal flow at 500 mb with a stationary front over south Florida, accounted for fifteen heavy rain events. The last synoptic pattern, Type IV, accounted for just eleven of the ninety-seven heavy rain events. This synoptic pattern was composed of a deep 500 mb low over southeast Canada with a trough extending into the northern Gulf of Mexico. A surface cold front stretched from the southeast U.S. into the central Gulf of Mexico.

These classification schemes represent the first step in forecasting heavy rain events as they alert the forecaster to which synoptic patterns produce heavy precipitation. Other important factors need to be examined to further understand the causes of heavy rain over south Florida. As mentioned earlier, meso-scale features contribute greatly to many inclement weather events. including heavy rain. Another important factor which has figured prominently in recent heavy rain studies is lower tropospheric warm advection. A study of both of these factors would add greatly to the understanding of heavy rain events over south Florida and likely improve forecasting of these events.

7. ACKNOWLEDGEMENTS

I would like to thank Mr. Ray Biedinger for useful criticism and review of the paper and to Ms. Joan David and Mrs. Mary Damiano for assistance in producing the graphics and the manuscript.

8. BIBLIOGRAPHY

Biedinger, Raymond E., 1985: "Climatology of Heavy Rain Producing Patterns in North Florida." NOAA Technical Memorandum, NWS SR 112, NWS Southern Region QPF Workshop, April 1985.

Belville, James D., and Noreen Stewart, 1983: Extreme Rainfall in Louisiana: The "New Orleans Type". Preprints 5th Conference on Hydrometeorology (Tulsa), Amer. Meteor. Soc., Boston, MA 279-283.

Bosart, Lance F., Barry E. Schwartz, 1979: Autumnal Rainfall Climatology of Bahamas. Monthly Weather Review. Vol 107, pp 1663-72.

Dimego, Geoffrey J., Lance Bosart, and G. William Enderson, 1976: An Examination of the Frequency and Mean Conditions Surrounding Frontal Intrusions into the Gulf of Mexico and Caribbean. Monthly Weather Review. Vol 104, 709-718.

Garcia, Oswaldo, Lance Bosart, and Geoffrey DiMego, 1978: On the Nature of Winter Season Rainfall in the Dominican Republic. Monthly Weather Review. Vol 106, 961-982.

Goodman, Ronald R., Richard Charnick, and Roger NcNeil, 1983: Forecasting Heavy Rain in Alabama. Preprints 5th Conference On Hydrometeorology (Tulsa), Amer. Meteor. Soc., Boston, MA 279-283.

Grice, Gary K., Robert Maddox, 1982: Synoptic Aspects of Heavy Rain Events in South Texas Associated with the Westerlies. NOAA Tech Memo. NWS SR 106, Fort Worth TX.

Maddox, Robert A., 1979a: A Methodology for Forecasting Heavy Convective Precipitation and Flash Flooding. National Weather Digest, Vol 4, No. 4, 30-42.

NOAA, 1948-84: Daily Precipitation Totals. Climatological Data, Florida. NOAA, EDIS, Federal Bldg, Asheville, NC.

----, 1968: Daily Series, Synoptic Weather Maps, Part I, Northern Hemispheric Sea Level and 500 Millibar Charts, Jan. 1948 to Apr. 1968, NCDC, Asheville, NC.

----, 1983: Daily Weather Maps-Weekly Series, April 1, 1968 to Dec 31, 1983. U.S. Government Printing Office. Washington, D.C.

FLOODING ON THE HIGH PLAINS
A CASE STUDY OF THE AUGUST 1, 1985 FLOOD AT CHEYENNE, WYOMING

Robert T. Glancy and John A. Daseler

National Weather Service Forecast Office
Cheyenne, Wyoming

1. INTRODUCTION

In recent years, there has been an increased awareness of flash flooding in the semi arid part of the United States from west Texas northward to eastern Montana. In this belt, several major floods have resulted in loss of life and massive destruction, including the Rapid City flood of June, 1972 (Dennis, et al, 1973), the Big Thompson Canyon flood of July, 1976 (Maddox, et al, 1977), and the Palo Duro Canyon flood of 1978 (Belville, et al, 1980). Analysis of each of these floods has shown that certain meteorological patterns can interact with the uneven topography to produce thunderstorms which drop large amounts of rain over small areas in short periods of time.

Such a flood occurred at Cheyenne, Wyoming on the evening of August 1, 1985. In an area where the average annual precipitation is only 13.41 inches, the storm dropped up to eight inches (Figure 1). Two creeks jumped their banks, and twelve people drowned. Three to four feet of water and hail ponded in the downtown area. Total storm damage exceeded 65 million dollars. This storm was also severe, dropping hail up to two inches in diameter and several funnel clouds which briefly dipped to the ground.

In this paper, we will analyze the synoptic and mesoscale parameters which caused the flood and identify those parameters which may be used in flash flood forecasting procedures in eastern Wyoming. We will also discuss the ramifications of the multiple event threat of the storm.

2. GEOGRAPHIC SETTING AND TOPOGRAPHY

Cheyenne is a town of 53,000 people located on a plateau in southeast Wyoming (Figure 2). The airport elevation is 6155 feet. The north-south Laramie Mountains lie 35 miles to the west with peak elevations in excess of 9000 feet. The land north and east of Cheyenne slopes gently downward to elevations near 4500 feet. A small east-west oriented ridge at about 6400 feet lies seven miles south of Cheyenne. As a result of the terrain, nearly all significant precipitation falls during upslope winds of 350 degrees clockwise through 200 degrees.

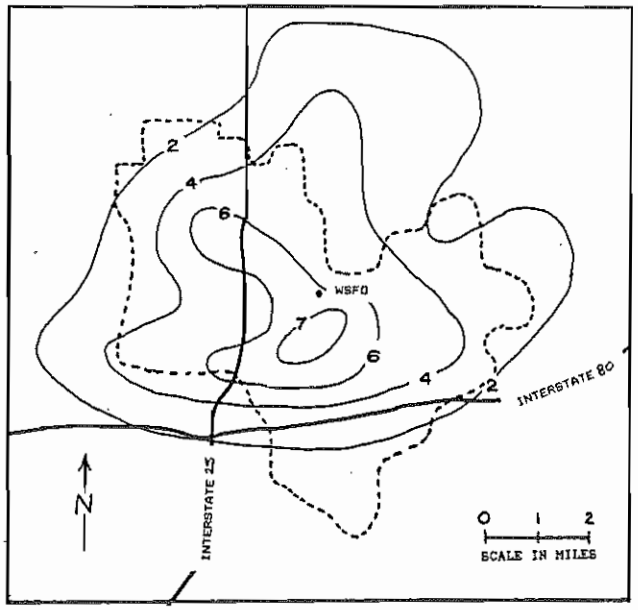

Figure 1. Rainfall from the Cheyenne storm, in inches. Dashed lines indicate city boundary.

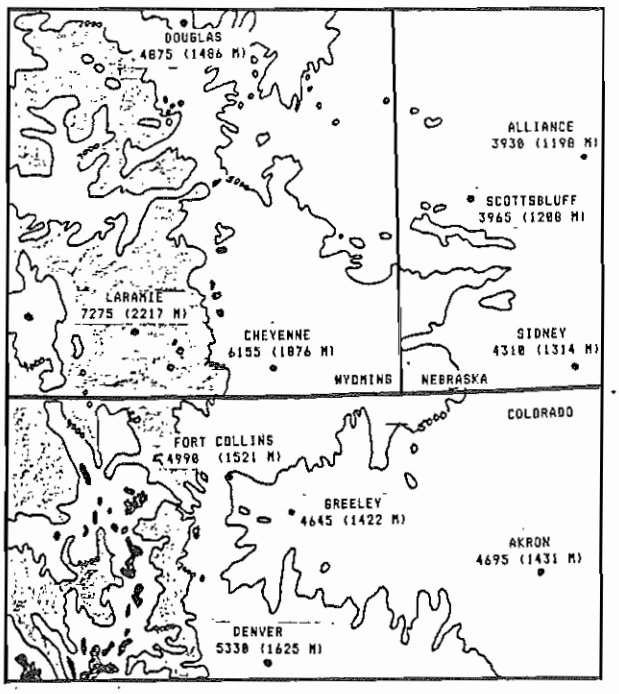

Figure 2. Topography map of area surrounding Cheyenne. Elevations are indicated at 5000, 7000, 9000, and 12,000 feet.

3. SYNOPTIC SETTING

The 12Z (6 AM - all times MDT) synoptic maps showed a stationary surface front along the Front Ranges of Wyoming and Colorado with a cool, moist airmass across the high plains (Figure 3). Fog and drizzle prevailed over a large area from Kansas to northeast Wyoming. At 500 mb (Figure 4), a ridge was located over the dakotas with a closed low over Oregon. A weak trough was moving northeast across Utah and southwest Colorado.

This type of synoptic pattern has been identified by Maddox, et al (1980) as one of four distinct patterns associated with flooding in the western U.S. (Figure 5). The 500 mb trough, a stationary surface front, deep moisture to the middle levels of the atmosphere, and strong conditional instability were all implicated by Maddox as factors in this flooding pattern.

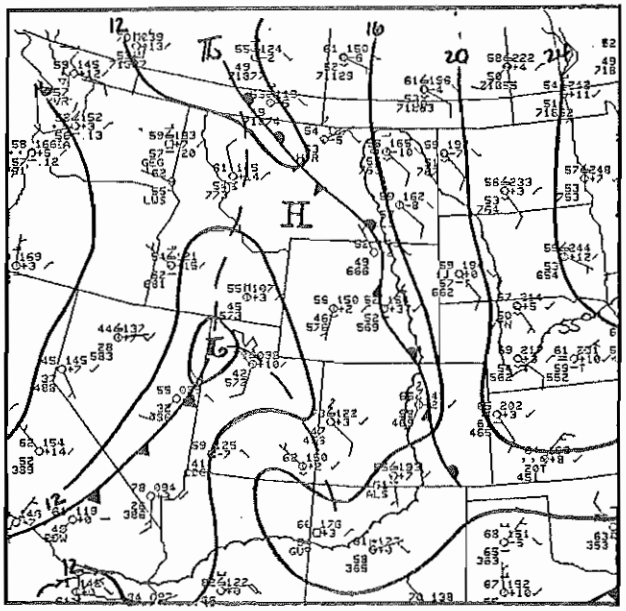

Fig. 3. Surface analysis for 12Z (6 AM) August 1. Scalloped line indicates dewpoints of 55 degrees.

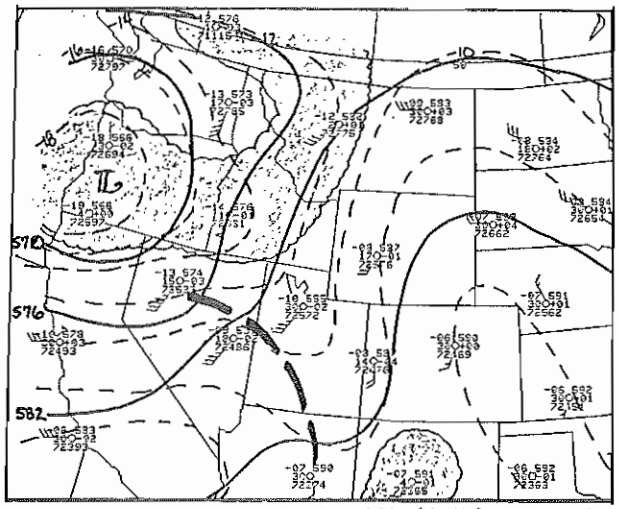

Fig. 4. 500 mb analysis for 12Z (6 AM) August 1. Heights - solid lines; isotherms - dashed lines; dewpoint depressions 5 deg. C - shaded area; trough position - heavy dashed line.

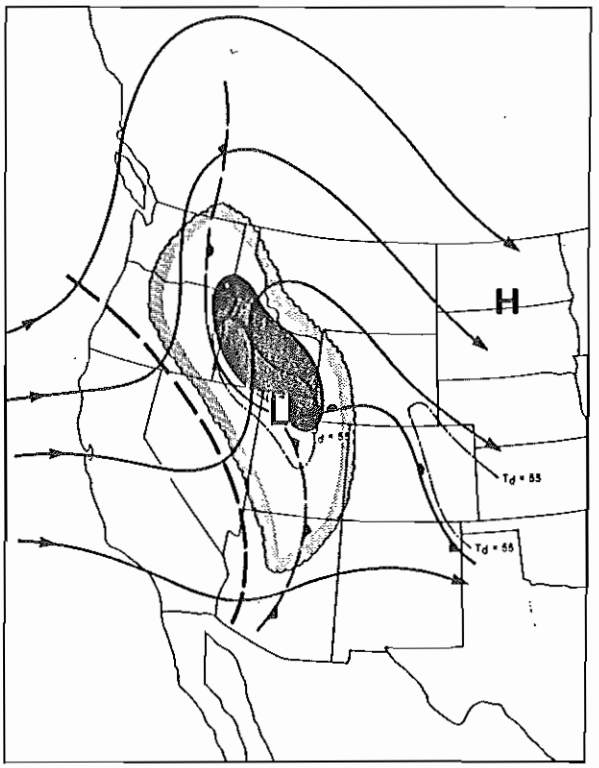

Fig. 5. Generalized 500 mb and surface patterns for a type of western flash floods. 500 mb flow - streamlines; 500 mb trough - heavy dashed line; 500 mb moisture - scalloped line; areas of high surface dewpoints - dot/dash line. Area of greatest flash flood potential in next 3 hours is shaded. From Maddox, et al (1980).

The 12Z Denver sounding (Figure 6) revealed considerable instability with a minus 4 lifted index expected in the afternoon. The airmass was fairly moist below 550 mb, with a precipitable water value of 0.87 inches, 128 percent of normal. South or southwest winds of 10-20 knots extended from the surface through 400 mb. Winds veered to the west and increased to 50 knots near 200 mb. The Lander, Wyoming sounding exhibited less moisture, but stronger winds. Winds were 10-25 knots from the southwest below 400 mb, with a maximum of 65 knots at 200 mb.

These parameters were all present on August 1st. The morning forecast had a 50 percent chance of thunderstorms, with the possibility of both severe weather and localized flooding. The primary threat was perceived to be severe weather due to the strong instability and stronger winds above 400 mb. Doswell (1980), found that the synoptic pattern for significant convection in eastern Colorado was very similar to Maddox's flooding pattern. The exception was that jet level winds were stronger in Doswell's study.

The other morning forecast problem was to isolate the threat area. Moist, unstable air lay across most of eastern Wyoming, but the threat area was narrowed by 1 pm when the National Severe Storms Forecast Center (NSSFC) issued a severe thunderstorm watch for southeast Wyoming and adjacent areas of Colorado and Nebraska.

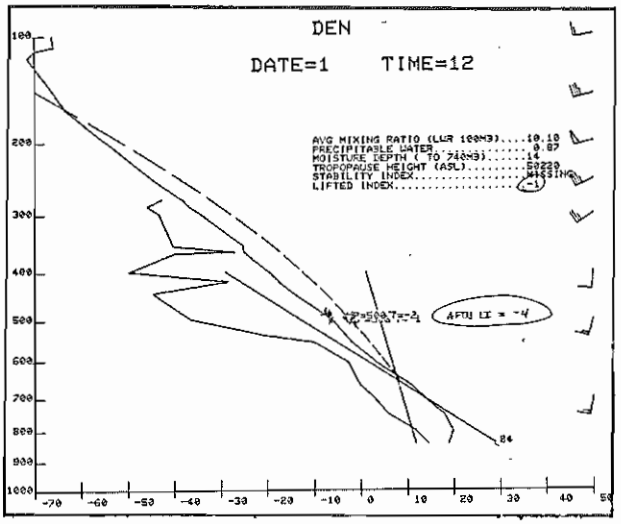

Fig. 6. Skew T sounding from Denver, Colorado at 12Z (6 AM) on August 1. Afternoon lifted index and convective temperature are calculated.

Fig. 7. Satellite pictures at 21Z (3 PM) August 1 and at 03Z (9 PM). Subtropical jet stream indicated by solid white line with arrows arcing across Arizona into Wyoming.

4. EVOLUTION OF FEATURES

4a. Upper Air

Satellite pictures showed the subtropical jet bulging northeast across Colorado in the afternoon of August 1st (Figure 7). An associated jet streak provided upper difluence over southeast Wyoming in the late afternoon and early evening of August 1st. Winds at Lander increased to 80 knots at 250 mb by 00Z (6 PM). This has been discussed as favorable vertical support for severe convection (Beebe and Bates, 1955, and McNulty, 1977). The jet streak has been noted in several flooding events including Austin, Texas (Grice and Maddox, 1982) and Palo Duro Canyon, Texas (Belville, et al 1980).

The 500 mb trough by 00Z (6 PM) extended from central Wyoming to central Colorado (Figure 8). There was an associated weak thermal trough.

Moisture increased at middle levels as the subtropical jet bulged to the northeast. By 00Z, the precipitable water at Denver was 0.99 inches, 152 percent of normal. Lander increased to 162 percent of normal. In the southerly circulation around the plains high, 850 mb dewpoints increased by 5 to 19 degrees at Rapid City, and by 4 to 16 degrees at North Platte.

The interpolated lifted index over Cheyenne was about a minus 6 at 00Z (6 PM).

Thus the synoptic pattern was very favorable for strong convective development. But why did the thunderstorm form over Cheyenne and remain stationary? We believe this was due to a unique set of afternoon mesoscale surface developments.

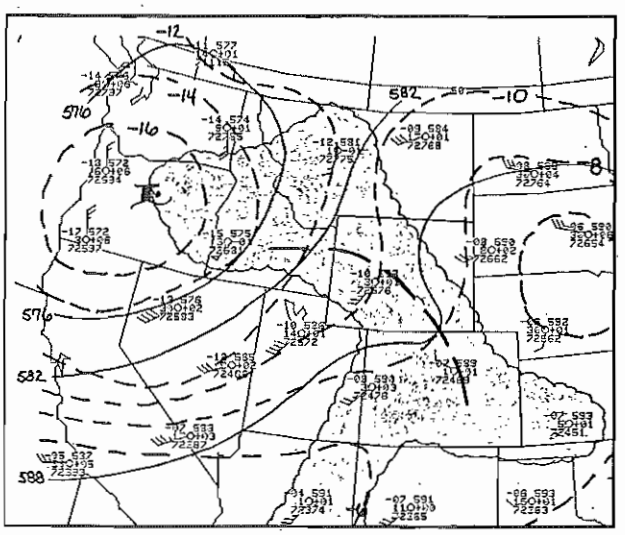

Fig. 8. 500 mb analysis for 00Z August 2 (6 PM MDT August 1). Analysis features same as for Figure 4.

4b. Surface

Upslope stratus cleared over eastern Wyoming by 18Z (12 noon), but overcast skies persisted over western Kansas and Nebraska through mid afternoon. This increased the thermal gradient in eastern Colorado and southern Wyoming, in turn setting up a thermal low along the stationary boundary between Denver and Cheyenne. Dewpoints were quite high, exceeding 60 degrees through most of the afternoon.

Convection began by 18Z southwest of Cheyenne. One important cell moved northeast, passing west and then north of Cheyenne between 20Z and 22Z. The first funnel cloud of the day was associated with this cell. It was sighted 14 miles north of Cheyenne between 2101Z and 2107Z (301 PM to 307 PM). An outflow boundary from this cell passed southwestward through Cheyenne about 22Z (4 PM), shifting the winds to northerly.

The event was truly mesoscale in nature, thus the data set is not complete. It was difficult to determine the mesoscale situation even on a detailed surface analysis (Figure 9). However, mesoscale development could be inferred using the sequence of Cheyenne observations (Figure 10), as well as by radar and spotter reports.

The outflow boundary intersected the thermal trough southwest of Cheyenne, and aided in the intensification of the thermal low. Winds at Cheyenne responded by turning east/southeast and increasing to 15-20 knots by 00Z (6 PM), producing a good upslope flow into the meso low.

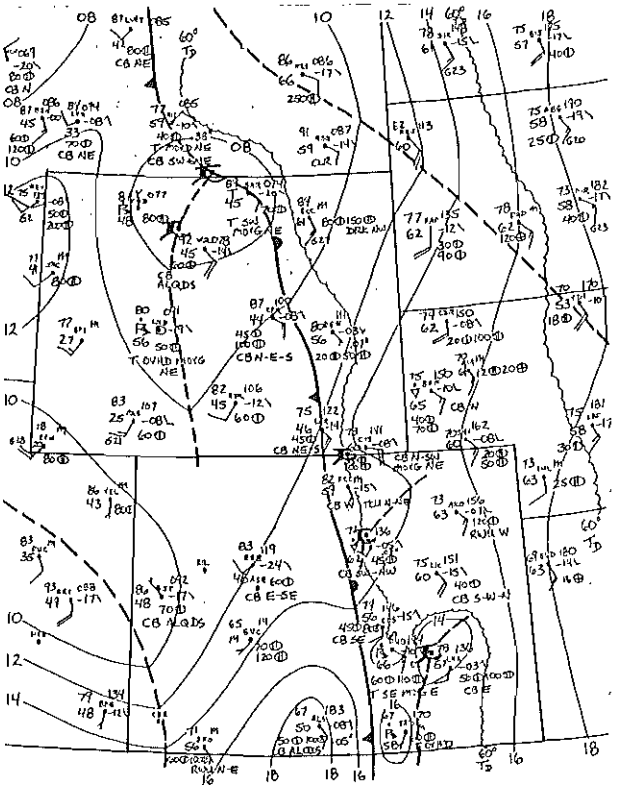

Fig. 9. Mesoscale surface analysis at 00Z August 2 (6 PM August 1). Scalloped line indicates 60 degree dewpoints.

TIME	CLOUDS	VSBY/WEATHER	SLP	T	TD	WINDS	ASI	REMARKS / ADDITIVE DATA
2047	40 SCT 100 SCT 250 -BKN	40	141	82	59	1316	021	CB RWU S-N STNRY TCU ALODS / 717 1963
2102		FUNNEL CLD						FUNNEL CLD B01 14N MOVG NE
2111	40 SCT E100 BKN 250 BKN	30 T				1813	020	FUNNEL CLD E07 TB09 OVHD MOVG E
2149	40 SCT E100 BKN 250 BKN	30 T	148	72	56	3507	020	T NE MOVG E CB ALODS MOVG E
2223	40 SCT 100 SCT E250 BKN	30				0609	020	TE22 MOVD E CB SE-NE MOVG E
2251	40 SCT 100 SCT E250 BKN	30	148	72	57	0713	020	CB NE-S MOVG NE TCU ALODS
2349	35 SCT 100 SCT 250 SCT	30	141	73	60	1019	018	CB N-SW MOVG NE / 808 1963 82
2356	35 SCT 100 SCT E250 BKN	30 T				1118	019	TB55 S-E MOVG E CB NE MOVG E
0022	M35 BKN 100 BKN 250 BKN	15 TRWA				1212	019	AB20 HLSTO 3/8 RB20 T OVHD MOVG E
0039	M35 BKN 100 BKN 250 BKN	15 TRW				0515	019	AE35 HLSTO 1/2 T OVHD MOVG E
0051	M35 BKN 100 BKN 250 BKN	10 TRW	150	61	56	0911	019	T S MOVG SE PCPN 051
0056	M35 BKN 100 BKN 250 BKN	2 TRW+A				1111	020	AB53 HLSTO 5/8 T OVHD MOVG SE
0111	M35 BKN 100 BKN 250 BKN	2 T+RW+A				0414	019	HLSTO 7/8 T OVHD STNRY FQT LTG
0129	M35 BKN 100 BKN 250 BKN	2 TRW+				0415	018	AE20 HLSTO 5/8 T OVHD STNRY FQT LTG
0124		FUNNEL CLD						FUNNEL CLD B24 5SW MVMNT UNKN
0141	M35 BKN 100 BKN 250 BKN	10 FUNNEL CLD TRW-				0515	019	FUNNEL CLD 3SW MOVG NE T OVHD MOVG N FQT LTG
0149	M35 BKN 100 BKN 250 BKN	5 FUNNEL CLD TRW	155	66	62	0214	020	FUNNEL CLD 3SW MOVG NE T OVHD MOVG NE PCPN 075
0211	W10 X	1 TRW+A				2814	024	AB05 HLSTO 3/8 FUNNEL CLD E07 T OVHD STNRY
0221	W5 X	1/2 TRW+				E2420	025	AE20 HLSTO 3/8 T OVHD STNRY FQT LTG
0227	W5 X	1/2 T+RW+A				E2435G49	023	AB25 HLSTO 7/8 T OVHD STNRY FQT LTG
0249	W2 X	1/4 T+RW+A				E1730	023	HLSTO 1 T OVHD STNRY PCPN 280 / 21505 FOUR
0311	E35 BKN 100 BKN 250 BKN	5 TRW				E1725	019	AE05 HLSTO 1 T N-SW MOVG SE FQT LTG
0334	35 SCT 100 SCT 250 SCT	15 RW-				E1820	021	TE33 MOVD SE FQT LTG SE
0343	35 SCT 100 SCT 250 SCT	15	163	61	56	E1825	022	RE40 PCPN 280 CB SE MOVG SE FQT LTG SE

Fig. 10. Hourly and special surface observations at the Cheyenne WSFO through the late afternoon and early evening of August 1 (21Z August 1 to 04Z August 2 or 3 PM to 10 PM). Abbreviations: SLP - sea level pressure; ASI - altimeter setting.

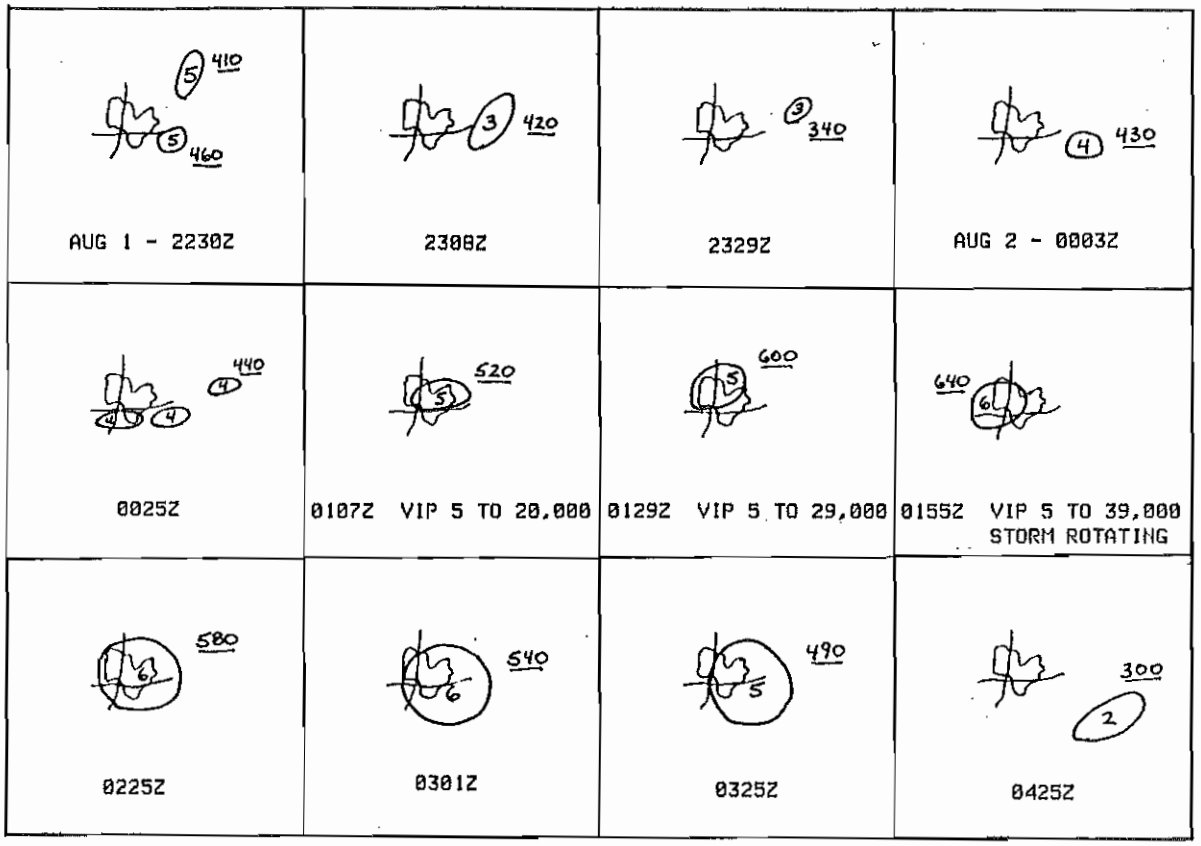

Fig. 11. Depiction of Alliance, Nebraska radar reports from 2230Z August 1 to 0425Z August 2 (430 PM to 1025 PM) on a background of the city boundary and the two interstates through Cheyenne. Maximum VIP levels are indicated for each cell. Underlined numbers indicate radar tops in hundreds of feet. Additive remarks are also shown.

As convergence increased into the meso low, radar data (Figure 11) from the NWS 10 cm WSR-74S radar at Alliance, Nebraska (AIA) showed convection developing westward toward the meso low by 0025Z (625 PM). The storm began to consolidate over Cheyenne between 630 PM and 700 PM. At 0107Z (707 PM), AIA measured a radar top of 52,000 feet. The storm then remained in the CHeyenne area for the next two hours. Storm rotation was noted from 0137Z (737 PM) to 0208Z (808 PM). Throughout this active stage of the storm, feeder cells were developing along the ridge south of Cheyenne and moving north in the geostrophic flow, merging into the storm over Cheyenne. This was observed by one of the authors 50 miles south in Fort Collins, Colorado.

The storm moved southeast after 03Z (9 PM) as it lost its upper support. The subtropical jet streak moved rapidly out of Wyoming in the evening. Extrapolation of the weak trough at 500 mb would have moved it across southeast Wyoming between 02Z and 03Z (8-9 PM). Coincidently, the updraft of the storm apparently collapsed, dropping an estimated 3.5 inches of rain at the Cheyenne WSFO between 02Z and 03Z (8-9 PM).

5. DISCUSSION AND CONCLUSIONS

Forecasters must watch both mesoscale and rapidly changing synoptic patterns in order to adequately prepare for short term flood forecasting. Features which appeared to influence the Cheyenne flood and which were also documented in other floods include:

a) Outflow boundaries pushing into higher terrain.
b) The development of a meso low along a preexisting boundary.
c) A push of subtropical moisture and/or a jet streak moving over the threat area.
d) Convection shown on radar to be moving/developing towards a meso low.

The identification of the immediate threat remains a problem since this type of flooding situation also occurs in an environment that frequently produces severe weather. The amount of moisture appears to be a key, and forecasters should closely monitor precipitable water values, satellite pictures, and other clues to excessive amounts of moisture in the atmosphere.

In southeast Wyoming, a 55 to 60 degree dewpoint appears to have some value for flash flood forecasting. A local study has shown that dewpoints of 58 degrees or higher are only observed about two percent of the time in mid summer at Cheyenne, and most flash floods on record in southeast Wyoming have occurred when the dewpoints were 58 degrees or higher.

A possible clue that severe weather and flooding could occur simultaneously is an advancing subtropical jet streak. The strong winds aloft could provide enough vertical lift for the development of hail and tornadoes. Of course, above normal amounts of moisture must also be present, as well as a surface mesoscale forcing mechanism such as terrain, an outflow boundary, or convergence into a meso low. The Cheyenne flood had all three of these mechanisms operating.

Convective situations which produce both flooding and severe weather on the high plains deserve further study. Future flooding events of this type should be documented in order to increase our understanding of these complicated events.

6. REFERENCES

Beebe, R.G., F.C. Bates, 1955: A mechanism for assisting in the release of convective instability. Mon. Wea. Rev., 83, 1-10.

Belville, J.D., G.A. Johnson, 1980: A synoptic and mesoscale analysis of the Palo Duro Canyon flash flood and associated severe weather. Preprints Second Conference on Flash Floods (Atlanta), AMS, Boston, 30-37.

Doswell, C.A., III 1980: Synoptic scale environments associated with high plains thunderstorms. Bull. Am. Met. Soc., 61, 1388-1400.

Grice, G.K., R.A. Maddox, 1982: Significant radar characteristics of the Austin, Texas flash flood. Preprints Fifth Conference on Hydrometeorology (Tulsa), AMS, Boston, 103-110.

Maddox, R.A., F. Caracena, L.R. Hoxit, C.F. Chappell: Meteorological Aspects of the Big Thompson Flood of 31 July, 1976. NOAA Tech. Rep. ERL 388 APCL 41, 83 pp.

Maddox, R.A., L.R. Hoxit, F. Canova, 1980: Meteorological characteristics of heavy precipitation and flash flood events over the western United States. NOAA Tech. Memo. ERL APCL-23, 87pp.

McNulty, R.P., 1977: On upper tropospheric kinematics and severe weather occurrence. Mon. Wea. Rev., 106, 662-672.

Dennis, A.S., R.A. Schleusener, J.H. Hirsch, A. Koscielski, 1973: Meteorology of the Black Hills Flood of 1972. Institute of Atmospheric Sciences, South Dakota School of Mines and Technology Report 73-4, 41pp.

NORTH TEXAS HEAVY RAIN ASSOCIATED WITH 500 MB CLOSED LOWS

Ernest L. McIntyre II

National Weather Service Forecast Office
Fort Worth, Texas 76102

1. INTRODUCTION

Maddox et al. (1979) considered 151 significant non-tropical heavy precipitation events across the United States and classified them according to similar synoptic and mesoscale mechanisms. Grice and Maddox (1982) analyzed heavy rains over South Texas and noted that the details of South Texas synoptic and meso-patterns were considerably different than the generalized models presented by Maddox et al. (1979). Read (1985) initiated the current study of North Texas heavy rain with an examination of summer season heavy rain events.

The purpose of this study is to expand the examination of North Texas heavy rain events by considering those events which developed in association with 500 mb closed lows. The approach of the paper is designed to help the WSFO Fort Worth forecaster recognize the upper air and surface patterns associated with this type of heavy rain event and assist him in the location and timing of flash flood watches.

2. DATA

Read (1985) examined rainfall records for North Texas climatological stations for the period 1974-1984 identifying all days on which five or more inches of rain fell in a 24-hour period. During the eleven year period twelve heavy rain events were associated with 500 mb closed lows. In addition, two heavy rain events associated with 500 mb closed lows occurred during the spring of 1985. These events were also included in the study.

Data sets for the synoptic time just prior to the onset of heavy rain were assembled for twelve of the events. Data sets for two events were incomplete. The data sets included charts for the standard levels 850, 700, 500, 300 and 200 mb and 3-hourly surface charts. In addition, hourly data and satellite imagery were available for the two 1985 events.

3. GENERAL CHARACTERISTICS

Table 1 lists the heavy rain events which comprise this study. Two of the events produced rainfall amounts of just over five inches while the event of May 12-13, 1982 produced the greatest amount with almost fourteen and a half inches. The number of North Texas climatological stations reporting rainfall amounts of five inches or more probably gives some indication of the geographical extent of the heavy rain and are also presented in Table 1.

Figure 1 shows the monthly distribution of the fourteen heavy rain events. Ten of the fourteen events occurred during the period March through June. Four events occurred in the fall (October-November).

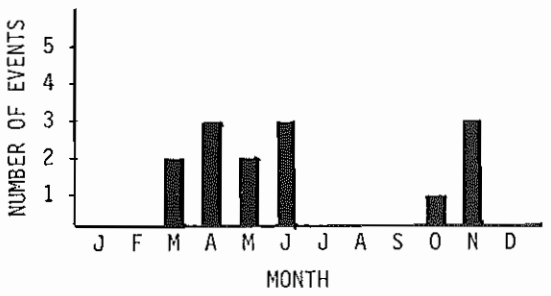

Figure 1. Monthly distribution of heavy rain events.

Figure 2 shows the nocturnal tendency of the heavy rain events. About seventy-five percent of the events began during the nighttime hours.

DATE	MAXIMUM RAINFALL	NUMBER OF STATIONS REPORTING AMOUNTS ≥ 5 INCHES
Jun 7-8, 1974	5.26	3
Oct 31-Nov 1, 1974	8.95	26
Mar 8, 1976	5.08	2
Mar 26-27, 1977	6.90	18
Apr 14-16, 1977	7.07	6
Apr 9-10, 1978	5.33	2
Nov 15-16, 1978	8.38	6
May 21, 1979	5.45	4
Jun 5, 1979	5.02	1
Nov 21, 1979	6.29	1
May 12-13, 1982	14.40	26
Nov 27, 1982	5.15	3
Apr 27-28, 1985	6.00	1
Jun 5-6, 1985	7.25	11

Table 1. Maximum rainfall for heavy rain events and number of North Texas climatological stations reporting amounts ≥ 5 inches.

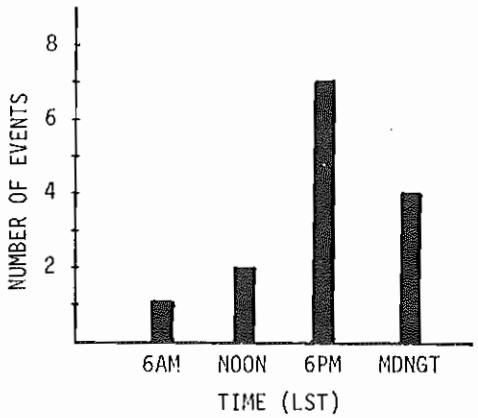

Figure 2. Time of onset of heavy rain events.

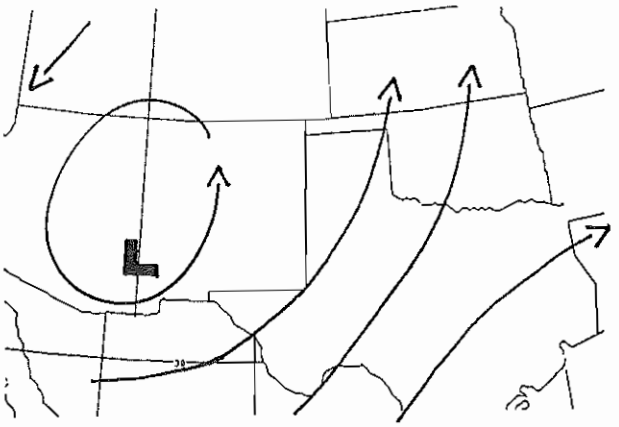

Figure 3. 500 mb flow pattern for a typical North Texas heavy rain event involving a 500 mb closed low.

4. THE 500 MB PATTERN

The 500 mb pattern associated with the North Texas closed low heavy rain events is easily recognizable. A typical pattern is shown in Figure 3. The 500 mb pattern exhibited a closed circulation within the southern branch of a split flow pattern. The closed lows were south of 40 degrees north latitude and between 105 and 112 degrees west longitude. Most of the events occurred with a large amplitude ridge over the eastern United States. The onset of the events usually occurred with the closed low well to the west of the heavy rain area.

NOAA's "Daily Weather Map" series was examined for the 1974-1984 period to determine the frequency of this 500 mb pattern. The pattern was observed to occur an average of 5.8 times each year. Rainfall of 5 inches or more was associated with the pattern an average of 1.1 times each year. During the eleven year period, the probability of heavy rainfall was approximately 20 percent each time the 500 mb closed low pattern was observed. Furthermore, rainfall of 3 inches or more was associated with the pattern just over 50 percent of the time.

5. OTHER UPPER AIR FEATURES

Figure 4 shows the mean temperature, dewpoint and wind at the standard levels at the onset of the North Texas closed low heavy rain events. Also shown are surface temperature and dewpoint values, and K-indices. The composite sounding is characterized by a strong low level jet at 850 mb and deep moisture.

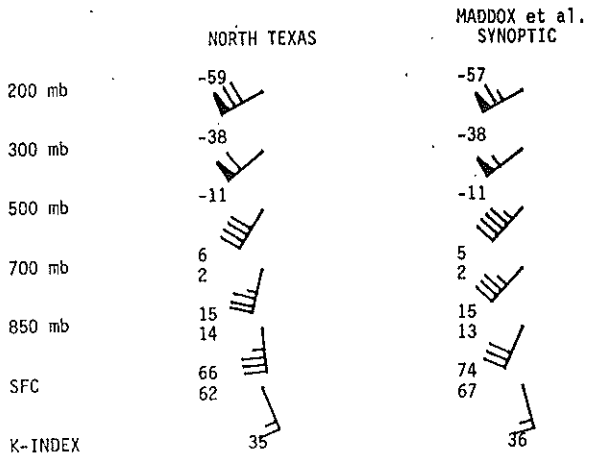

Figure 4. Mean values of temperature, dewpoint, winds and K-value for North Texas closed low heavy rain events and for United States synoptic-type flash flood events from Maddox et al. (1979).

The North Texas composite sounding is compared in Figure 4 to the Maddox et al. (1979) composite sounding for synoptic-type flash flood events. Very close agreement is observed at 500 mb and above. At 850 mb and at 700 mb, winds were more southerly in the North Texas events and at the surface were a little more southeasterly.

Although surface temperatures and dewpoints were generally in the 60's and 70's for the North Texas events, two events occurred with temperatures and dewpoints in the 40s. Warm advection was present at the 850 mb level in most of the events and was present at 700 mb in all events. The axis of the 850 mb moisture was over the heavy rain area in most of the events but was just to the east of the area in two events.

The heavy rain area was in the right rear quadrant of an upper tropospheric jet in about half of the cases. Upper tropospheric diffluence was present in all of the cases.

6. THE SURFACE BOUNDARY

The surface boundary provides a focal point for the development of strong convection. The position of the boundary determines the geographic location of the heavy rain. The surface boundaries associated with the North Texas events were varied and patterns other than those presented below may be possible.

Two of the North Texas events were associated with east-west oriented stationary fronts. The heavy rains in each of these cases occurred a couple of hundred miles north of the surface boundary, in the vicinity of the 850 mb front. Figure 5 shows the surface

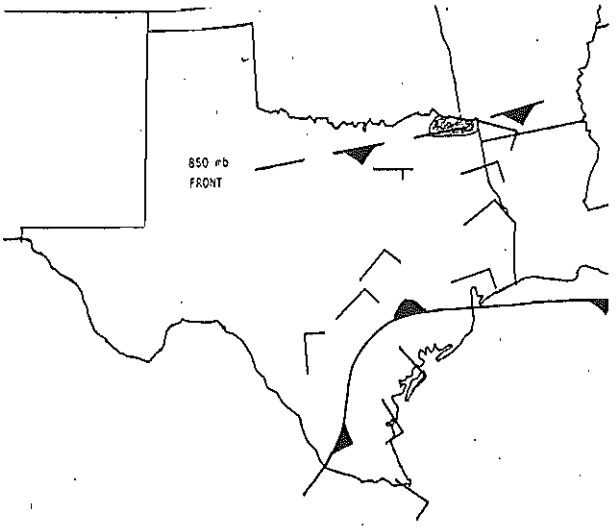

Figure 5. Typical surface pattern where heavy rain (shaded area) fell well north of an east-west oriented stationary front.

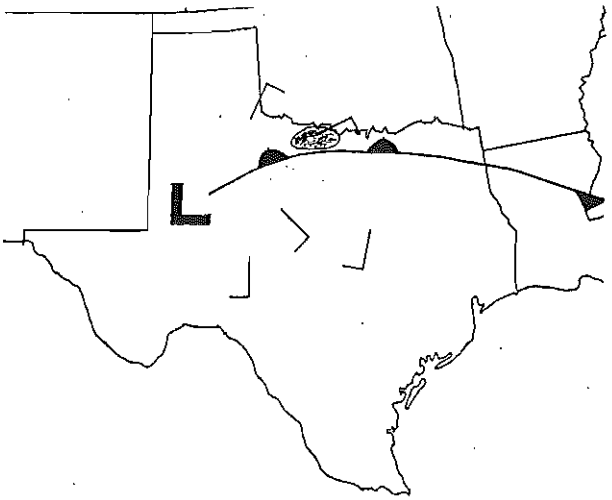

Figure 6. Typical surface pattern where heavy rain (shaded area) fell just north of a warm front.

features typical of these events along with the position of the 850 mb front.

Another event occurred just to the north of a slow-moving east-west oriented warm front as depicted in Figure 6.

Five events occurred along northeast to southwest oriented stationary or slow-moving cold fronts. The heavy rain areas in these cases were along and just north of the frontal boundary (Figure 7).

One event was associated with a nearly north-south oriented slow-moving cold front. As shown in Figure 8, the heavy rain in this case fell in an area which was centered just east of the front.

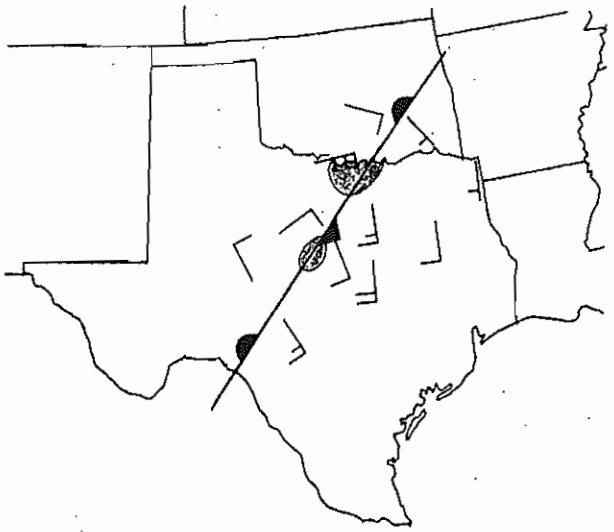

Figure 7. Typical surface pattern where heavy rain (shaded areas) fell along and just north of a northeast-southwest oriented stationary front.

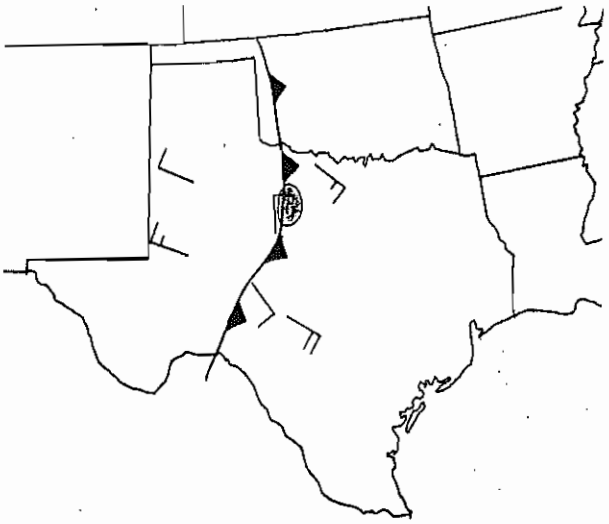

Figure 8. Typical surface pattern where heavy rain (shaded area) fell along a north-south oriented cold front.

The orientation of the frontal boundaries was related to the 500 mb patterns. When the 500 mb closed low was situated in a north-south oriented trough with the closed low to the west of Texas, the fronts tended to be oriented more nearly north to south.

When the 500 mb closed low was situated northwest of Texas or when the 500 mb low was in a northeast to southwest oriented trough, with a strong short wave moving through the westerlies north of Texas, the surface fronts tended to be oriented more nearly northeast to southwest.

Three of the North Texas events occurred along thunderstorm outflow boundaries which were a good distance from any frontal boundaries. In all three cases well-defined outflow boundaries developed on the south or southeast side of on-going convective activity and moved slowly toward the south or southeast (Figure 9).

In most cases the surface boundaries and heavy rain areas of the North Texas events corresponded closely to those described by Maddox et al. (1979) in their synoptic, frontal and mesohigh-type events. The exceptions were the overrunning events which occurred well to the north of a surface boundary.

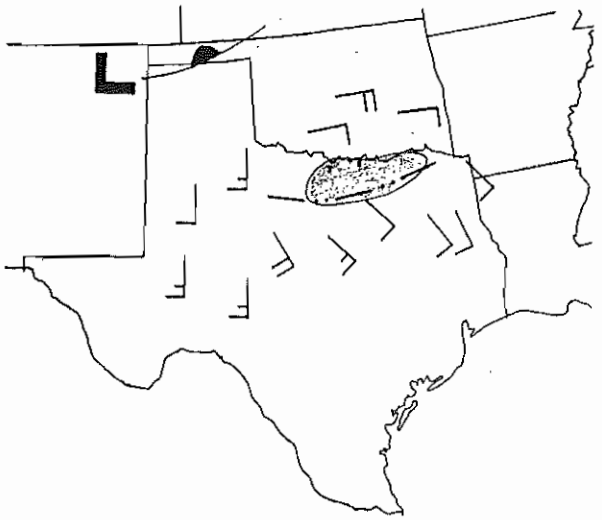

Figure 9. Typical surface pattern where heavy rain (shaded area) fell along and north of a thunderstorm outflow boundary.

7. TIMING OF THE HEAVY RAIN EVENTS

As described in Figure 2, the majority of North Texas heavy rain events associated with 500 mb closed lows began during the evening or nighttime hours. In order to alert the greatest number of people to the flash flood potential, it is therefore important that watches be issued during the late afternoon or early evening, which may be several hours before the onset of the event.

Figure 3 indicated that the onset of heavy rain in North Texas occurred with the 500 mb closed low well to the west of Texas. Figures 10 and 11 present almost concurrent radar and 500 mb vorticity patterns for two of the events. The figures indicate that strong convection can begin well ahead of significant 500 mb positive vorticity advection.

Radar and satellite data were not available to determine if a similar relationship existed in all the cases of

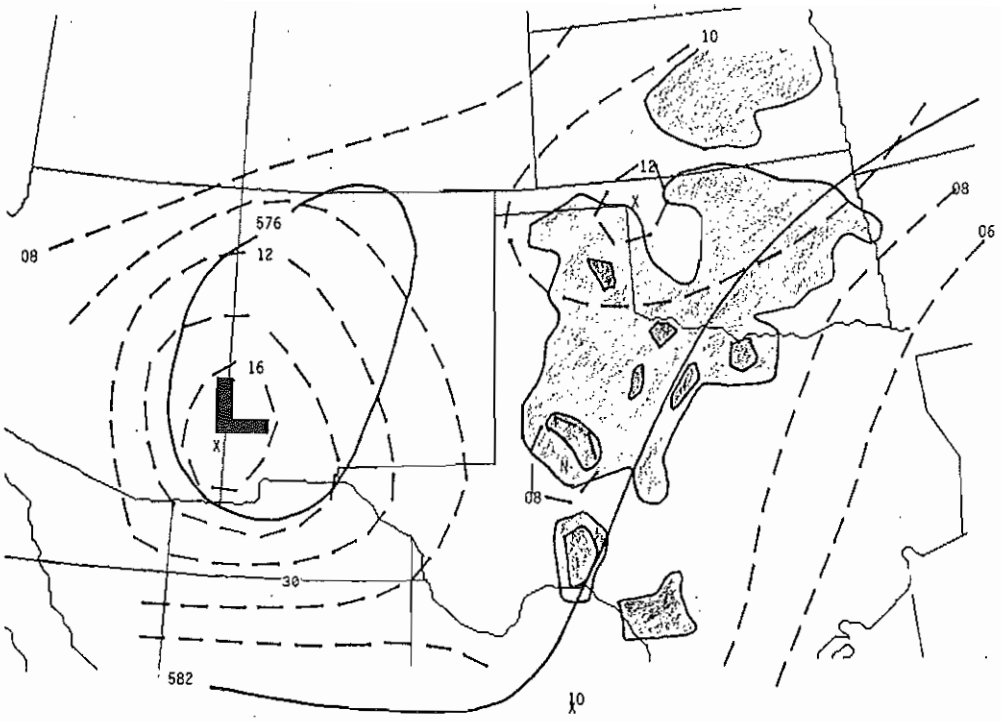

Figure 10. 500 mb vorticity (dashed lines), 500 mb heights and radar contours for 12z June 10, 1985.

this study. But the evidence presented indicates that North Texas forecasters should not wait for impressive positive vorticity advection before considering heavy rainfall. It appears that weak short waves embedded in the flow around the low, along with lower-level mechanisms such as frontal convergence and warm advection are sufficient to initiate the significant convection.

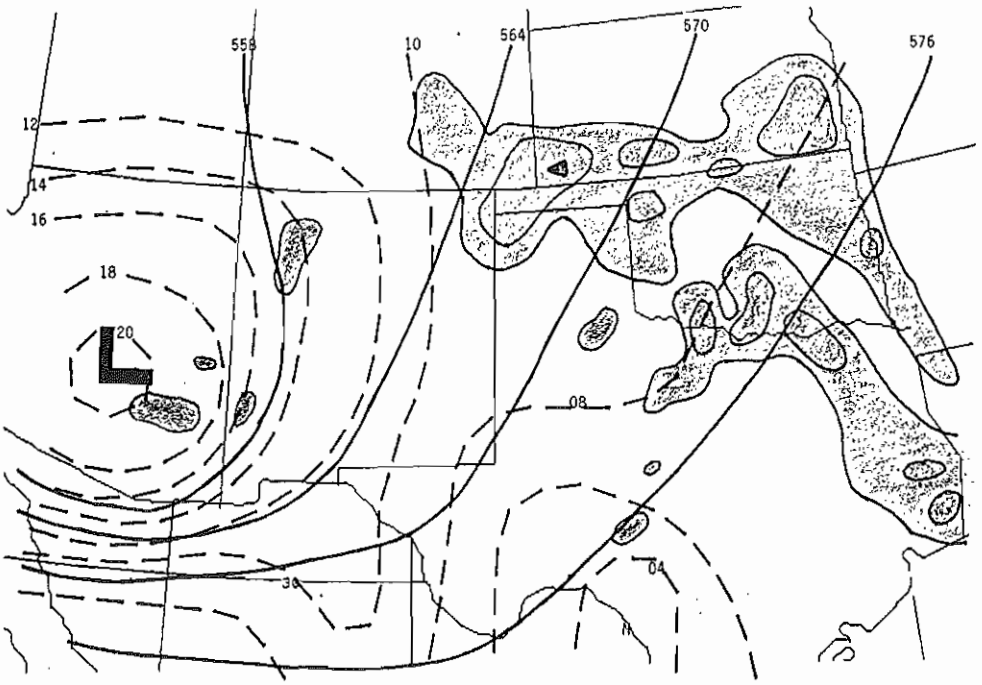

Figure 11. 500 mb vorticity (dashed lines), 500 mb heights and radar contours for 12z May 12, 1982.

8. DISCUSSION

Is it possible to forecast heavy rain events associated with 500 mb closed lows? It should be in North Texas, given the infrequency of the 500 mb pattern and the relatively high rate of occurrence of heavy rains associated with the pattern.

North Texas forecasters should consider the possibility of heavy rain with the 500 mb pattern whenever (1) a front is across North Texas parallel to the upper level flow and (2) instability and moisture are present across the area.

Those events where heavy rains occur without a frontal boundary are certainly less forecastable. However, in such cases areas of convection should be watched closely for the development of outflow boundaries. The events which occur without any type of surface boundary (e.g. similar to those in this study which occurred near the 850 mb front) are the most difficult. Hopefully more attention can be focused on these in the future so that a better understanding can be developed.

9. REFERENCES

Maddox, R.A., C.F. Chappell and L.R. Hoxit, 1979. Synoptic and mesoscale aspects of flash flood events. Bull. Amer. Meteor. Soc., 60, 115-123.

Read, W.L., 1985. Heavy rain associated with northwest flow aloft. 1985 Southern Region OPF Workshop.

PUERTO RICO'S SEVERE RAINFALL EVENT MAY 15-19, 1985: AN INCIDENT OF HEAVY RAINFALL PRODUCTION IN THE CARIBBEAN INFLUENCED BY NON-TROPICAL CIRCULATION PATTERNS

Jere R. Gallup

NOAA-National Weather Service
Weather Service Forecast Office
San Juan, Puerto Rico 00913

1. INTRODUCTION

This paper describes one of the important meteorological patterns that seasonally results in heavy rainfalls over tropical latitudes. It is termed non-tropical to distinguish it from other tropical systems and wind patterns responsible for heavy rains that occur during the summer and early fall months and because its essential origin is non-tropical.

During the period 15-19 May 1985, a developing upper-level trough in the westerlies penetrated southward into the north central Caribbean and was eventually reflected within the low-level wind field. The atmospheric changes that resulted from this system produced the first major flood event in recent years of such a widespread nature, affecting almost all the northern, central and eastern drainages of Puerto Rico. Flooding was also reported in some western and southern parts of the island but was generally of a minor nature. Damage figures from federal estimates amounted to $37 million with several bridges washed out, 10 to 12 homes washed away in the Utuado and Jayuya area, but amazingly only one fatality. Evacuations were large with 3,500 to 4,000 people in flood shelters.

Heaviest total accumulations (figure 1) fell over the interior highlands of central and eastern Puerto Rico supporting the assumption that orographic influences had much to do with the event. Some outstanding rainfall rates that characterize the efficiency with which rainfall was being produced were 14.20 inches in 24 hours at Adjuntas, 3.50 inches in one hour and 0.55 of an inch in 10 minutes read from the Valenciano gage at San Lorenzo (part of the Enhanced Alert System from telemetering rainfall).

This report presents the evolution of this situation in a chronological setting introducing certain signature patterns that occurred within the atmosphere prior to and during the flood event. Five fundamental analogs this event shares with other past ones that have reached noteworthy proportions are also highlighted. These are (1) upper troughs or lows that have altered the low-level wind pattern with consequent deformation zones capable of producing deep and rather significant axes of lateral convergence, (2) subtropical Atlantic ridge implications, (3) orographic triggers, (4) zones of anticyclonic shear or divergence aloft usually associated with subtropical jets, troughs or lows, and (5) the superposing of low and high-level mechanisms for net vertical motion. Many of these factors combine to modify an environment that is characteristically dry and stable and then focus and prolong the convection over an area enough for serious flooding. There is some examination also given to the conspicuous peak in the annual rainfall distribution that occurs in May.

2. BACKGROUND

As described by Riehl (1954), usually the atmosphere over the tropical Atlantic and Caribbean is dynamically stable because of the presence of very dry and warm air aloft overlying more moist, Atlantic maritime air at lower levels. This comes from the fact that the subtropical ridge over the Atlantic dominates most of the year. Subsiding air produced by this semi-permanent feature spreads outward over the region restricting most vertical motion to the first 10,000 ft. Compressional warming and drying of the middle and lower atmosphere by subsidence produces the trade wind inversion which serves to cap almost all but sufficiently forced convection. Thus regulating the atmosphere, it can be watched as an important indicator for forecasting convective changes in the tropics. First described by Piazzi-Smyth (1856), its presence can be detected almost yearlong in the tropics as a major controlling influence on the weather. In the annual mean vertical sounding for 15N latitude (figure 2) taken from the U.S. Standard Atmosphere Supplement, 1976 (1977), this lower-tropospheric temperature inversion is easily identified separating the more moist, well mixed surface layer beneath from the dry and stable layer above.

An interesting fact about this May flood is that it coincides with one of the biannual peaks in rainfall that climatically occurs over the Caribbean region during the month of May (figure 3). Commonly known in Puerto Rico as the

"Aguaceros de Mayo", its seasonal arrival is often rather abrupt and intense after just following the driest months of the year. This climatic peak in May rainfall also coincides closely with the timing of the extreme rains and flooding that just recently occurred over the Virgin Islands in late April of 1983 and of other similar heavy rainfalls that periodically have occurred in the past.

The explanation for this monthly maximum in the region's rainfall climate, occurring outside the season when tropical influences are greatest, has been a puzzlement for some time. It is not attributable to the north-south oscillation of the equatorial trough which together with disturbances in the easterlies generate most of the broad summer-season rise in rainfall over the Caribbean. More probable is the explanation that May is the mid-point for the transition season in the Caribbean. Westerly troughs in the mid and upper troposphere, still in phase with the mean long-wave pattern over the western Atlantic that time of year, continue occasionally to drop sharply southward over the region. At the same time, however, these troughs tend to be weaker. They stagnate early and become cutoff more often. The polar westerlies have retreated more northward where they offer less support, and wave progression eastward soon cuts off their southern extensions. The implications are that these cutoff mid-latitude troughs are an important part of the explanation behind the May rainfall maximum.

There is another contributing factor to this annual rainfall maximum that occurs in May. Over the western portions of the Atlantic and Caribbean, subsidence is for a brief time much less pronounced during the late spring (April-May). The summer transition into the deeper easterly trades is setting up. As Gutnik (1958) showed in his description of the climate of the trade wind inversion in the Caribbean, the mean frequency of the trade wind inversion decreases abruptly from April to May demonstrating its absence or weakness for a greater percentage of the time. Because of this, mid and upper troughs in the mid-latitude circulation are having somewhat more success in replacing dynamic stability than in just previous months when the trade inversion was both steeper and based lower. A look at the mean thunderstorm days taken from the Local Climatological Data, 1984, Annual Summary, San Juan, Puerto Rico also shows this sudden break down in low-level stability that combines with still vigorous dynamics occurring at mid and upper levels in the atmosphere. The April to May increase in thunderstorm days (from one to five) is by far the most significant increase of the year.

As Riehl (1954) has discussed, mass transfer does occur across the trade inversion. The actual process of lifting the base of the inversion as well as its eventual weakening or destruction is accomplished in this manner. Cloud growth increases penetration into the lower portion of the inversion layer. Cooling effects result from rapid evaporation into the dry layer and from parcel expansion. In this way the warm and dry layer takes on the characteristics of the cloud layer and the depth of the moist column increases. However, for this process to overcome such a stable and dominant regulator of the tropical weather regime as the trade inversion presents during much of the year, there must be a well defined reversal in the vertical motion field.

At the lower levels in the atmosphere, vertical motion is largely controlled by divergent or convergent wind patterns as well as orographic boundaries. Axes of wind convergence and orographic barriers appear to be the most common features that focus convective intensities in the tropics. These are also the features along which the strongest positive low level forcing occurs. Surface troughs and lows as well as other weather systems in this region are often just attendants to the true forcing and focusing mechanisms at work..the wind speed and flow patterns. For this reason, most tropical meteorologists think of winds first when they are making a forecast, and rightly so.

Dynamic systems at higher levels in the atmosphere often work in combination with low-level disturbances to enhance their convection or development or become the originating factor behind their initial formation as described by Sadler (1967). Upper/middle-level cyclones and troughs of any significant depth and persistence will usually be represented by some changes at the surface within the tropical wind field. Weather associated with these changes usually is aligned along significant axes of lateral convergence or along zones of cyclonic shear and curvature produced by the deformation that occurs in the low-level wind patterns. For significant weather to be generated, the convergence usually needs to be pronounced through a rather deep layer of the lower atmosphere, and processes aloft should also be favorable for divergence. The anticyclonic shear and divergence aloft associated with an upper cyclone, trough or jet provide for the strong upward transport of moisture that occurs as well as the complete destabilization that must occur throughout the atmospheric column for heavy rainfalls.

3. MAY 1985 EVENT

3.1 500 mb and Surface Analyses

Upper/middle-level troughs over the Caribbean during the mid-latitude spring and fall transitions are often notable for their persistent and prolific production of rainfall. Part of the explanation for this is their tendency to stall in the lower latitudes where they frequently cutoff and become embedded within the subtropical circulation. Here, they stagnate while deriving most of their support outside polar influences until again they become reinforced by a new short wave undergoing an eastward progression within the long-wave pattern.

Often the product of such a pattern is that the extended cloudy and wet spells accompanying these troughs can become serious flood problems in the Caribbean region. Such a situation (figure 4) developed across the eastern Caribbean during this flood event. In the 500 mb analysis for 1200 GMT 15 May, the initial stages of a trough cutting off near 70 degrees west longitude are occurring. Cold air advection upstream brought additional deepening and southward penetration of the trough during the following 24 hours.

Weather analyses on 15-16 May quickly began to look favorable for a heavy rain situation. An initial weakness in the low-level pressure pattern to the west of Puerto Rico on 15 May developed into a closed low north of Hispaniola in the 0000 GMT surface analysis for 16 May (figure 5). The surface low had become a reflection of the stationary mid and upper-level trough that was being reinforced and intensified by the cold air advection.

3.2 San Juan Soundings, 11-14 May

Usually, comparisons can be easily made between tropical soundings that are stable and those undergoing changes more favorable for rainstorms. As sinking motion is overcome and dynamic processes become favorable for positive vertical motion, a complete transformation in the character of the temperature and moisture distribution occurs within the atmosphere's vertical profile. San Juan's soundings for 11-14 May (figures 6, 7, 8 and 9) illustrate quite well these changes immediately prior to the beginning of heavy rains during the May 1985 flood. Notable differences did occur resulting in a greater moisture depth and the disappearance of an elevated trade inversion by 14 May.

Initially, the San Juan sounding of 1200 GMT 11 May (figure 6) showed relatively strong stability due to subsidence above 715 mb. Based at that level, adiabatic processes had produced a 2.6 C temperature inversion through a layer of 2,900 ft and dewpoint depressions of 30 C. From the influence of a mid-level Atlantic ridge center just north of Puerto Rico, descending motion was predominate with a warm and dry layer between the 715-500 mb levels. Twenty-four hours later the 1200 GMT 12 May sounding (figure 7) indicated less pronounced subsidence with an isothermal layer near the former inversion and some mid-level intrusion of moisture beginning to occur below 500 mb. Any ascending motion or vertical transport of moisture, however, was still almost absent in the 1200 GMT sounding for 13 May (Figure 8). Sinking motion had, in fact, lowered the base of the dry layer to almost 800 mb.

The 1200 GMT sounding of 14 May (figure 9) provided the first strong evidence to the forecaster that the vertical motion field was finally beginning to fully reverse. The significant dryness above 800 mb was rapidly supplanted by a moist layer of 11,880 ft in thickness, up to about the 500 mb level. Moisture was also increasing at lower levels. Weak subsidence above 800 mb on the 13th had ended rapidly as the developing mid and upper-level trough gained greater influence over the region. This was causing a positive reversal in the vertical motion field at all levels along with greater moisture intrusion.

Overall, an approximate 1-5 C of cooling occurred between the 800-400 mb levels in the soundings 11-14 May. The result was even more apparent with the sounding of the 14th showing a conditionally unstable lapse rate and extensive moisture all the way up. The Showalter Index had fallen from a +3 to +-0 along with the level of free convection (LFC) lowering from 821 mb to 954 mb in the 24-hour period. Most important too was the absence of any remnant trade inversion by the 14th as upward motion brought more cooling into the layer. These changes in the character of the sounding were the most important evidence the forecaster had that the upper trough was gaining final dominance.

As is typical of these situations, very moist tropical air at lower levels becomes concentrated through mass convergence and atmospheric overturning through a deeper layer. This erased the normal stable cap of dry and warm air aloft and set the stage for the heavy rainfall amounts that fell during the following 24-hour periods. Usually to produce such excessive rainfall amounts the atmosphere must be organized optimally throughout the atmospheric column to promote good vertical motion. Three notable factors that played a part in accomplishing this feat and which were brought together into a final orchestration were the combined presence to an orographic barrier, an asymptote of convergence, and a subtropical jet.

3.3 Orographic Influences

A shift to moderate southerly winds at low levels began around 1200 GMT 15 May and was in place the night of the 16th. The average wind vectors in the lower 5,000 ft changed from 140/14 to 170/17; eventually average winds veered to south southwest.

With this wind pattern, orographic influences have a most important bearing on rainfall production because of the mountain escarpment that flanks the south coast of Puerto Rico and provides abrupt rises in elevation of 3,000 to 4,000 ft MSL (figure 10). In the tropics orographic lifting is probably the most effective converter of low-level moisture into intense rainfall rates. It also satisfies the requirement of focusing the low-level vertical motion and concentrating the coverage of heavy rainfall to the topography. This is evident in (figure 1) where isohyets of heavy rainfall conform to the higher elevations.

Atmospheric steering winds were significantly deep from the south and southwest. The fact that the south coastal plain received much less rainfall is a strong indication that

positive dynamics within the upstream flow were not sufficiently great to support the more intense flood producing rainfall rates. Radar also indicated that the heaviest cells were firing off over the ridge line and valleys just inland that drain extensively to the north coast. Transported within the flow, incipient cells off the water were observed merging and regenerating into the heavier solid convection that remained almost stationary.

As explained by Maddox et al. (1979) upslope transport of moist unstable air due to orographic lifting can of itself become a primary boundary focusing mechanism. This is especially true where the upslope lifting process carries air parcels to or above the LFC above which bouyant energy can be supplied from the external environment. Because of downslope effects, San Juan's sounding (north coast) at lower levels is not representative of the south coast of Puerto Rico. Comparisons cannot be made. However, St. Martin's soundings provided LFC values from around 1,600 to 2,200 ft during the event which should compare more favorably (minimal terrain influence) even though their geographic location was outside the maximum concentration of low level moisture. Considering this then, in a more moist environment upslope lifting over elevations of approximately 1,500 ft alone could have easily triggered thunderstorms even though positive energy values above 15,000 ft were not especially great for perpetuating strong vertical motion. The San Juan sounding, for example, showed only minimal upper level cooling over Puerto Rico during the entire episode. Possibly this accounts for most radar measured tops below 35,000 ft.

3.4 Asymptote of Convergence

A streamline convergent flow axis (asymptote of convergence) developed within the lower levels of the atmosphere and was oriented almost directly across Puerto Rico.

This feature resulted from the low-level circulation preceding the steadily deepening surface trough over the central Caribbean and the southerly flow out of the tropical Atlantic around the nose of the retreating Atlantic ridge (figure 11). It can be seen that the deformation field presented by the streamlines is relatively disorganized over the southern Caribbean; however the prominence of the lateral convergent flow axis across Puerto Rico cannot be neglected. Analyses at both the surface and 700 mb show its presence. Its existence throughout the lower atmosphere and the fact that winds were increasing from the south into the confluent area are good evidence of strong positive vertical velocities, provided an outflow mechanism aloft was also at work. Finally, the feature became a primary factor, along with the orographic lifting, for focusing convection and providing for the repeated development of heavy rains over the flood stricken area.

3.5 Subtropical Jet

At 200 mb the 1200 GMT analysis for 18 May (figure 12) showed the subtropical high had strengthened along 10 degrees north latitude with a pronounced subtropical jet running northward over Hispaniola. In just the previous 12-hour analysis (0000 GMT 18 May, not shown), the mid-latitude westerlies had been prominant over the Greater Antilles with only 30 kt maximum winds. Therefore, the subtropical jet had introduced itself into the affected area on short notice. Along the subtropical jet axis just west of Puerto Rico, a 70 kt maximum wind was derived from satellite estimates.

The influence of the subtropical jet most probably brought all the processes together and resulted in the most serious onslaught of heavy rain during the night of the 17th and throughout the day of the 18th. In the tropics getting all your soldiers in a row is usually what is required for producing a significant weather event. Just having the low levels favorable for upward vertical motion and not having the mid and upper levels also combining for net vertical motion throughout the atmospheric column usually results in less striking weather scenarios. The introduction of the jet maximum over the area, although not especially strong, did provide a sufficient outflow mechanism. Also, the jet maximum in (figure 12) appears to be favorably positioned for moderate anticyclonic shear and divergence aloft over Puerto Rico.

4. FORECASTS AND WARNINGS

Forecasts and warnings went well with the situation. In both the public forecasts and summaries, the public was alerted to the possibility of heavy rains as much as 24 hours ahead of the actual beginning of rainfall. Forecasts had followed similar patterns in the past and satellite pictures had been showing intense convection over Hispaniola the day prior. The initial flash flood watch and warning preceded the first reports of flooding with lead times of four and three hours respectively. Of great benefit to operations was the first trial use of the newly installed telemetering raingage network (Enhanced Alert System) with real time rainfall data being received from the upper Loiza basin in eastern Puerto Rico.

The watch and warnings were well defined to the eastern two-thirds of Puerto Rico during the first two episodes of flooding on 15 May and again on the 17th. The extension of the watch area westward to involve all of Puerto Rico by the morning of the 18th appeared also to be timely.

As with many orographic produced rainfalls in the tropics, tops do not have to be excessive nor do thunderstorms have to be occurring for rainfalls to reach extreme proportions. Especially in tropical settings this can be the case where the supply of moisture is almost limitless, and the combined triggering mechanisms can sometimes be of a very subtle nature or hidden within the resolution of the available data network. The forecaster on duty during the period when heaviest rains fell over the central and western mountain stations

asserted that radar tops were stratiform, staying within a range of 20 to 30 thousand feet and considerably lower than previous flood associated tops. Also, radar reflectivity values were not large. The relating of radar intensities to actual observed rainfall works well in the tropics most of the time. Under circumstances like those observed in this case, I suggest that the forecaster's educated intuition and local knowledge can at times be not only the sole but often the best tools he has available.

5. GUIDANCE

Basic guidance as is available to the forecaster in the States is almost entirely absent in Puerto Rico. The progs that are available are usually smoothed considerably and give only a general idea of regional changes. In most instances, however, it has been found that the stateside guidance and models do well enough in predicting for this area during the time of year when polar influences are greatest, but most NMC map boundaries cut off north and west of the Caribbean. Use of these charts then is left to extrapolation into our area. One simple improvement would be to extend the map backgrounds for the Limited Area Fine Mesh (LFM) and Nested Grid Model (NGM) generated graphics to include the Caribbean and Atlantic east to 60W and south to 15N.

Improved guidance would also increase the confidence the forecaster needs for making predictions in the tropics. The ideal guidance for forecasting in this region would be a model sophisticated enough to output data fields showing boundary-layer winds on a horizontal grid with sufficient density to streamline even the mesoscale features. Also, another bit of guidance helpful to the forecaster would be horizontal depictions at both low and high levels in the atmosphere that provide analyzed values of computed relative vorticity and velocity divergence. However, it is my opinion that good mesoscale interpretation and treatment of satellite data offers the best future for forecast improvement in this area.

The lack of timely and comprehensive data does not provide for the detailed analysis needed for interpretation and forecasting of such weather events in the tropics. There needs to be more telemetering of weather data so that real time information is constantly available to the forecaster and hydrologist. Expanded data collection from reliable bouys and land based observation points should be a priority item.

6. SUMMARY/CONCLUSIONS

The months of May in the Caribbean region have in the past been notable producers of heavy rainfalls, falling outside the tropical months that contribute to most of the region's annual supply. This paper proposes some of the possible controlling influences behind why May is such a climatically wet month in the northern Caribbean region.

Certain signature patterns this flood event shares with others of similar magnitude have been highlighted. Streamline axes of convergent flow, at times intersecting with other meso-boundaries, are important in the tropics for focusing convective intensities and when defining significant weather phenomenon. Many of the mechanisms or features considered important to flash flooding have already been included in the literature (Maddox et al., 1979). These have been described primarily for mid-latitude cases, but some have also been observed applying here. Two of the most important focusing mechanisms which are germane to this flood event, the first of which is unique from earlier classification, are (1) low level axes of convergent flow (asymptotes of convergence) resulting from deformation in the mesoscale wind field and (2) the orographic barriers and vertical lift that some of the islands present within the smooth uninterrupted wind stream. The fact that these are either slow moving or non-migratory features are what make them so significant to flooding. In the synoptic scale, the consideration of what is happening throughout the atmospheric column leads us to the third ingredient behind the heavy May rains: the location of the subtropical jet maximum west of the area, favorably positioned as a good outflow mechanism aloft.

Most important to any significant weather event appears to be the combined influences of several mechanisms at work, both temporally and spatially. The whole result they produce is much greater than the sum of what each individually would have contributed. The intersection of these mechanisms or the motion fields being produced by them, exemplified in this case where the convergent axis met with the mountain slope, largely defines the heaviest rain area. A very gradual westward migration in the convergent axis resulted in the displacement of the heaviest rains from eastern Puerto Rico into the west central sectors toward the end of the five day period; otherwise, the heavier rains would have been more restricted in their coverage. Even so, the flow pattern in the May event remained remarkably constant considering its position and strength.

7. ACKNOWLEDGEMENTS

The author wishes to thank Dr. J. A. Colon, NWS San Juan, for his valuable review and comments. Thanks also go to Mr. Felix Rodriguez del Rio, USGS San Juan, for help in finalizing the figures and to Ms. Pura Torres for her expert preparation of the manuscript. Dr. H. P. Gerrish, NHC Miami; Mr. D. C. McDowell, Univ. of Puerto Rico; and Ms. Kay Hale of the Univ. of Miami were helpful in obtaining valuable reference material.

8. REFERENCES

Caracena, F., and J. M. Fritsch, 1983: Focusing mechanisms in the Texas hill country flash floods of 1978. Mon. Wea. Rev., 111, 2319-2332.

Colón, José A. Climatologia. In Geovision de Puerto Rico, pp. 45-120. Edited by Maria Teresa B. de Galiñanes, Rio Piedras: Editorial Universitaria, 1977.

Frank, N.L., 1969: The inverted v cloud pattern --an easterly wave? Mon. Wea. Rev., 97, 130-140.

Gerrish, H.P., 1967: Mesoscale studies of instability patterns and winds in the tropics. Report No. 14, Contract No. DA 28-043-AMC-00443(E), Inst. of Marine Science, Univ. of Miami, 72 pp.

Gutnick, M., 1958: Climatology of the trade wind inversion in the Caribbean. Bull. Amer. Met. Soc., 39, 410-420.

Maddox, R.A., F. Caracena, L.R. Hoxit and C.F. Chappel, 1977: Meteorological aspects of the Big Thompson flash flood of 31 July 1976. NOAA Tech. Rep. ERL 388-APCL 41, 83 pp.

_____, C.F. Chappell and L.R. Hoxit, 1979: Synoptic and meso-a scale aspects of flash flood events. Bull. Amer. Meteor. Soc., 60, 115-123.

Palmer, C.E., C.W. Wise, L.J. Stempson, and G.H. Duncan, 1955: The practical aspect of tropical meteorology. AWS Manual 105-48, Vol I, 195 pp.

Piazzi-Smyth, C., 1858: Astronomical experiment on the peak of Teneriffe. R. Soc. London, Philosoph. Trans., 48, 465-533.

Riehl, H., 1954: Tropical Meteorology, McGraw-Hill, New York, NY, 428 pp.

Sadler, J.C., 1967: The tropical upper tropospheric trough as a secondary source of typhoons and a primary source of trade wind disturbances. Final Report, contract No. AF 19 (628)-3860, HIG Rept 67-12, Hawaii Institute of Geophysics, 44 pp.

Simpson, R.H., 1970: A reassessment of the hurricane prediction problem. ESSA Tech. Memo. WBTM SR-50, 16 pp., U.S. Wea. Bur., Southern Region.

U.S. Department of Commerce, NOAA. Local Climatological Data, 1984, Annual Summary, San Juan, Puerto Rico.

U.S. Standard Atmosphere Supplement, 1976, prepared under the sponsorship of: ESSA, NASA, and USAF; GPO, Wash. D.C., 1977, 289 pp.

Weldon, R.B., 1979: Cloud patterns and the upper air wind field. NWS Satellite Training Course Notes, Part IV, NESS, Applications Division.

9. FIGURES

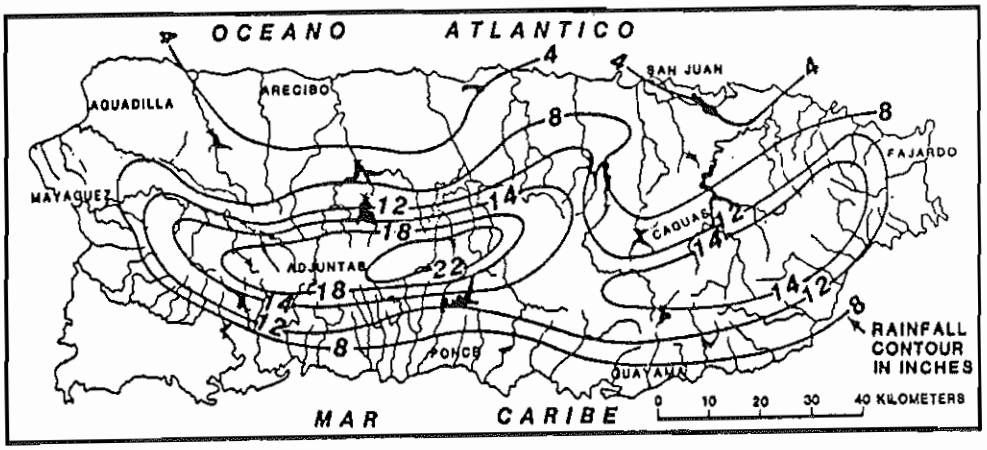

FIGURE 1.--Total rainfall distribution during May 15-19, 1985.

(Preliminary data from the National Weather Service)

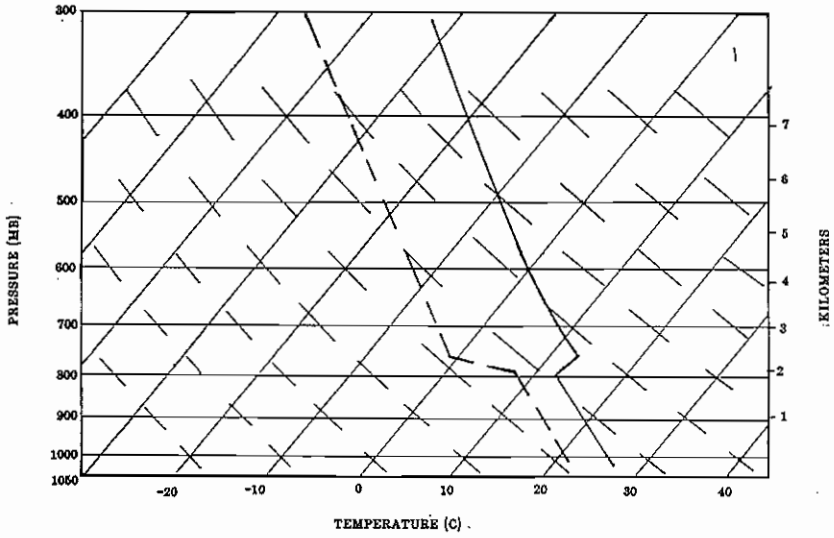

Figure 2. 15 N Standard Atmosphere Plotted on Skew-t Diagram, Solid Line Temperature, Dashed Line Dewpoint. (U.S. Standard Atmosphere Supplement, 1976)

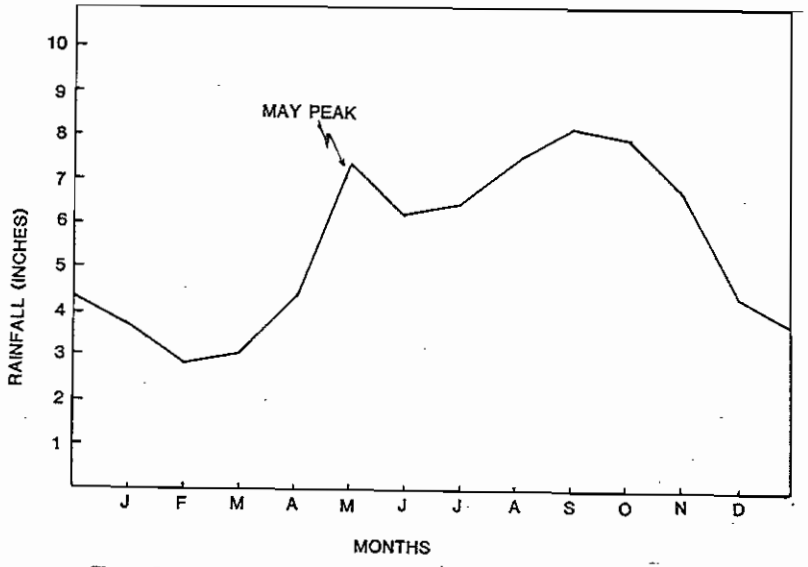

Figure 3. Annual Variation in Average Rainfall for Puerto Rico (J.A. Colon)

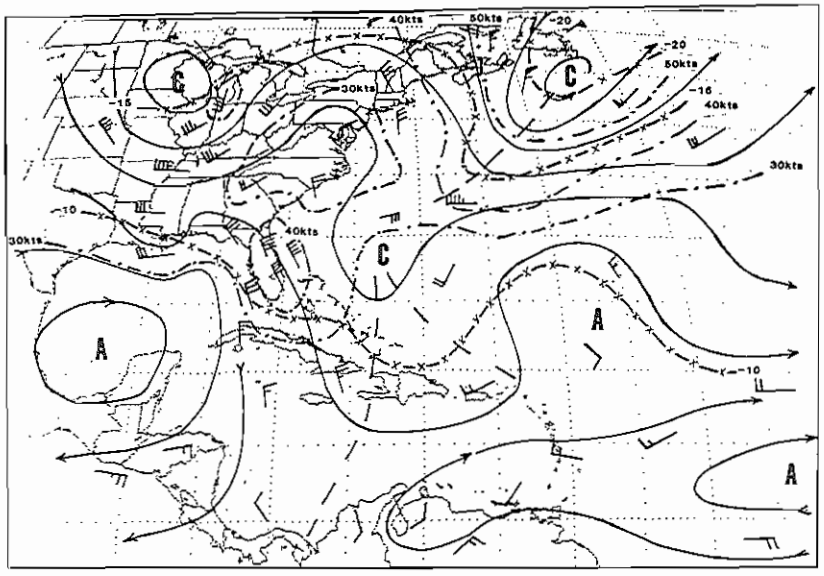

Figure 4. 1200 GMT 15 May 1985 500 mb Analysis: Streamlines, Isotachs and Isotherms.

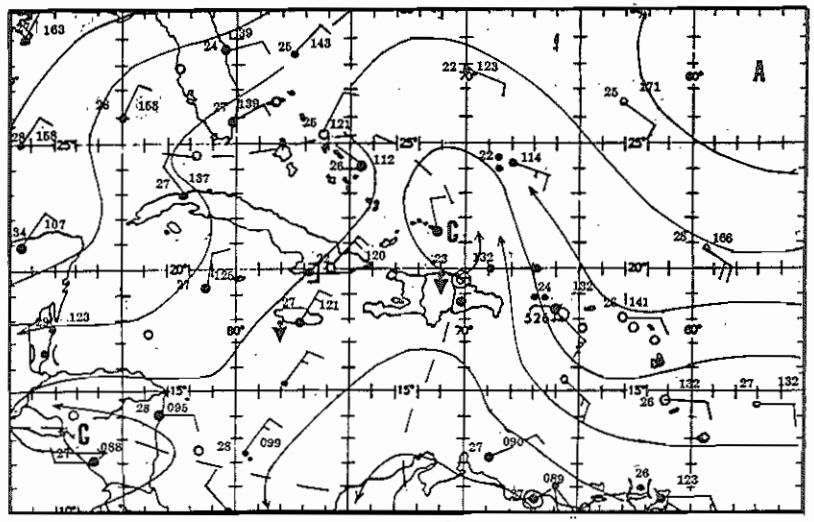

Figure 5. 0000 GMT 16 May 1985 Surface Analysis: Streamlines.

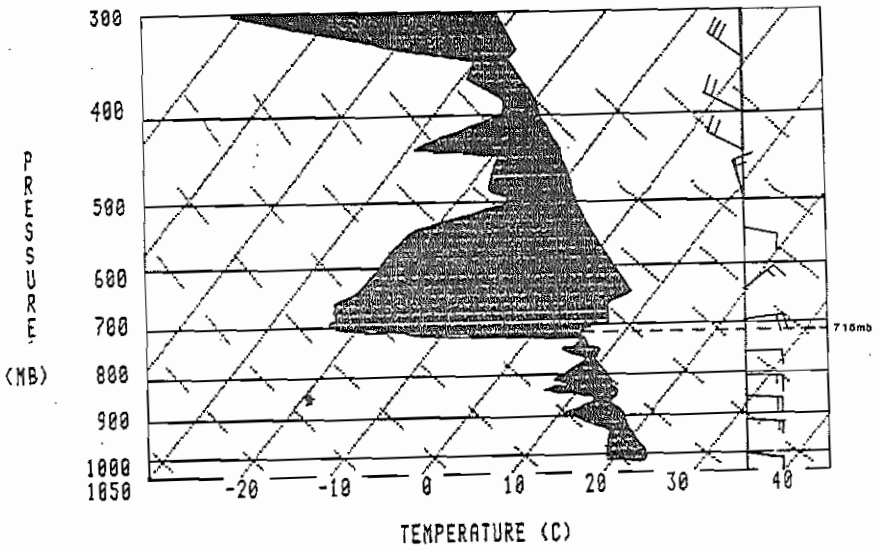

Figure 6. San Juan Sounding (Skew T/Log P) 1200 GMT 11 May 1985

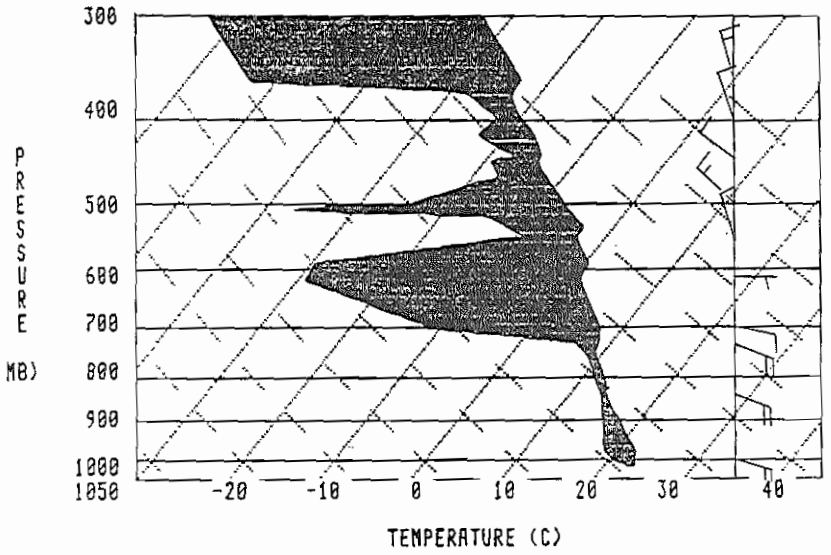

Figure 7. San Juan Sounding (Skew T/Log P) 1200 GMT 12 May 1985

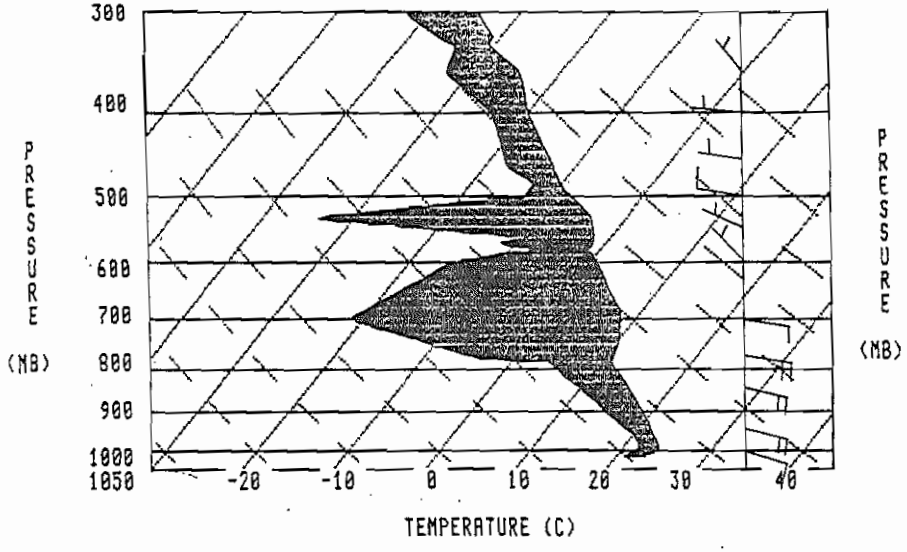

Figure 8. San Juan Sounding (Skew T/Log P) 1200 GMT 13 May 1985

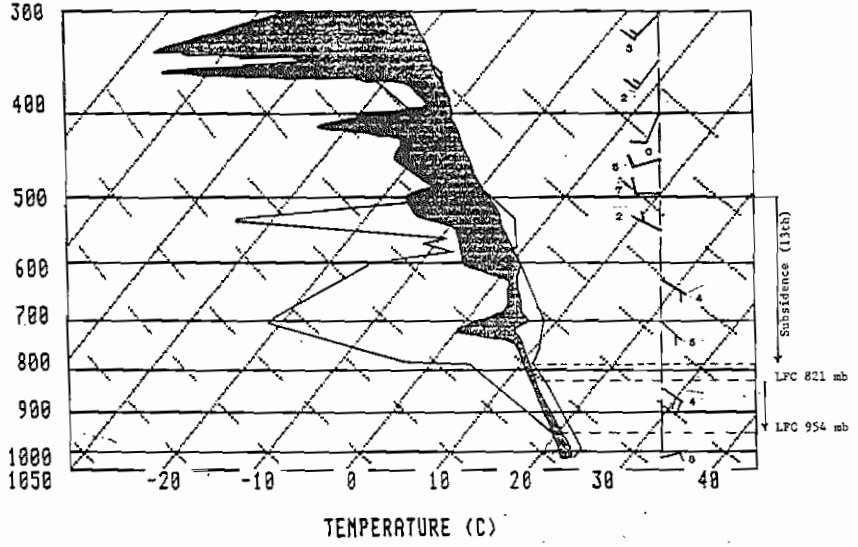

Figure 9. San Juan Sounding (Skew T/Log P) 1200 GMT 14 May 1985
and Previous 24 Hour Trace.

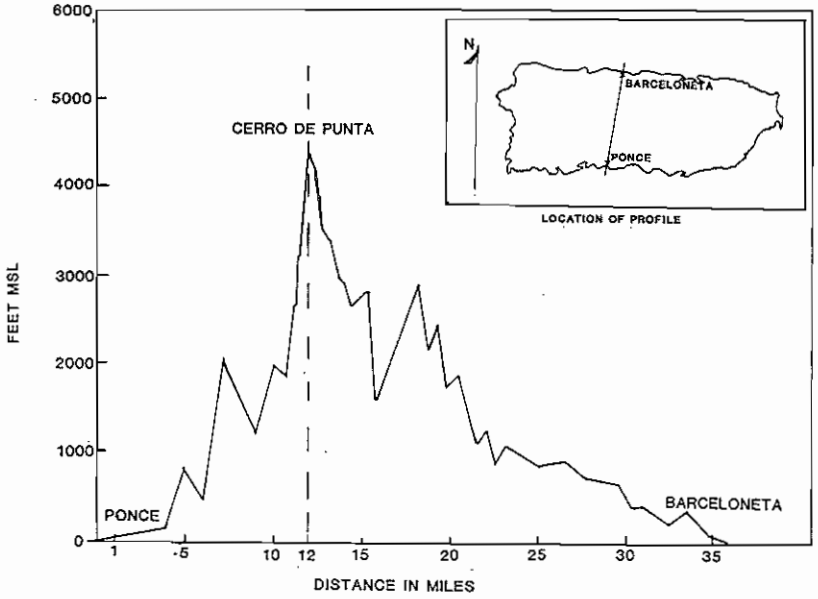

Figure 10. Cross-sectional Profile of Puerto Rico.

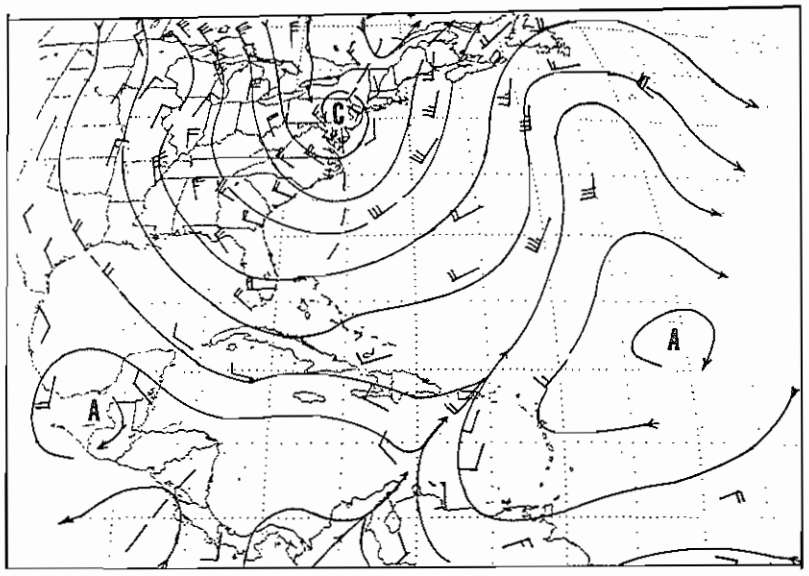

Figure 11. 0000 GMT 18 May 1985 850 mb Analysis: Streamlines and Convergent Asymptote.

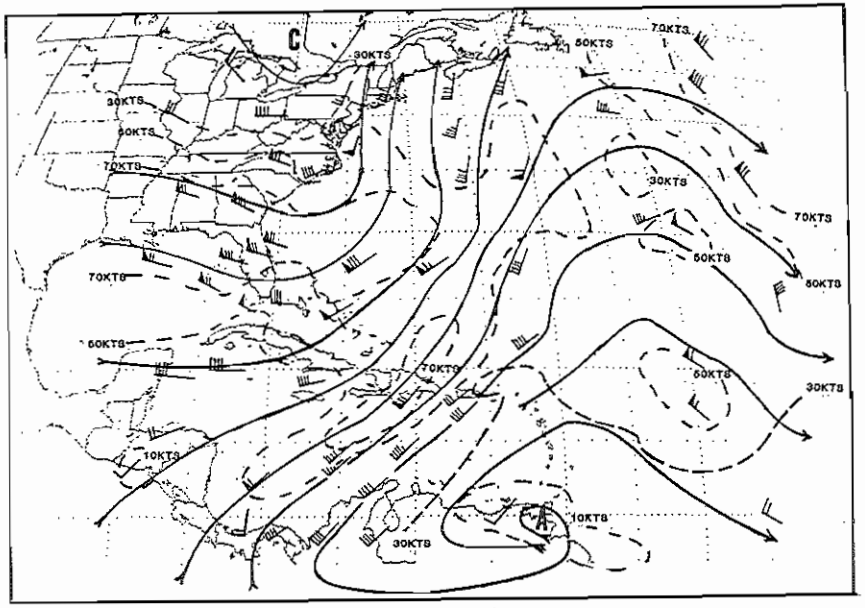

Figure 12. 1200 GMT 18 May 1985 200 mb Analysis: Streamlines, Isotachs.

THE RELATIONSHIP OF QPF TO THE MANAGEMENT OF HYDROELECTRIC POWER ON THE SANTEE RIVER BASIN IN NORTH AND SOUTH CAROLINA

Samuel E. Baker

National Weather Service Forecast Office
West Columbia SC, 29169

1. INTRODUCTION

Hydroelectric power is well developed in many parts of the United States. In some areas, dam and reservoir projects were designed specifically for hydropower. Many of these projects have large storage capacity and relatively undeveloped shorelines. Reservoirs designed primarily for hydroelectric power generation use a large part of their volume to store runoff water for use as needed at a future time. Reservoir levels can be raised or lowered to result in the most effective use of the water.

In the Eastern part of the country, however, many hydropower projects are located in areas where the river valleys are narrow with steep sides. This results in reservoirs which have small storage capacity. Other reservoirs have highly developed shorelines which are very sensitive to changes in water level. In both of these cases the usable storage capacity of the reservoir is limited and runoff must be used for hydropower as it comes down the river, or be wasted over the spillway.

An accurate Quantitative Precipitation Forecast (QPF) can be used by water managers to help estimate the amount of water that will be available for hydropower generation. This enables the power system manager to use hydropower before the runoff reaches the reservoir on the assumption that the water will be replaced after the rain. The savings in fuel costs can be substantial, and this is a benefit for all power users.

This paper describes hydroelectric development in the Santee River Basin in North and South Carolina. The process of estimating the amount of runoff water is described and an attempt is made to establish an economic relationship between an accurate QPF and hydropower generation.

2. DESCRIPTION OF THE SANTEE BASIN

2.1 Area Drainage area is 15,700 sq mi. The Basin lies in two states; 5,300 sq mi in North Carolina and 10,400 sq mi in South Carolina. The Santee Basin is 275 miles long and 115 miles wide. It extends diagonally in a NW-SE direction from the Blue Ridge to the Atlantic Ocean (fig.1).

2.2 Topography The Santee River Basin is comprised of three well defined physiographic provinces.

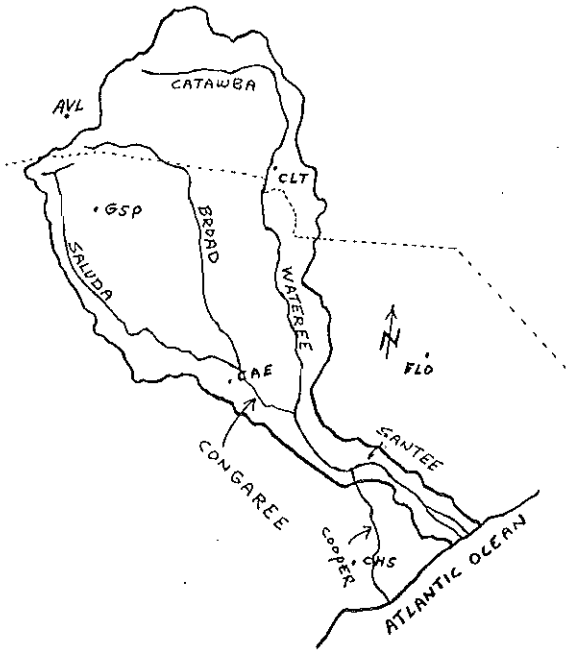

FIGURE 1 MAJOR RIVERS IN THE SANTEE BASIN

The Northwest section is in the Blue Ridge Mountains. The Piedmont extends from the foothills of the mountains to within 100 miles of the Atlantic Coast. The Coastal Plain forms the Southeastern portion of the Basin between the Fall Line and the Atlantic Ocean. Elevations range from almost 6000 ft. at Grandfather Mountain in North Carolina to sea level. The largest portion of the Basin is in the Piedmont with an elevation range from 1200 ft. at the Foothills to 200 ft. at the Fall Line.

2.3 Climate Normal annual precipitation ranges from over 80 inches in the extreme Western corner of the Basin to 43 inches at the Charlotte WSO. Overall the average precipitation is 50 inches per year (NOAA a-c). Annual evaporation ranges from 32 inches in the Mountains to 44 inches in the Coastal Plain (Farnsworth et al, 1982).

Evapotranspiration closely approximates the free water surface evaporation and ranges from around .6 in. in January to near 5.5 in. in July.

Temperatures range from near zero for short periods in the Winter to over 100 degrees for several days at a time in the Summer. Snow occurs in the Mountains from late December until March. Snowpack is not a significant factor in spring runoff and ice does not affect streamflow.

2.4 Hydrology Five major rivers make up the Santee system (fig. 1). The slope of these rivers, or drop in elevation divided by the length, in part determines their hydroelectric potential. Travel time of runoff through the system is important in water management planning. Shorter travel times make advance planning more critical for efficient water use.

The major rivers and characteristics are:

Saluda River The Saluda River and tributaries carry runoff from the western sections of the Basin. With headwaters on the Blue Ridge, the Saluda runs 145 miles south and southeast to Columbia, SC. Total drop in elevation is 1300 ft. Travel time for runoff ranges from 30 to 36 hours depending on the flow.

Broad River The Broad River drains the central section of the Basin and runs southerly for 166 miles from the Blue Ridge to Columbia. Total drop in elevation is 1800 ft. Travel time is 31 to 38 hours.

Catawba-Wateree The River begins as the Catawba River north of Old Fort, NC and carries runoff from the northern and eastern slopes of the Basin. The Catawba runs east and then south into South Carolina where its name changes to the Wateree. Total run from the mountains to the Congaree is 295 miles. Total drop in elevation is 2080 ft. Travel time is 43 to 53 hours.

Congaree River The Broad and Saluda Rivers join at Columbia, SC to form the Congaree. The Congaree runs southeast for 51 miles to join the Wateree River near the head of Lake Marion. Total drop in elevation is 80 ft. Travel time is 15 to 18 hours.

Santee River The Congaree and Wateree Rivers join to form the Santee. The Santee then flows southeast for 143 miles to the Atlantic Ocean. Total drop in elevation is 110 ft. Travel time is 17 to 20 hours.

2.5 Development The Santee Basin is highly developed from a hydroelectric standpoint. There are 35 hydroelectric plants presently operating in the Basin. Of this number, 34 are riverine plants and one is a pumped storage facility.

The number of plants on each major river are:

Saluda	8	
Broad	7	with 1 pumped storage
Catawba-Wateree	15	
Congaree	1	
Santee	3	

Power Development development of the Santee Basin began in the 1770's when a canal was surveyed from the Santee River to the Cooper River near Charleston, SC. Textile mills located on rivers in the Basin in the 1800's in order to utilize the water as an energy source. Mechanical problems associated with connecting water wheels to power shafts led to the use of water driven generators to run electric motors. Several small hydroelectric plants were built to provide power for the mills. Most of these generating plants are still in operation today.

A power company was formed in 1904 to develop the hydroelectric potential of the Catawba-Wateree River. Hydroelectric development continues to the present and sites for future projects are under active study.

A fossil fuel crisis in the early 1970's led to a renewed interest in hydropower. Several of the old plants that were near retirement have been refurbished. Recent problems with nuclear power plant cost and certification have also increased interest in the use of hydroelectric power.

Today, hydroelectric power is an integral part of the generating capacity of major power companies in the Santee Basin.

Power Use Three major power companies operate in the Santee Basin. Duke Power Company operates 21 hydroplants with a capacity in excess of 861 megawatts. South Carolina Electric & Gas operates 4 riverine plants and the pumped storage facility at Monticello for a total generating capacity of over 740 megawatts. The South Carolina Public Service Authority, known as Santee Cooper, operates three hydroplants with a total capacity of over 85 megawatts.

Several small hydroelectric plants are operated by textile mills or city power companies. The total power capacity of these small plants is less than 10 megawatts.

Limitations on Lake Levels The US Army Corps of Engineers has developed guidelines for reservoir managers to follow when changing lake levels. These "rule curves" specify the desired water level according to season.

Many hydroelectric reservoirs in the Southeast are located in densely populated areas and have highly developed shorelines. Lakeside property owners, boaters, fishermen and other recreationists are very sensitive to changes in water level. Intense public pressure is brought to bear on reservoir managers when lake levels are changed beyond the usual amount.

The above considerations severely restrict the reservoir manager when using water for hydropower. Storing water for future use raises the lake level and using water too long before a runoff event may lower the water by an unacceptable amount.

Careful planning is necessary to fully utilize the water resource in the Santee Basin. A knowledge of the amount of water to be available for use in the next 2 or 3 days is extremely valuable when scheduling hydropower into a daily generation scheme.

3. HYDROPOWER AS RELATED TO OTHER TYPES

3.1 Energy Costs To discuss the relationship that exists between electric power generated by hydroplants and that generated by other energy sources a brief explanation is necessary. First, a discussion of the cost of electric power to the consumer. This cost will

be called the electric bill. The electric bill is made up of three cost components:

A. Physical plant
B. Return on rate base
C. Fuel component

Hydroelectric power has a definite advantage over other types for components A. and C. Many hydroelectric plants in the Santee Basin were constructed in the early 1900's or at least before World War II. This means that the physical plant cost was amortized long ago and present costs are primarily for maintenance. Since the "energy crunch" of the 1970's, a fuel charge has been tacked onto most electric bills. For power generated at a hydroelectric facility the fuel cost is quite low when compared to a coal or gas fired steam plant.

3.2 Response Time vs System Demand Electrical demand or system load is always changing. During certain times of the day, high demand causes a "peak" on the system. Since electrical power cannot be stored, the generating capacity of the system must be increased rapidly to handle the "peaks". These daily peaks normally last only a few hours.

Of the three main types of power generation (fossil, nuclear and hydro), hydro is the fastest to bring on line. Nuclear plants are primarily operated at a steady load to provide a power base for the system. Steam plants are cycled on and off the line as power demand factors change, i.e., day of the week and temperature. Hydro plants are normally used for quick response to "peak" demand for power.

Both nuclear and fossil fuel plants use steam as a medium to convert heat to electric power. Time is required to make steam by heating water. Bringing a fossil fuel plant on line from a "cold start" condition can take anywhere from 6 to 22 hours. A hydroplant can be brought on line in a matter of two or three minutes. Even a pumped storage facility in a pumping configuration can be switched over to generating in less than 5 minutes.

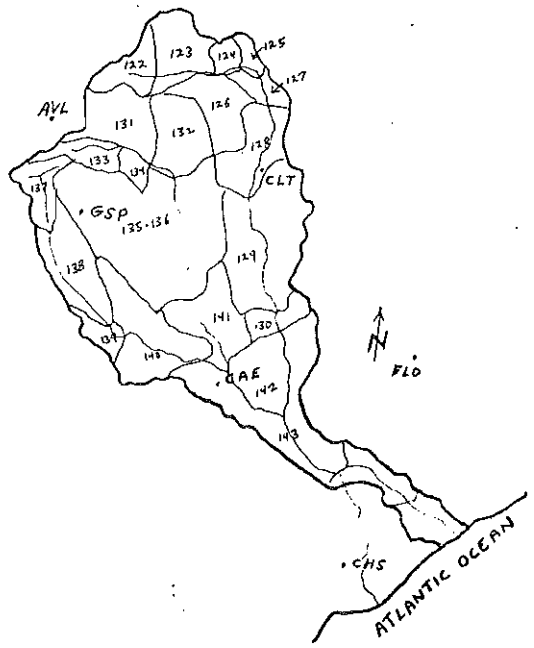

FIGURE 2 DRAINGAGE AREAS IN THE SANTEE BASIN

4. METHOD OF RUNOFF CALCULATION

In order to determine the amount of water that will be available for conversion to power, the QPF must be used to compute surface runoff. The amount of runoff and also the timing will be needed to effectively use the QPF in hydropower planning.

The Santee Basin is comprised of smaller drainage areas that are used in the calculations (fig. 2). In some cases, these basins are the drainage areas for the different hydroelectric plants. In others, the runoff from several basins may combine to suppy water for a hydroelectric facility. In all cases, the water that is used for production of hydropower at an upstream plant can be reused again downstream.

Unit hydrographs (fig. 3) are used to compute the amount and timing of runoff from a particular basin. These hydrographs are usually set up in six hourly increments. This allows the volume of water entering the reservoir each six hours to be easily calculated.

BASIN 122 Drainage area for Bridgewater

RUNOFF	TIME IN HOURS / DISCHARGE IN 1000 cfs				
	6	12	18	24	30
.10	3.0	.5	.3	.2	.1
.20	6.0	1.0	.6	.4	.2
.40	12.0	2.0	1.2	.8	.4
1.00	30.0	5.0	3.0	1.9	.9

FIGURE 3 UNIT HYDROGRAPH FOR BASIN 122

Two steps are used to compute the amount of surface runoff from a particular rainfall event or QPF:

1. RE= QPF - SMD (1)

Where: RE is RAINFALL EXCESS
QPF is QUANTATIVE PRECIP FORECAST
SMD is SOIL MOISTURE DEFICIENCY
All units are inches.

2. Enter the (RE/SRO) relationship for the basin with RE and read the SRO. Where: SRO is SURFACE RUNOFF in inches.

RE/SRO# 7 RAINFALL EXCESS vs SURFACE RUNOFF

RE (inches)		SRO (inches)
10.0	–	5.00
	–	
9.0	–	
	–	4.00
8.0	–	
	–	
7.0	–	3.00
	–	
6.0	–	
	–	2.00
5.0	–	
	–	1.50
4.0	–	
	–	1.00
3.0	–	
	–	.60
2.0	–	.40
	–	.25
1.0	–	.15
	–	.07
0.0	–	0.00

The runoff volume (ROV) can now be calculated by:

$$ROV = SRO \times DA \quad (2)$$

where: DA is the DRAINAGE AREA in sq miles
ROV is in acre-ft

The runoff timing can now be determined by using the unit hydrograph for the basin (Fig. 3). This allows a computation of how much of the ROV will enter the basin outlet point, i.e., reservoir in each six hour period (fig. 6).

To calculate how much water is needed to utilize full generation at a particular hydro plant, it is necessary to know the effective head of the plant and the generating capacity.

Hydro-electric production and stream flow are related by (Long, 1980):

$$P = \frac{Qhe}{11.815} \quad (3)$$

where: P is PLANT CAPACITY in Kilowatts
Q is STREAMFLOW in cubic feet/second
h is EFFECTIVE HEAD in feet
e is EFFICIENCY OF SYSTEM

assuming e= .85 the equation becomes:

$$P = .0719\ Qh \quad (4) \quad \text{or} \quad Q = \frac{P}{.0719\ h} \quad (5)$$

Table 1 displays the generation capacity (P) and effective head (h) for 31 hydroelectric plants in the Santee basin. Using equation (5), the maximum flow can then be calculated. A comparison of the runoff flow from the runoff hydrograph and the max flow at the plant will quickly show if maximum generation can be sustained for long enough to be scheduled into the system.

By using the QPF to estimate runoff in advance of the precipitation, additional hours of full generation can be utilized before the runoff begins. Therefore, the system manager can generate more power using relatively cheap hydroelectric facilities than he could if no QPF information was used. Table 2 shows the gross value of power produced per hour with full generation conditions.

5. A SCENARIO FOR USE OF THE QPF TO MAXIMIZE HYDROPOWER

5.1 Preexisting Conditions The following conditions are assumed to exist for this scenario:

(a). All lakes and reservoirs are at the desireable full pool level.

(b). Soil moisture deficiency equals 1 inch for the entire Santee Basin.

(c). System load and all generating facilities are in normal operational status.

5.2 The QPF The quantitative precipitation forecast is prepared for two time periods:

DAY 1 From 12z today until 12z tomorrow (24 hours).

DAY 2 From 12z tomorrow until 12z, day after tomorrow (24 to 48 hours).

TABLE 1 MAXIMUM POWER CAPACITY AND FLOW

POWER PLANT	HEAD (h) [ft]	POWER (P) [kw]	FLOW (Q) [cfs]
SALUDA DAM	50	2,711	754
PIEDMONT	26	1,750	936
HOLLIDAYS BR	35	4,000	1,590
BOYDS MILL	35	1,200	477
BUZZARD ROOST	55	15,000	3,793
LAKE MURRAY	155	200,000	17,946
TUXEDO	120	5,000	580
TURNER	70	5,500	1,093
STICE SHOALS	30	2,000	927
GASTON SHOALS	40	9,140	3,178
99 ISLANDS	55	18,000	4,552
LOCKHART	52	12,000	3,210
NEAL SHOALS	24	4,000	2,318
PARR	35	14,000	5,563
COLUMBIA	32	10,000	4,346
LAKE TAHOMA	30	240	111
BRIDGEWATER	135	20,000	2,060
RHODISS	60	25,500	5,911
OXFORD	89	36,000	5,626
LOOKOUT	78	18,720	3,338
COWANS FORD	112	372,000	46,195
MT ISLAND	78	50,000	8,916
SPENCER MTN	20	640	445
WYLIE	70	52,000	10,332
FISHING CR	61	30,000	6,840
GREAT FALLS	71	69,000	13,516
ROCKY CREEK	58	69,000	16,546
WATEREE	78	56,000	9,985
WILSON DAM	28	1,107	550
JEFFERIES	75	16,177	3,000
ST STEPHEN	49	84,000	23,843

TABLE 2 GROSS VALUE OF POWER PRODUCED

(rate per kilowatt-hour)	$.06	$.07
SALUDA DAM	$162.66	$189.77
PIEDMONT	$105.00	$122.50
HOLLIDAYS BR	$240.00	$280.00
BOYDS MILL	$72.00	$84.00
BUZZARD ROOST	$900.00	$1050.00
LAKE MURRAY	$12000.00	$14000.00
TUXEDO	$300.00	$350.00
TURNER	$330.00	$385.00
STICE SHOALS	$120.00	$140.00
GASTON SHOALS	$548.40	$639.80
99 ISLANDS	$1080.00	$1260.00
LOCKHART	$720.00	$840.00
NEAL SHOALS	$240.00	$280.00
PARR	$840.00	$980.00
COLUMBIA	$600.00	$700.00
LAKE TAHOMA	$14.40	$16.80
BRIDGEWATER	$1200.00	$1400.00
RHODISS	$1530.00	$1785.00
OXFORD	$2160.00	$2520.00
LOOKOUT	$1123.00	$1310.40
COWANS FORD	$22320.00	$26040.00
MT ISLAND	$3000.00	$3500.00
SPENCER MTN	$38.40	$44.80
WYLIE	$3120.00	$3640.00
FISHING CREEK	$1800.00	$2100.00
GREAT FALLS	$4140.00	$4830.00
ROCKY CREEK	$4140.00	$4830.00
WATEREE	$3360.00	$3920.00
WILSON DAM	$66.42	$77.49
JEFFERIES	$970.62	$1132.39
ST STEPHEN	$5040.00	$5880.00

A 24 hour QPF is sufficient for the purpose of power planning. Six hour QPFs would perhaps give more accuracy but the additional calculations would probably preclude their use.

For the purpose of this scenario the QFP will be:

DAY 1 (fig. 4): Three inches over the northwest sections of the Basin including all of the North Carolina portion. Two inches over the rest of the Basin including the coastal plain portions.

DAY 2 (fig. 5): Two inches over the central portions of the Basin with one inch over the northern and southern portions.

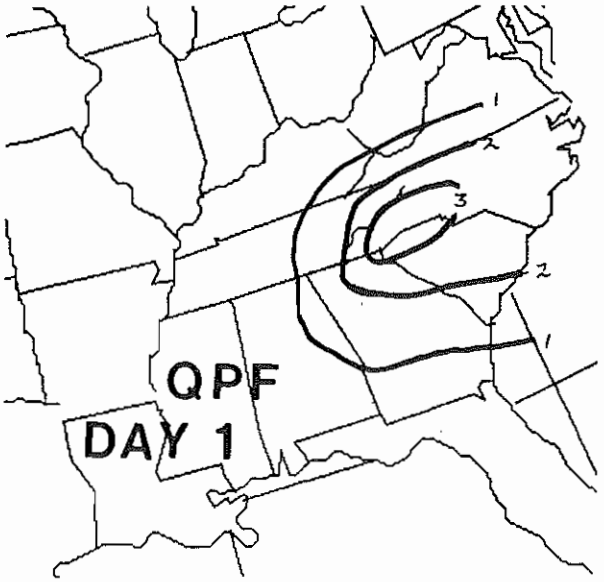

Figure 4 DAY 1 QPF

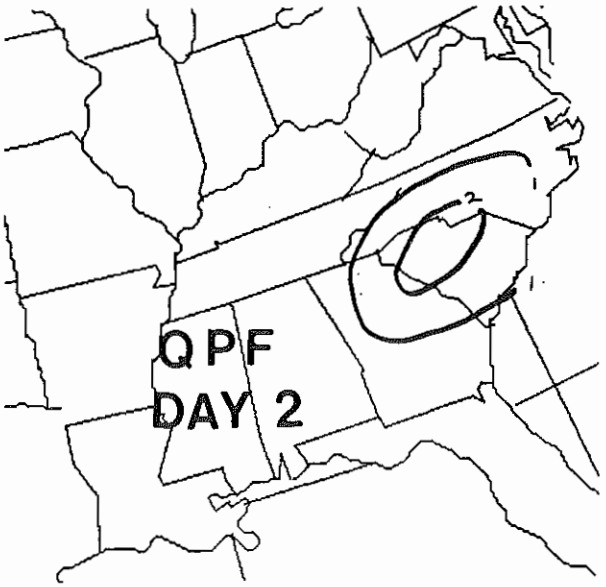

FIGURE 5 DAY 2 QPF

Using formula (1) and the SMD of 1 inch, the RE for DAY 1 is: 2 inches over the northern sections and 1 inch elsewhere. Applying this RE of 2.0 inches to the graph for drainage area 122 (RE/SRO #7) yields an SRO of .40 inches. The SRO ranges from .35 to 1.2 inches in the Basin (Table 3). The DAY 2 QPF results in RE of 1 to 2 inches and SRO of .20 to 1.20 (table 4).

TABLE 3 (DAY 1 QPF)

	(inches)			(in)	(sq mi)	(ac ft)
BASIN#	QPF	RE	RE/SRO	SRO	DA	ROV
122	3	2	7	.40	380	8106
123	3	2	7	.40	708	15104
124	3	2	7	.40	222	4736
125	3	2	7	.40	139	2965
126	3	2	11	1.20	630	40320
127	3	2	11	1.20	289	18496
128	3	2	11	1.20	600	38400
129	3	2	12	.90	1730	83039
130	3	2	14	1.20	320	20480
131	3	2	7	.40	864	18432
132	3	2	10	.70	626	23370
133	3	2	7	.40	212	4523
134	3	2	7	.40	108	2304
135-136	2	1	12	.40	2763	58944
137	3	2	7	.40	415	8853
138	2	1	11	.35	735	13720
139	2	1	11	.35	200	3733
140	2	1	12	.40	991	21141
141	2	1	12	.40	857	18283
142-143	2	1	14	.55	1780	52213

TABLE 4 (DAY 2 QPF)

	(inches)			(in)	(sq mi)	(ac ft)
BASIN#	QPF	RE	RE/SRO	SRO	DA	ROV
122	1	1	7	.20	380	4053
123	1	1	7	.20	708	7552
124	1	1	7	.20	222	2368
125	1	1	7	.20	139	1482
126	1	1	11	.30	630	10079
127	1	1	11	.30	289	4624
128	2	2	11	.30	600	9599
129	2	2	12	.90	1730	83035
130	2	2	14	1.20	320	20479
131	1	1	7	.20	864	9215
132	1	1	10	.30	626	10015
133	1	1	7	.20	212	2261
134	1	1	7	.20	108	1152
135-136	2	2	12	.90	2763	132616
137	1	1	7	.20	415	4426
138	2	2	11	.30	735	11759
139	2	2	11	.30	200	3200
140	2	2	12	.90	991	47565
141	2	2	12	.90	857	41133
142-143	1	1	14	.50	1780	47464

By entering the unitgraph for basin 122 (fig. 3), with the SRO for day 1 and day 2; the six hourly flows can be combined to get a runoff hydrograph (fig. 6).

RUNOFF HYDROGRAPH FOR BASIN 122

elapsed time in hours/ flow in 1000 cfs									
Bridgewater	6	12	18	24	30	36	42	48	54
SRO day 1	12	2.0	1.2	.8	.4				
day 2					6.0	1.0	.6	.4	.2
total flow	12	2.0	1.2	.8	6.4	1.0	.6	.4	.2

FIGURE 6 RUNOFF HYDROGRAPH FOR BRIDGEWATER

A runoff hydrograph for downstream hydroplants can be made by preparing a runoff hydrograph for the particular downstream basin and then adding the upstream hydrograph. The upstream hydrograph must be delayed by an amount approximately equal to the travel

time between points. Figure 7 shows the runoff hydrograph for Rhodiss (basin 123) with the Bridgewater hydrograph added in with an 18 hour delay.

RUNOFF HYDROGRAPH FOR BASIN 123

Rhodiss	6	12	18	24	30	36	42	48	54
SRO flow	16	6	3.6	2.4	2.4	3.8	1.8	1.2	.4
Bridgewater			12.0	2.0	1.2	.8	6.4	1.0	.6
total flow	16	6	15.6	4.4	3.6	4.6	8.2	2.2	1.0

FIGURE 7 RUNOFF HYDROGRAPH RHODISS

This method of downstream routing ignores the effect of channel storage in the river or reservoir between the outlet of basin 122 and 123. This method should be accurate enough for planning purposes, however.

By comparing the amount of water needed for full generation with the amount of water that will be available at the various power plants. The amount of time that full generation can be used and the approximate "lead" time can now be determined. Table 5 shows the results of these calculations and gives an estimate of the additional hours of generation gained by using the QPF.

It is easy to see that the value of the additional power produced is substantial. In this senario, the value of the QPF amounts to over half a million dollars.

TABLE 5

STATION	HYDRO GENERATION [hrs]		ADDITIONAL WITH QPF INPUT [hrs]	
BRIDGEWATER	42	$50,400	12	$14,400
RHODISS	54	$82,620	12	$18,360
OXFORD	54	$116,640	12	$25,920
LOOKOUT	54	$60,642	12	$13,476
COWANS FORD	24*	$267,840	6*	$66.960
MT. ISLAND	54	$162,000	12	$36,000
SPENCER MTN	54	$2,074	12	$461
WYLIE	66	$205,920	12	$37,440
FISHING CREEK	54	$97,200	12	$21,600
GREAT FALLS	54	$223,560	12	$49,680
ROCKY CREEK	54	$223,560	12	$49,680
WATEREE	66	$221,760	12	$40,320
TUXEDO	54	$16,200	6	$1,800
TURNER	60	$19,800	12	$3,960
STICE SHOALS	66	$7,920	12	$1,440
GASTON SHOALS	60	$32,880	6	$3,288
99 ISLANDS	60	$64,800	6	$6,480
LOCKHART	66	$47,520	3	$2,160
NEAL SHOALS	66	$15,840	6	$1,440
PARR SHOALS	66	$55,440	12	$10,080
COLUMBIA	66	$39,600	12	$7,200
SALUDA	54	$8,784	12	$1,952
PIEDMONT	66	$6,930	6	$630
HOLLIDAYS BRIDGE	54	$12,960	6	$1,440
BOYDS MILL	66	$4,752	6	$432
BUZZARD ROOST	66	$59,400	12	$10,800
LAKE MURRAY	66	$792,000	12	$144,000
JEFFERIES	66	$64,061	12	$11,647
ST. STEPHEN	66	$332,640	12	$60,480
TOTALS		$3,295,743		$643,526

* 1/2 GENERATION

6. SUMMARY AND CONCLUSIONS

An accurate QPF can be used to great advantage by managers of electric generating systems. Knowledge of the amount of precipitation expected can enable system managers and dispatchers to utilize hydroelectric power several hours earlier than if they waited for the runoff to begin. At many hydroelectric sites in the Southeast, local restrictions on the changing of lake levels preclude substantial drawdown prior to runoff and/or storage of runoff for later use. In these cases, a short term drawdown may be acceptable if the water will be replaced in a few hours. Efficient use of hydropower during other than "peak periods" requires planning the system configuration several hours ahead. A QPF can aid the system manager by allowing him to plan on the use of hydropower.

In the Santee basin, each hour of generating time using hydropower is worth approximately $72,278. In the scenario above, The QPF would have resulted in an additional 3 to 12 hours of generating time. The gross value of this power would be $643,526. If the DAY 1 QPF indicated no precipitation and the DAY 2 QPF indicated substantial runoff; the value could double to over a million dollars.

REFERENCES

Farnsworth, R.K., E.S. Thompson, and E.L. Peck, 1982: Evaporation Atlas for the 48 Contiguous United States. NOAA Tech. Rpt. NWS 33, Office of Hydrology, National Weather Service, Washington, DC June 1982, 26 pp

Long, John F., 1980: Small Scale Hydropower Resource Assesment Report for S.C. US Dept. of Energy and S.C. Land Resources Conservation Commission, 68 pp, 4

NOAA, 1982: Monthly Normals of Temperature, Precipitation, and Heating and Cooling Degree Days 1951-1980, South Carolina. Climatology of the United States No. 81, National Climatic Center, Asheville, NC

NOAA, 1985: Climatological Data Annual Summary, North Carolina 1984, Volume 89 Number 13. Climatic Data Center, Asheville, NC

NOAA, 1985: Climatological Data Annual Summary, South Carolina 1984, Volume 87 Number 13. Climatic Data Center, Asheville, NC

THE EFFECTS OF URBANIZATION ON THE MINGO CREEK WATERSHED

Timothy P. Marshall

Haag Engineering Co.
2455 S. McIver Dr.
Carrollton, Texas 75006

1. INTRODUCTION

Urbanization of flood plains presents additional challenges to the hydrometeorologist in flood forecasting and warning. One of the problems associated with urbanization is increased runoff rates from paved surfaces, storm sewers, and river channelization. A recent flood on the Mingo Creek watershed in Tulsa, Oklahoma, provided an opportunity to study the flood flow problems in this rapidly growing area.

Mingo Creek begins in southeast Tulsa, Oklahoma and flows northward to Bird Creek. The topography changes from rolling hills in the south to a broad, gently sloping flood plain in the north. Prior to 1950, the watershed remained virtually undeveloped. Land use was primarily agricultural. Since then, Tulsa has expanded rapidly eastward. Without regard to flood control, large residential areas have been constructed on the flood plain of Mingo Creek. Some homes, apartment complexes, and mobile home parks lie adjacent to the creek's channel.

On May 27, 1984, the worst flash flood in recorded history occurred along the Mingo Creek watershed. Rainfall varied from 5 to 15 inches, with the heaviest amounts reported in the center of the watershed. Most of the rain had fallen within a four hour period. Five fatalities occurred on swollen Mingo Creek tributaries. Although the meteorology situation was ideal for flash flooding, certain urbanization factors appeared to have contributed to the increased flood levels.

A ground survey was conducted within a few days after the flood disaster. The purpose of the survey was to document flood elevations and obtain channel dimensions. Subsequent study revealed channel flow problems that included highway berms, underdesigned culverts, and other channel constrictions which restricted flood flow. In several areas, flood water accumulated behind obstructions causing extensive flooding beyond the 100 year flood plain. Results of the ground survey are presented along with comments on watershed planning and management.

2. URBANIZATION HISTORY

Mingo Creek has been a problem watershed ever since the first settlers arrived in the mid 1800's. Most early floods inundated farm land and were not life threatening. Recent floods occurred in 1943, 1959, 1961, 1968, 1970, 1974, 1976, and 1984. Generally, flooding has resulted when rainfall exceeded 5 inches. Flooding has been associated with slow moving thunderstorms which happen primarily in spring and summer months. Although flooding has been prevalent on the watershed for a long time, flood control was not implemented until 1975.

Urbanization has grown rapidly since the mid 1950's, when the city of Tulsa encompassed about 10 percent of the Mingo Creek watershed area. By 1984, approximately 90 percent of the 61 square mile watershed was within the city limits of Tulsa. Figure 1 shows the increase in watershed urbanization from 1955 to 1982. Rapid urbanization occurred initially west of the Mingo Creek mainstem. Large residential subdivisions, highways, shopping centers, office and industrial buildings were constructed. A recent study by HTB, Inc., (1981) mentioned that the riparian region of Mingo Creek was so heavily populated there was little open land left for construction of flood detention ponds. Flood control costs have escalated in recent years, since proposals have included buying back developed land for detention pond construction.

3. MINGO CREEK FLOOD CONTROL HISTORY

At the time of the May 27, 1984 flash flood, several flood control improvement projects were under construction and several were already

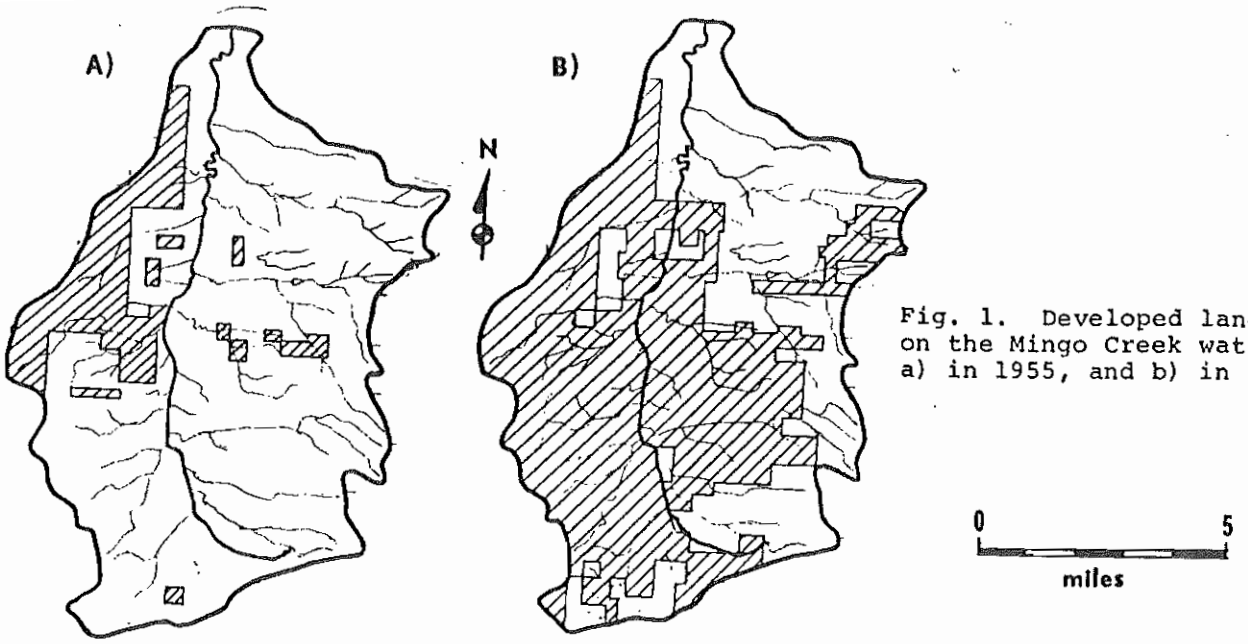

Fig. 1. Developed land area on the Mingo Creek watershed a) in 1955, and b) in 1982.

completed on the Mingo Creek watershed. Improvement projects included channel widening, channel straightening, and the addition of detention basins to pond flood waters. Design criteria considered full urbanization of the watershed with a 100 year return period for flooding.

The U.S. Army Corps of Engineers (Corps) was originally asked to complete an interim flood control study of Mingo Creek in May, 1966. Although a flood in June, 1968 caused about 150,000 dollars in property loss, the study was discontinued in 1972 when flood control costs exceeded benefits. However, a flood in June, 1974 prompted a restudy of flood control plans, as property losses approached 20 million dollars. Even though a higher cost-benefit ratio was determined, lack of funding precluded further study.

Recognizing the serious nature of flooding along Mingo Creek, the City of Tulsa undertook its own flood control project in 1975 without federal assistance. Subsequently, ordinances were passed by the city council in 1977 restricting future flood plain development. Prior to the 1984 flood, three miles of channel had been widened, and one detention pond had been constructed. Twenty-two homes were purchased and removed to clear land for a second detention pond.

Another devastating flood on Mingo Creek happened in 1976, causing 26 million dollars in property loss (Corps, 1977). The Corps was again authorized to continue their flood control plan for Mingo Creek. A final project report was completed in 1980. According to the Federal Emergency Management Agency (1984), the Corps' 93.2 million dollar plan entails the construction of 23 detention ponds and channelization of 7.5 miles of the Mingo Creek mainstem and tributaries. After extensive review by the Corps, the flood control plan was submitted to Congress for approval in April 1984. The next flood disaster on Mingo Creek occurred the following month.

4. SURVEY RESULTS

A field survey was conducted after the flood to investigate channel flow restrictions. The survey entailed measuring channel characteristics such as depth and width. In addition, bridge dimensions and the extent of vegetation cover were recorded. Results showed flood water ponded upstream of bermed highways, channel constrictions, and channel obstructions (i.e. encroaching vegetation).

4.1 Highways Berms

There were five highway berms which traversed the Mingo Creek flood plain. These highways were: the Broken Arrow Expressway (Rt. 51), Skelly Drive (I-44), Admiral Street, Crosstown Expressway (I-244), and Pine Street. In each case, flow was directed through designed culverts which restricted discharge. Once the creek topped its banks, flood waters were essentially dammed by highway berms, and water proceeded to spread out horizontally.

Figure 2 shows the effect of the Broken Arrow Expressway berm on ponding flood waters along Bell and Fulton tributaries. The topagraphy on both sides of the highway was similar, with a gradual slope downward to the north. North of the highway, flood flow remained close to the 100-year design flood. However, south of the highway, water pooled and spread out, inundataing residential and business areas. Basin

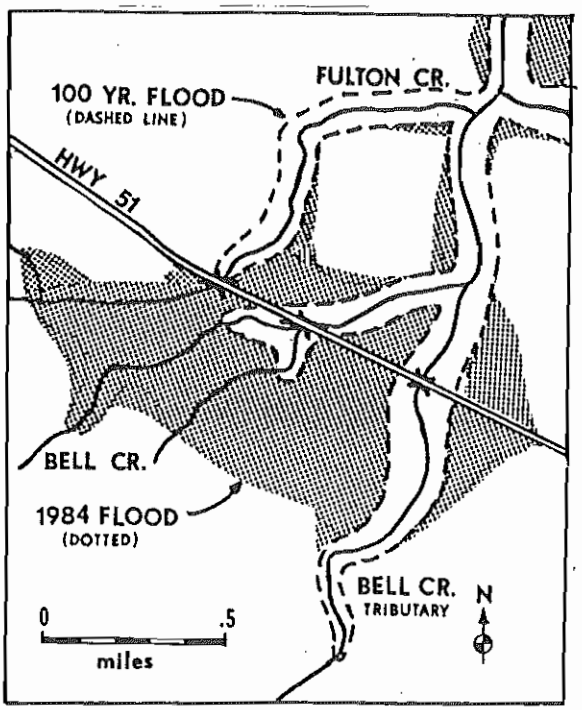

Fig. 2. Plan view of the Broken Arrow Expressway traversing Mingo Creek tributaries. Bold line represents creek channel, dashed line is 100 year flood level, and shaded area indicates extent of flooding on May 27, 1984 beyond the 100 year flood level.

transfer occurred between creeks. The resulting lake stretched more than a mile wide.

One method to minimize the damming effect of flood waters in the flood plain would have been to construct highways on columns rather than berms as shown in Figure 3. This would alleviate the ponding problem and allow flood waters to continue downstream. Although initial costs are much higher to elevate highways on columns, it is believed property losses would have been greatly reduced.

4.2 Channel Constriction

There were several areas along Mingo Creek where the channel width narrowed, and culvert sizes were smaller than those upstream. Water elevations upstream of flow constrictions were increased. Across the width of some culverts there was a two foot head difference. Generally, as the channel length increases, bridge culvert size should increase also.

Bridge and culvert data from the Corps (1970), show several locations where culvert sizes along the mainstem of Mingo Creek were smaller than adjacent culverts upstream. Widths of bridge openings are plotted in Figure 4. Of the twenty bridges traversing Mingo Creek, at

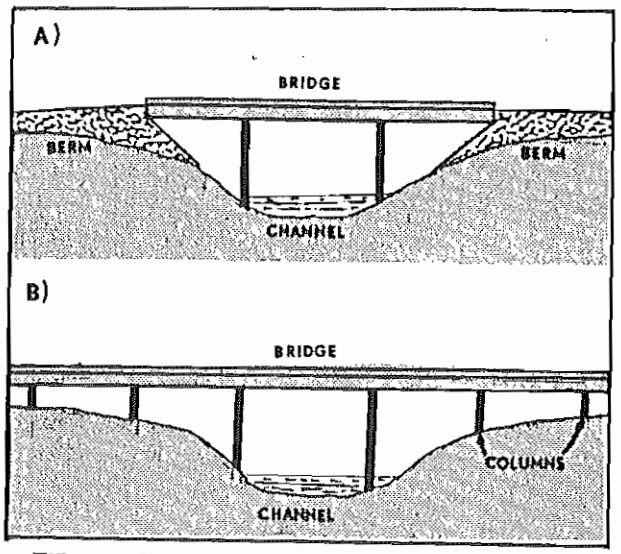

Fig. 3. Flood plain bridges a) as designed on Mingo Creek, and b) as recommended to minimize the ponding problem.

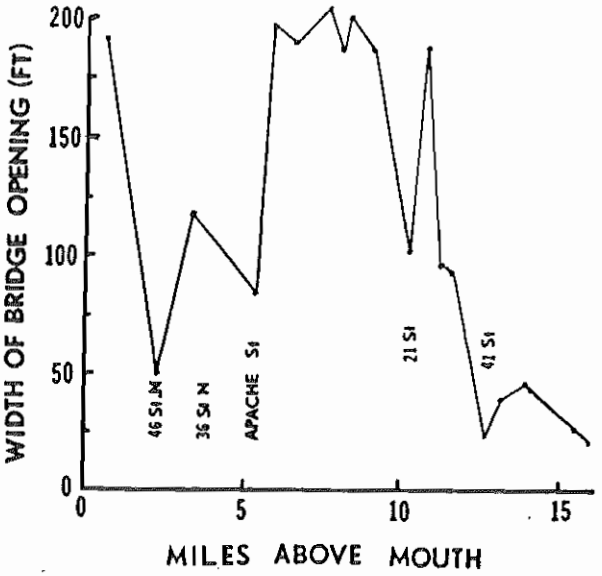

Fig. 4. Width of bridge openings on Mingo Creek from mouth to headwaters. Flow constrictions occurred at underdesigned culverts (labeled).

least five culverts had widths 15 to 50 percent smaller than the adjacent ones upstream. Some of this difference can be explained by the ages of the bridges. In general, it was found that bridges constructed recently tend to have larger culvert openings than older bridges.

4.3 Channel Vegetation

The sloping sides of the mainstem of Mingo Creek had been excavated, surfaced with grasses, and appeared to be well maintained. On the other hand,

Fig. 5. Excavated channel on Bell Creek with concrete box culvert.

Fig. 6. Unimproved channel on Bell Creek has dense vegetation cover. View is only a few hundred yards upstream of Figure 5.

tributaries of Mingo Creek, predominantly in undeveloped areas, had trees and brush growing along the creek.

Figures 5 and 6 allow comparison of the amount of channel vegetation along Bell Creek near the Broken Arrow Expressway. Where the highway crosses the creek, a concrete box culvert was constructed, the channel sides excavated, and the slope was cleared of dense vegetation. Only a few hundred yards upstream in an undeveloped area, the situation was much different. The creek was cloggged with trees and undergrowth. After the May, 1984 flood, debris marks revealed that the water exceeded the bank height by at least three to four feet.

Obstructions in the flow most likely caused a decrease in water velocity and an increase in water height. Investigation of land use upstream of the undeveloped area revealed a large residential subdivison with a concrete lined creek channel. High water velocities in the developed area appreared to contribute to the back flow problem downstream.

5. CONCLUSIONS

Rapid urbanization of the Mingo Creek watershed has increased the backwater problem. In the flood in May, 1984 pooling of water occurred upstream of highway berms, underdesigned bridge culverts, and areas with dense channel vegetation. Mitigation of ponding flood waters will involve elevating bridges on columns instead of berms, widening older bridges which have small culverts, and minimizing channel vegatation on the creek mainstem as well as tributaries.

Urbanization has outpaced flood control on Mingo Creek. Although Mingo Creek has had a long history of flooding, flood control began only within the last decade. Without federal support initially, the City of Tulsa has had to fund local flood control projects. Urban problems were recognized more than twenty years ago but, flood control planning and implementation was a long, involved process. It is hoped that the problems presented herein are considered in planning and construction for future flood control projects.

6. ACKNOWLEDGEMENTS

I would like to thank the U.S. Army Corps of Engineers, Tulsa Division and Mr. Randy Zipser of the Oklahoma State Water Resources Board for providing background information on Mingo Creek. Mr. Ben Barker of the Tulsa National Weather Service Office provided detailed meteorology information on the May, 1984, flood. Mr. Richard Madison of Haag Engineering Company offered helpful comments and suggestions in review of this material.

7. REFERENCES

Federal Emergency Management Agency, 1984: Interagency Flood Hazard Mitigation Report, FEMA-709-DP. 18pp.

HTB Inc., 1981: Mingo Creek Master Drainage Plan for Tributaries between I-44 and Broken Arrow Expressway. 144 pp.

U.S. Army Corps of Engineers, 1970: Flood Plain Information on Mingo Creek, Southwestern Division, Tulsa, Division. 32 pp.

U. S. Army Corps of Engineers, 1977: Report on Flood of 30 May 1976, Southwestern Division, Tulsa, District. 30pp.

THE USE OF WATER VAPOR IMAGERY IN THE ANALYSIS AND FORECASTING OF HEAVY PRECIPITATION

Roderick A. Scofield and Theodore W. Funk

NESDIS/Satellite Applications Laboratory
Washington, DC 20233

1. INTRODUCTION

Water vapor imagery (6.7 μm) is one of the GOES-VAS products obtained from the multispectral imaging mode and is currently available every 6 hours. This paper discusses the use of the imagery in the analysis and forecasting of heavy precipitation. The moisture structure of the atmosphere, both in the horizontal and vertical, is an important factor in the development of heavy precipitation systems. Moisture variances can be quite extreme within the mesoscale range. Water vapor imagery has the capability to provide moisture information at a much finer resolution than conventional data sources.

In addition to presenting features in the water vapor imagery associated with advection and vertical motion, this paper discusses the use of 6.7 μm imagery in the analysis of the middle Atlantic record flood event of November 1985.

2. WATER VAPOR IMAGERY CHARACTERISTICS

As shown by Weldon and Steinmetz (1983), the 6.7 μm moisture channel imagery depicts the total radiance emitted by water vapor in an atmospheric column, with a peak response in the middle troposphere from about 300 mb down to 600 mb. Water vapor imagery displays regions of middle-level moisture and clouds. Distinct patterns of cooler, more moist areas (light tones) and warmer, drier areas (dark tones) are readily detected. These features are related to areas of both synoptic and mesoscale advection and vertical motion. When animated, the features exhibit excellent spatial and temporal continuity.

The convention used on the moisture channel imagery is similar to that for the unenhanced infrared:

1. Very light gray shades (lightest third of gray shades) indicate:
   (a) middle or high clouds are present and are being detected as in standard IR imagery or
   (b) a relatively deep layer of moist air is present above 700 mb - typically 300 to 400 mb deep;
2. If gray shades are very dark (darkest third of gray shades):
   (a) no cold middle and high clouds are present and
   (b) little or no water vapor is present in the middle or upper troposphere (above 800 or 700 mb depending on the latitude and time of year);
3. Gray shades in the middle third of shades can be attributed to a wide range of combinations of moisture amount and vertical distribution.

3. PRODUCTION OF DARK REGIONS IN THE WATER VAPOR IMAGERY

The production of dark regions in the water vapor imagery refers to a decrease in image brightness following a feature embedded in the upper flow. In this section the emphasis is on darkening, not with the existence of dark regions. Physical processes leading to moisture channel darkening are cold advection at middle and high levels coupled with strong upper-level convergence-both processes lead to strong sinking and a deepening of the dry layer. This allows the satellite to sense further down to a warmer level in the troposphere. Subsynoptic scale dark regions (possibly associated with jet maxima) can move with the flow evolving into a large variety of patterns, orientations, and locations with respect to the circulation features.

Weldon (1985) identified four types of warming:

1. Base warming - at the base of troughs often associated with jet maxima or streaks in "digging" situations;
2. Cyclonic surge - a warm zone turns into

the cyclonic flow and takes the elongated shape into the storm slot; this is often associated with upper air cyclogenesis and surface deepening (surface deepening continues until the warm zone reaches the left or poleward side of center);

3. Anticylonic surge - often associated with upper air anticyclogenesis and closing of ridge;

4. Head warming - occurs on the poleward or upstream side of a comma head deformation zone; this is associated with the opening up or "shearing out" of the upper low and filling of the surface low.

Presently, Ellrod (1985) found darkening with time in the water vapor imagery to be a good indicator of significant high altitude turbulence.

4. FEATURES IN THE WATER VAPOR IMAGERY ASSOCIATED WITH ADVECTION AND VERTICAL MOTION

The 6.7 μm moisture channel imagery is quite adept at diagnosing middle and upper tropospheric meteorological phenomena by defining the continuity of moisture and cloud fields associated with them. For this purpose, the imagery especially is helpful in regions devoid of upper air wind reports and is often more useful than the IR imagery, particularly in clear areas. Below is a list and brief description of phenomena detectable in the imagery that normally are related to advection and vertical motion. Examples are presented in Fig. 1.

a. Middle and upper level circulation systems: Significant curvature in the moisture patterns of water vapor imagery often defines and locates middle and upper tropospheric circulation systems. This is quite evident in Fig. 1a which shows several cyclonic vortices over the Pacific Ocean. These vortices, however, generally are not detectable as easily in the corresponding IR image (Fig. 1b), since the region is relatively cloud free. Thus, important information about circulation systems is best contained in the moisture channel imagery.

b. Jet streams: Jet streams usually are positioned along and parallel to elongated, well-defined gradients of gray shades. The polar jet stream axis normally is positioned between lighter gray shades on the poleward side and a darker band on the equatorward side. Conversely, the subtropical jet stream axis normally is located between lighter gray shades on the equatorward side and a darker band on the poleward side. The stronger the jet, the better defined is this light-dark edge. An example of a dual jet pattern is presented in Fig. 1c. Here, the polar jet curves cyclonically along line A-B while the subtropical jet extends along line C-D.

c. Jet maxima: Jet maxima, like jet streams, often are positioned along elongated, well-defined gradients of gray shades. However, a wind maximum within a jet stream usually is associated with a sharper edge than along the rest of the jet axis. In Fig. 1d, a jet maximum through California (along line A-B) is located in the base of a deep shortwave trough. The dark zone immediately to the south defines the exact position of the maximum.

d. Deformation zones: Deformation zones are bands in which air parcels or clouds undergo stretching in one direction and contraction in the orthogonal direction. Weldon (1979) has shown that they are related best to the cols of the motion field for stationary and very slow moving systems and to the cols of the relative vorticity field for eastward moving systems. Furthermore, they are systematically located in advance (to the rear) of and perpendicular (parallel) to the maximum wind. In the water vapor imagery, deformation zones often clearly are detectable as sharp boundaries between light and dark gray shades where stretching is occurring along and parallel to the boundary and contraction is occurring orthogonal to it. Animated imagery is particularly important in detecting the stretching and contraction associated with these zones. A classic example of a deformation zone in a slow moving system that is orthogonal to the maximum wind is given in Fig. 1e. The zone is aligned from A to B along the gradient of gray shades. The superimposed 500 mb streamlines reveal that the band is located in the col of the motion field. Just south of the zone under the light gray shading, radar (not shown) depicts precipitation in a northwest to southeast oriented band from eastern Ohio and western Pennsylvania to off the North Carolina coast.

e. Cutoff lows: Fig. 1f presents a cutoff low off the Baja of California (center at A). As is evident in this example, the circular moisture pattern clearly reveals cutoff lows. Again, this especially is true when cloudiness associated with these lows is minimal.

f. Convectively unstable situations: These situations occur when middle-level dry air surges into and over low-level moist air resulting in convective instability. This mesoscale moisture pattern often is not evident in the standard IR imagery. Fig. 1g depicts a squall line over northern and central Texas, whose southern portion (A) is positioned within a narrow dry, dark slot extending across Mexico into central Texas. The advection of this middle-level dryness into Texas, coupled with moisture at low levels, resulted in a convectively unstable environment in which a cold front released the instability and set off heavy thunderstorms. Anthony and Wade (1983) have shown that if the dry area surges downwind of moist, unstable lower levels and the middle and upper-level flow is at least slightly different, then severe thunderstorms likely will develop.

g. Rapid darkening to the rear of convective clusters: Thunderstorm-induced rapid darkening in the moisture channel imagery likely is the result of drying air due to subsidence immediately to the rear of the convective cluster. Spayd (1985a) has presented such an example (Fig. 1h-i). Fig. 1h shows a convective system at A with a dark region at B. Four hours later (Fig. 1i), the area at B had darkened (dried) considerably as the convective complex at A intensified and caused descent to its rear.

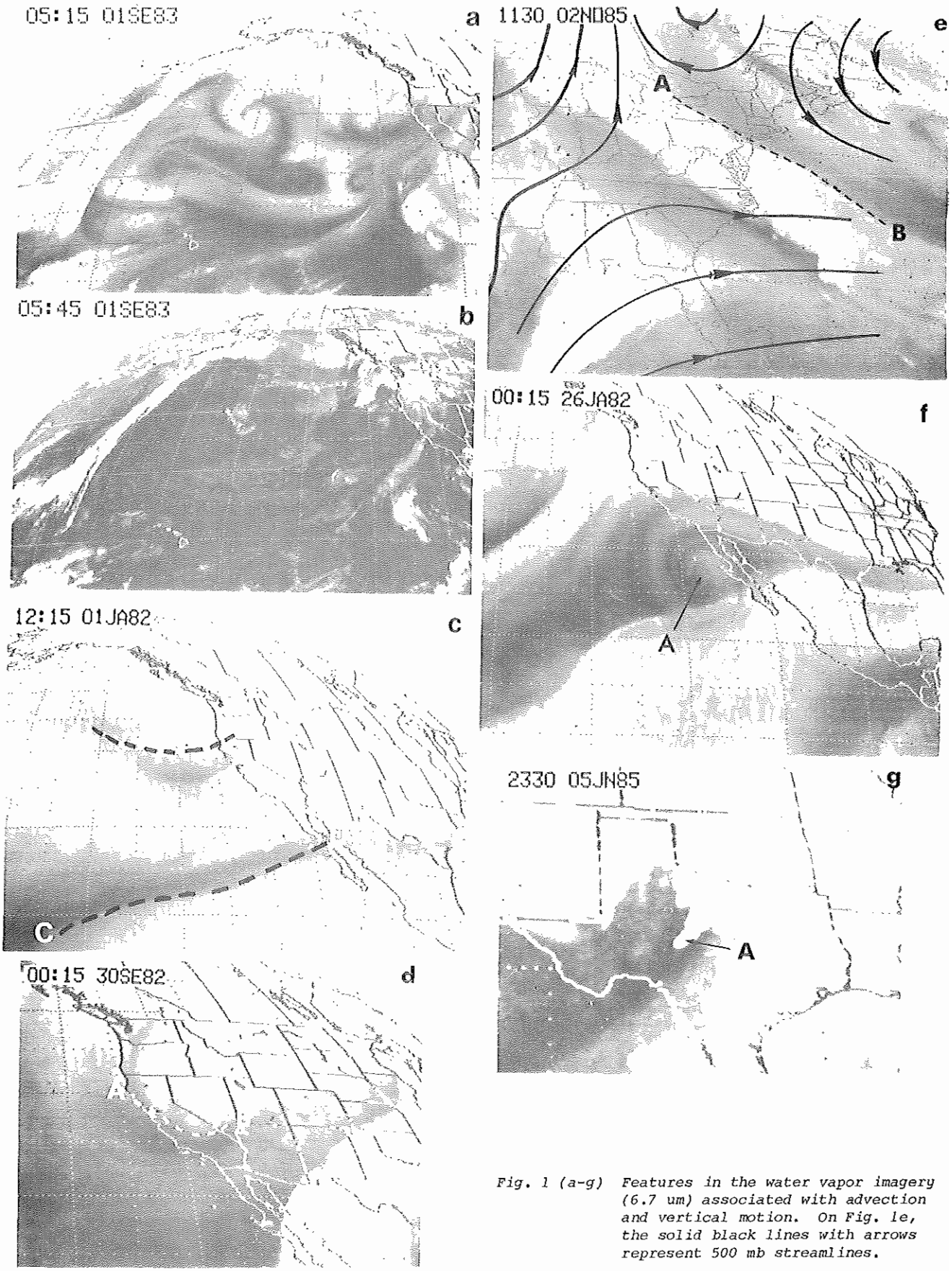

Fig. 1 (a-g) *Features in the water vapor imagery (6.7 um) associated with advection and vertical motion. On Fig. 1e, the solid black lines with arrows represent 500 mb streamlines.*

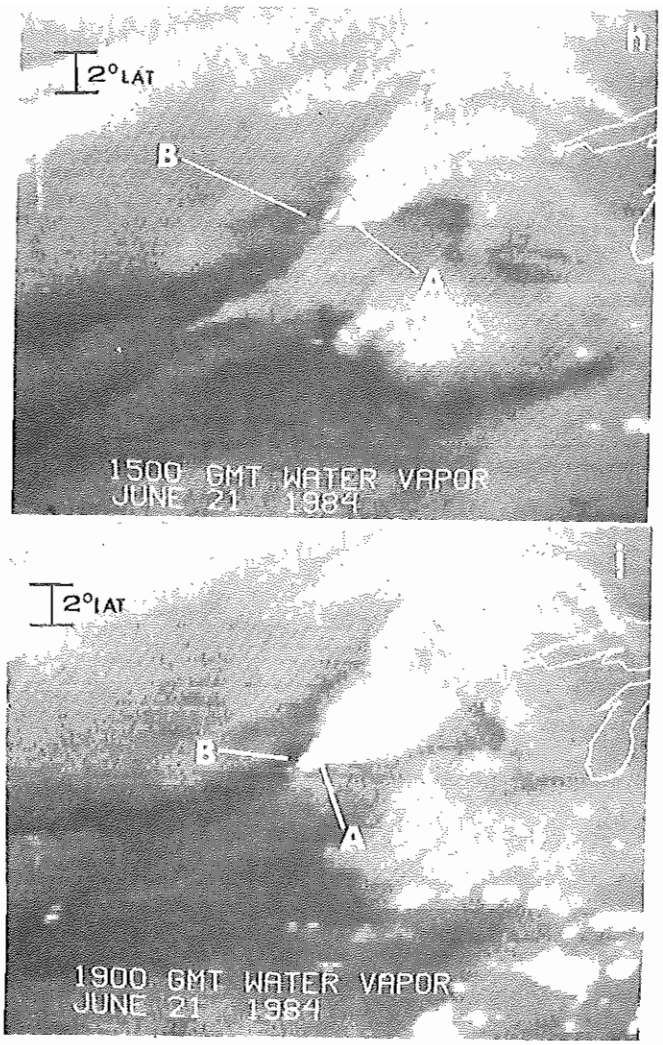

Fig. 1 (h-i) (Continued).

5. MIDDLE ATLANTIC RECORD FLOOD EVENT OF NOVEMBER 1985

Record rainfall and flooding hit the middle Atlantic states during the first week in November 1985. Generally light to moderate rainfall amounts occurred across the region on November 1-2. However, very heavy rainfall fell on November 3-4, as a weak low pressure system in the Gulf of Mexico rapidly developed into a major storm system as it slowly moved northeast into the middle Atlantic states. The intense low, combined with a distinct trough extending north to the Great Lakes, caused two-day rainfall totals of 5-10 inches from much of central Virginia to central West Virginia. Four-day maximum amounts from November 1-5 exceeded 10 inches over west central Virginia with Montebello, VA receiving over 18 inches.

The event provides an excellent example of how 6.7 μm moisture channel imagery can provide indications of rapid surface development and deepening. The imagery for this case is presented in Fig. 2. At 2330 GMT 3 November, a jet maximum was located upwind and in the base of the 500 mb trough (axis from eastern Missouri to Louisiana). This maximum was associated with a dark area, i.e., base warming (Weldon, 1985) (denoted by A) in Louisiana. A surface low was in southeast Georgia with a central pressure of 1005 mb, the same as 12h earlier (not shown). However, by 1200 GMT 4 November, the low, now in south central North Carolina, began deepening rapidly with a central pressure of 1001 mb. The development is indicated on the 1130 GMT 4 November water vapor image. As observed on upper air synoptic charts, the jet streak induced rapid surface development as it rounded the deepening shortwave and was oriented parallel to the distinct moisture gradient through northern Florida northward to extreme eastern Kentucky. The dark (dry) region previously in Louisiana had darkened and surged northeastward along the length of the jet axis, a feature that Weldon (1985) and Smigielski and Ellrod (1985) have noted is an indication of rapid surface cyclogenesis and deepening. This slot region apparently is due to sinking and drying associated with the jet circulation (Anderson et al., 1982).

The comma configuration continued to develop markedly at 2330 GMT 4 November. The dry slot had darkened considerably from 12h earlier and had rotated around the vortex into the middle Atlantic states. A dual jet pattern was quite apparent. The polar jet dipped south through the Midwest along the distinct light-dark gradient and curved cyclonically around the trough base while the subtropical jet advanced northeastward from the Gulf of Mexico to just off the North Carolina coast. Apparently, resulting strong upper-level convergence caused descent, thereby continuing the pronounced darkening process of the slot. The rapid darkening correlated with explosive surface deepening as the low pressure center, located just south of Roanoke, VA, fell to 994 mb. It reached a minimum pressure of 992 mb at 0900 GMT 5 November as the dry air continued wrapping into the vortex as depicted on the 0530 GMT 5 November image. However, by 1130 GMT 5 November, its pressure rose to 995 mb as the dark slot had reached the left or poleward side of the vortex center (in northern Virginia) and had begun to diffuse. The slot position and diffusion correlated with weakening of the low, a correlation that Weldon (1985) and Smigielski and Ellrod (1985) also have noted. Finally, by 2330 GMT 5 November, the slot had filled in around the low center (in eastern Maryland) which correlated with a rising central pressure of 999 mb. The jet stream, as depicted by the circular dark band, completely encircled it.

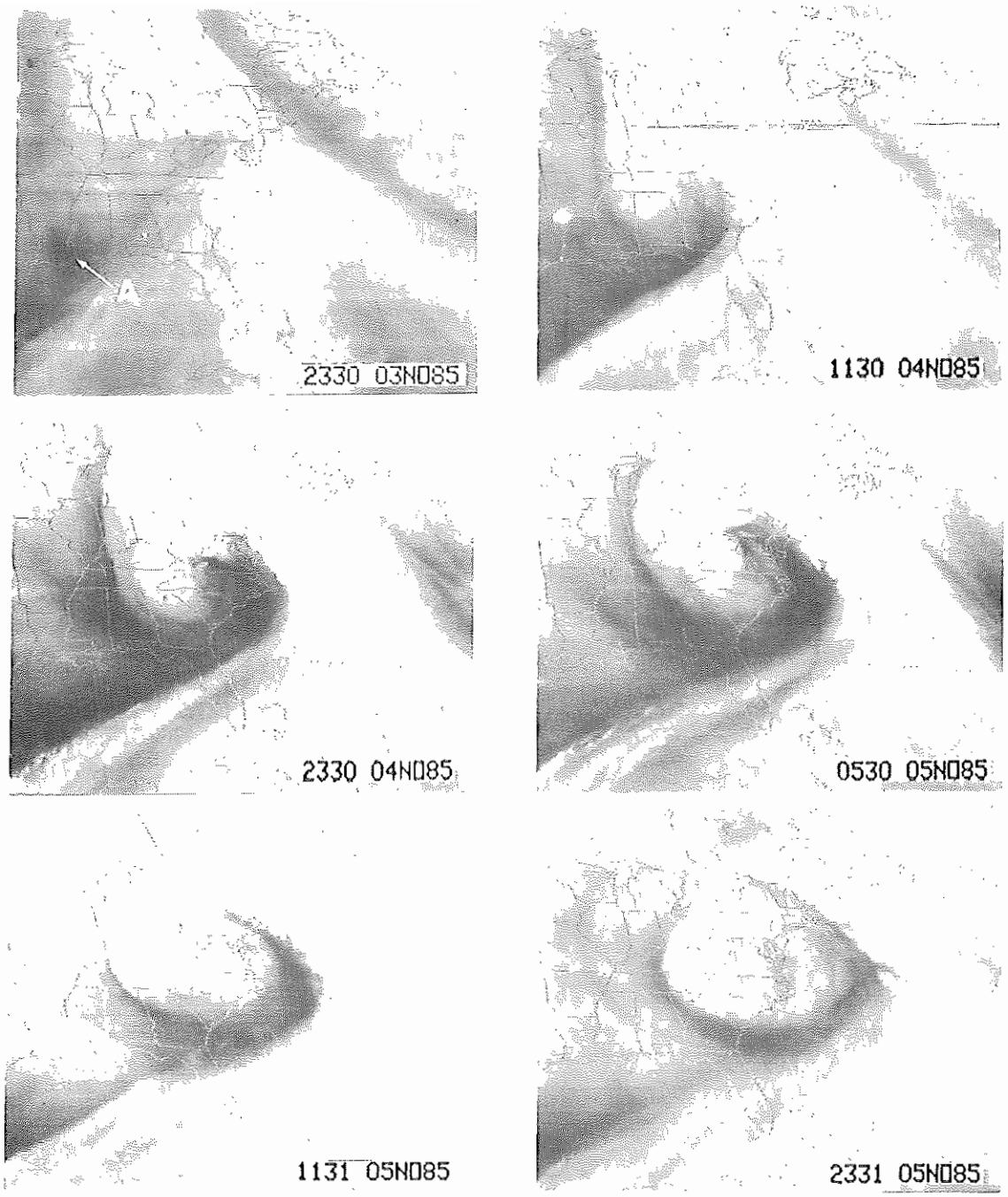

Fig. 2 Water vapor imagery (6.7 um) from the middle Atlantic states record flood event of November 1985.

This event also demonstrates the usefulness of water vapor imagery in showing that boundaries in the imagery can be related to the development of heavy rainfall producing convection. The imagery at 1130 GMT 4 November (Fig. 3) depicts bright cloud tops over West Virginia and eastern Ohio. General rainfall over the area was due to the advection of warm air and positive vorticity into a strong low-level convergence zone north of the surface low. However, heavy (even severe) thunderstorms were occurring over west central and southwest Virginia (area A) on the southern edge of the rain area. The convection, which persisted until 1800 GMT over west central Virginia and produced 4.69 inches of rain at Roanoke, VA between 1200 and 1800 GMT, occurred on the moisture gradient along the eastern boundary of the rapidly developing and darkening dry air slot. The slot likely introduced middle-level dryness (as depicted at B on the 1130 GMT image) over abundant low-level moisture, which resulted in convective destabilization and the onset of convection along a frontal boundary over the region. The boundary is less evident on the IR imagery (not shown). New thunderstorms, which produced about an additional inch at Roanoke, occurred over west central Virginia between 1800 GMT and 0000 GMT 5 November.

These cells (area C) again had appeared on the distinct leading edge of a dark "finger" of the dry slot from southern to western Virginia (area D) on the 2330 GMT 4 November image (Fig. 3). Since the main slot extended through eastern Maryland, this "finger" may result from compensating subsidence to the rear of the convection during the 12h period. Spayd (1985a and 1985b) has also presented examples of the development of heavy rainfall producing convection along boundaries in the water vapor imagery.

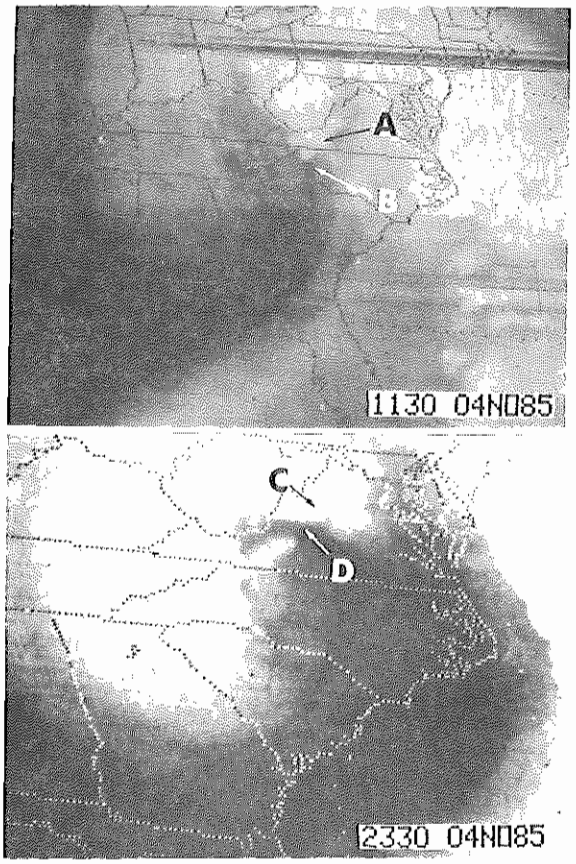

Fig. 3 Water vapor imagery (6.7 um) at 1130 and 2330 GMT 4 November 1985 from the middle Atlantic states record flood event. Convective clusters at A and C and dark, dry regions at B and D are annotated.

To summarize, the 6.7 μm moisture channel imagery proved to be an important indicator of synoptic-scale cyclogenesis and mesoscale convective development during the November 1985 catastrophic flood event across the middle Atlantic states. The current and future effort is to utilize the imagery as an aid for better anticipating and forecasting heavy precipitation events such as the one just described. In this effort, Gurka (1985) has presented cases in which the water vapor imagery provided valuable information to supplement numerical prediction models in forecasting the movement and behavior of heavy rainfall producing winter storms.

6. OUTLOOK

As our knowledge of how to use the water vapor imagery increases, a better understanding of the initiation, focusing, and maintenance of heavy precipitation will result. Animated and more frequent 1 to 2h interval imagery is necessary in order to better analyze features associated with advection and vertical motion.

7. ACKNOWLEDGEMENTS

The authors thank Gary Ellrod, NESDIS/Satellite Applications Laboratory, for his constructive criticism in the preparation of their manuscript. The authors also thank John Shadid for his drafting and layout, Gene Dunlap for prints of the satellite pictures, and Tina Cashman for typing this manuscript.

8. REFERENCES

Anderson, R. K., J. J. Gurka, and S. J. Steinmetz, 1982: Application of VAS multispectral imagery to aviation forecasting. Proceedings of the Ninth Conference on Weather Forecasting and Analysis, June 28-July 1, 1982, Seattle, Washington, AMS, Boston, MA 227-234.

Anthony, R. W. and G. S. Wade, 1983: VAS operational assessment findings for spring 1982/1983. Proceedings of the Thirteenth Conference on Local Storms, Tulsa, Oklahoma, AMS, Boston, MA, 358-364.

Ellrod, G. P., 1985: Detection of high level turbulence using satellite imagery and upper air data. NOAA Technical Memorandum NESDIS 10, Satellite Applications Laboratory, NOAA/NESDIS, Washington, DC, 30 pp.

Gurka, J. J., 1985: The use of 6.7 micron water vapor imagery for improving precipitation forecasts. Proceedings of the Sixth Conference on Hydrometeorology, October 29 - November 1, 1985, Indianapolis, IN, AMS, Boston, MA, 260-265.

Smigielski, F. J. and G. P. Ellrod, 1985: Surface cyclogenesis as indicated by satellite imagery. NOAA Technical Memorandum NESDIS 9, Satellite Applications Laboratory, NOAA/NESDIS, Washington, DC, 30 pp.

Spayd, L. E., Jr., 1985a: Application of GOES VAS data to NOAA's interactive flash flood analyzer. Proceedings of the International Conference on Interactive Information and Processing Systems for Meteorology, Oceanography, and Hydrology, January 7-11, 1985, Los Angeles, CA, AMS, Boston, MA, 240-247.

Spayd, L. E., Jr., 1985b: Preliminary uses of GOES VAS data to estimate and nowcast heavy convective rainfall. Proceedings of the Sixth Conference on Hydrometeorology, October 29 - November 1, 1985, Indianapolis, IN, AMS, Boston, MA, 252-259.

Weldon, R., 1985: Conclusions and generalizations on water vapor imagery gray shades versus moisture distribution. Training Notes, Satellite Applications Laboratory, NOAA/NESDIS, Washington, DC, 4 pp.

Weldon, R. and S. Steinmetz, 1983: Characteristics of water vapor imagery. Unpublished report, Satellite Applications Laboratory, NOAA/NESDIS, Washington, DC, 22 pp.